

UCSF

UC San Francisco Electronic Theses and Dissertations

Title

Diversifying olfactory cell fates

Permalink

<https://escholarship.org/uc/item/9tw8b8mw>

Author

Sagasti, Alvaro,

Publication Date

2001

Peer reviewed|Thesis/dissertation

Diversifying Olfactory Cell Fates

by

Alvaro Sagasti

DISSERTATION

Submitted in partial satisfaction of the requirements for the degree of

DOCTOR OF PHILOSOPHY

in

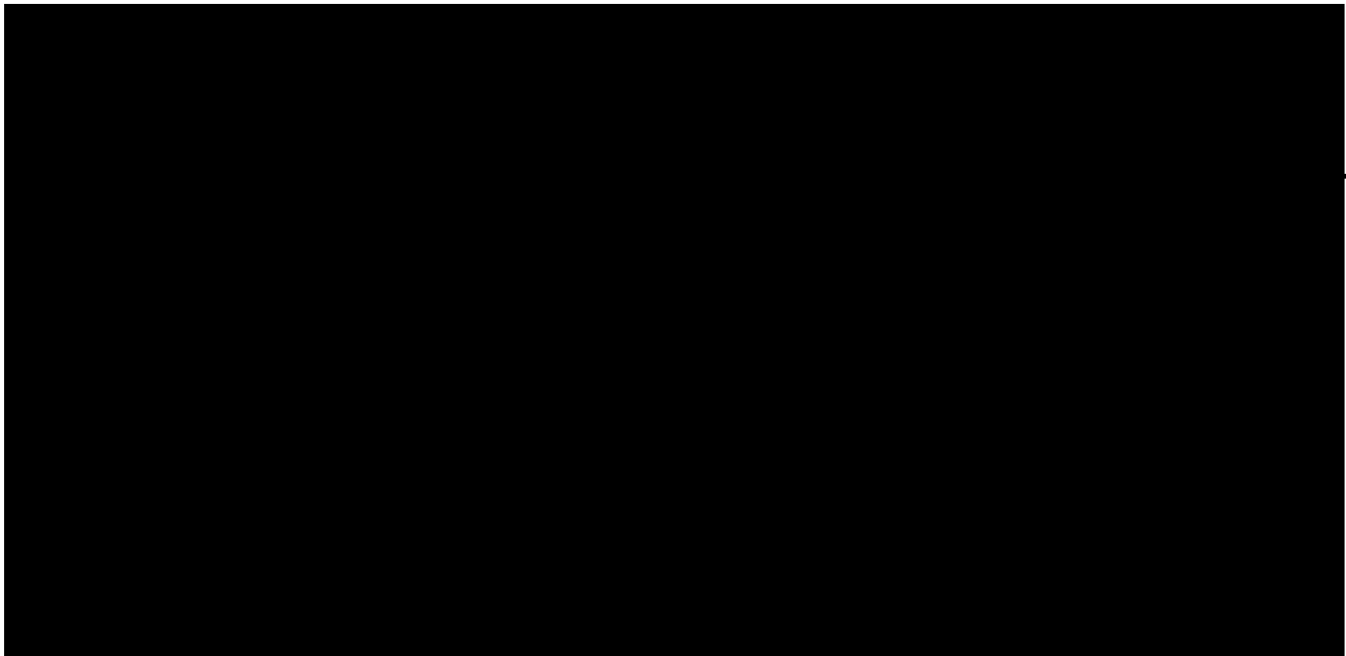
Genetics

in the

GRADUATE DIVISION

of the

UNIVERSITY OF CALIFORNIA, SAN FRANCISCO



Copyright © 2001

by

Alvaro Sagasti

Acknowledgments

Many people have contributed to the success of the work described in this thesis. Those contributions include assistance with specific experiments as well as many less tangible, but no less important, contributions to my scientific education and personal well-being.

I have acknowledged many of the people who have made specific contributions at the end of each published paper, but I want to mention again Oliver Hobert, Naoki Hisamoto, Miho Tanaka-Hino, and Kunihiro Matsumoto. These scientists have been excellent collaborators whose work and insight were vital to making the projects described in chapters 2 and 4 successful.

I am particularly indebted to my closest collaborator in the Bargmann lab, Emily Troemel. Emily's influence on my work extends far beyond the specific reagents and experiments she contributed to our collaborative papers. The entire Bargmann lab deserves credit for providing a constant, insightful critique of my work, and more generally for helping to educate me about how to be a good scientist. I especially want to thank David Tobin for his patience and careful scientific judgement.

I wish to thank the broader UCSF community for making graduate school a fun and exciting time in my life. In particular, I want to thank my thesis committee members, the Bargmann, Kenyon, Martin, and Tessier-Lavigne labs, participants in the developmental biology journal club, my classmates and my friends.

Finally, I want to thank Cori Bargmann for being an ideal advisor. Her wisdom, scientific excitement, broad knowledge, rigorous standards, and warm personality have made my years in her lab a great privilege.

Genes & Development
From: Alvaro Sagasti [asagast@itsa.ucsf.edu]
Sent: Friday, August 10, 2001 7:48 PM
To: genesdev@cshl.org
Subject: copyright permission

Friday August 10, 2001

Genes & Development
Cold Spring Harbor Laboratory Press
Box 100, 1 Bungtown Road
Cold Spring Harbor, New York 11724-2203

To Whom it may concern:

I am writing to request permission to include a copy of the following paper in my thesis dissertation:

Sagasti, A., Hobert, O., Troemel, E.R., Ruvkun, G., Bargmann, C.I. Alternative olfactory neuron fates are specified by the LIM homeobox gene *lim-4*.

Genes Dev. 1999 Jul 15;13(14):1794-1806.

The dissertation will be microfilmed by University Microfilms Incorporated and they request permission to supply single copies upon demand. Since I must submit my thesis by August 27, I would greatly appreciate it if you could respond next week by fax to: (415) 476-3493. Please contact me by e-mail if you questions.

Thank you very much.

Sincerely,

Alvaro Sagasti
Department of Anatomy
UC San Francisco

Permission granted by the copyright owner,
contingent upon the consent of the original
author, provided complete credit is given to
the original source and copyright date.

By Cheryl H. Powers 8/13/01
Date

COLD SPRING HARBOR LABORATORY PRESS

FCR/mm/aug 01.114
22 August 2001

Alvaro Sagasti
Dept of Anatomy
UC San Francisco

Dear Mr/Ms Sagasti

CELL, Vol 105, 2001, pp 221-232, Sagasti et al, " The CaMKII UNC-43..."
Vol 99, 1999, pp 387-398, Sagasti et al, "Lateral signalling..."

As per your letter dated 16th August 2001, we hereby grant you permission to reprint the aforementioned material at no charge in your thesis subject to the following conditions:

1. If any part of the material to be used (for example, figures) has appeared in our publication with credit or acknowledgement to another source, permission must also be sought from that source. If such permission is not obtained then that material may not be included in your publication/copies.
2. Suitable acknowledgment to the source must be made, either as a footnote or in a reference list at the end of your publication, as follows:

"Reprinted from Journal title, Volume number, Author(s), Title of article, Pages No., Copyright (Year), with permission from Elsevier Science".
3. Reproduction of this material is confined to the purpose for which permission is hereby given.
4. This permission is granted for non-exclusive world English rights only. For other languages please reapply separately for each one required. Permission excludes use in an electronic form. Should you have a specific electronic project in mind please reapply for permission.
5. This includes permission for UMI to supply single copies, on demand, of the complete thesis. Should your thesis be published commercially, please reapply for permission.

Yours sincerely

Frances Rothwell (Mrs)
Global Rights Manager

Advisor Statement

Chapter 2 was published in *Genes and Development*, volume 13, pages 1794 to 1806. Oliver Hobert isolated the *lim-4* cDNA, made the *lim-4::GFP* transgene, and created figure 2. Emily Troemel made the *str-2::ODR-10* transgene. All other work was performed by Alvaro Sagasti.

Chapter 3 was published in *Cell*, volume 99, pages 387 to 398. This work was an equal collaboration between Emily Troemel and Alvaro Sagasti. Emily created and characterized the *str-2::GFP* transgene, performed ablations, performed the candidate mutant analysis, and wrote the manuscript. Alvaro Sagasti analyzed the *str-2::GFP* expression in axon guidance mutants, performed the screen for mutants that express *str-2* in both AWC cells, and performed the majority of the epistasis analysis.

Chapter 4 was published in *Cell*, volume 105, pages 221 to 232. Members of Kunihiro Matsumoto's laboratory isolated a partial *nsy-1* cDNA, engineered the *nsy-1* gain-of-function transgene, and performed the biochemical experiments in figures 1B and 2G. All other work was performed by Alvaro Sagasti.

Cori Bargmann, Ph.D.
Associate Professor
HHMI and UCSF, Department of Anatomy

Abstract

Biological complexity requires the development of a diverse array of cell types. A molecular genetic approach was used to investigate two mechanisms by which cellular diversity is generated in the nervous system, using the *C. elegans* olfactory cells, AWA, AWB, and AWC, as a model. One of these mechanisms acts cell intrinsically and the other requires a cell-cell interaction.

The *lim-4* mutant was isolated in a visual screen for mispecification of olfactory cell fates. In *lim-4* mutants signal transduction genes, cell morphology, and the synaptic connections of AWB neurons are transformed towards an AWC fate. LIM-4 encodes a LIM homeobox gene that is expressed in AWB. Ectopic expression of LIM-4 in the AWC neuron pair is sufficient to force those cells to adopt an AWB fate. The previously described AWA nuclear hormone receptor ODR-7 also represses AWC genes, as well as inducing AWA genes. These results suggest a mechanism by which a generic olfactory cell fate diversifies to create several functionally different cell fates, ultimately endowing the animal with a more complex behavioral repertoire.

A further level of cell fate diversification occurs in the AWC olfactory neurons. A stochastic, coordinated decision ensures that the candidate odorant receptor *str-2* is expressed in only one AWC neuron in each animal—either the left or the right neuron, but never both. A lateral interaction between the two AWC neurons generates

asymmetric *str-2* expression in a process that requires AWC axon contact. A mutant screen was conducted to identify genes involved in AWC lateral signaling. Analysis of these mutants revealed that this interaction induces *str-2* expression by reducing calcium signaling through a calcium channel and the CaM kinase II *unc-43*.

nsy-1, another mutant isolated in the AWC asymmetry screen, encodes a homolog of the human MAP kinase kinase kinase ASK1, an activator of JNK and P38 kinases. Based on genetic epistasis analysis and biochemical experiments, we propose that the *nsy-1* MAP kinase cassette is directly activated by *unc-43*. Mosaic analysis demonstrated that UNC-43 and NSY-1 act primarily in a cell-autonomous execution step that represses *str-2* expression in one AWC cell, downstream of the initial lateral signaling pathway that coordinates the fates of the two cells. These results, coupled with the observation that NSY-1 and UNC-43 have well-conserved mammalian homologs, raise the possibility that the calcium-to-MAPK signaling cassette used in AWC signaling may be used for cell fate diversification in other animals.



Cori Bargmann
Graduate Advisor
Professor
HHMI and UCSF, Department of Anatomy

Table of Contents

Chapter 1	1
Introduction: Diversifying olfactory cell fates	
Chapter 2	43
Alternative olfactory neuron fates are specified by the LIM homeobox gene <i>lim-4</i>	
Chapter 3	57
Lateral signaling mediated by axon contact and calcium entry regulates odorant receptor expression in <i>C. elegans</i>	
Chapter 4	70
The CaMKII UNC-43 activates the MAPKKK NSY-1 to execute a lateral signaling decision required for asymmetric olfactory neuron fates	
Chapter 5	83
Conclusions and future directions	

Chapter 1

Introduction

Diversifying Olfactory Cell Fates

Every organism begins life as a single cell. Understanding the processes that transform a fertilized oocyte into a multi-cellular organism is one of the central challenges of biology. How can a single cell give rise to the thousand specialized cells that make up a nematode worm, let alone the millions of cells that make up a human? During development cells divide rapidly to build up the organism's bulk, but cell division is not sufficient to create a complex organism. As cells divide they must coordinate their fates with their neighbors and become specialized to perform specific functions. For example, some cells make up the skin of an animal, others its digestive system, and others the neurons which allow it to sense and respond to its environment. Differences in the complement of genes transcribed into messenger RNA by each cell account for their unique identities.

Precise control of cell fate diversification and coordination is particularly critical in the nervous system: neurons must take on specialized roles and make specific connections with one another to build the electrical circuits that allow the nervous system to function. Without a diverse array of sensory neurons, interneurons, and motor neurons to form these circuits, animals would not be able to sense or respond properly to their environment. The role that specific cells play in neuronal circuits has been clearly demonstrated for behavioral responses to sensory stimuli in simple animals like the

mollusk *Aplysia* or the nematode *C. elegans*. Behavioral sophistication can in principle be achieved by making these circuits more complex. It is likely that increasing diversification of neuronal cell fates during evolution created animals with correspondingly more complex behavioral repertoires. Many of the same mechanisms that generate diversity in a simple nervous system, such as that of *C. elegans*, are therefore likely employed to create the much more complicated nervous systems of vertebrates.

The generation of cellular diversity can be programmed into the embryonic lineage and executed by asymmetric cell divisions, or it can be induced by interactions between cells in the embryo. Most of these interactions occur during development and generate cell types that remain stable throughout the life of the animal.

This thesis describes efforts to use molecular genetic approaches to define some of the mechanisms by which cellular diversity is generated in the nervous system, using *C. elegans* olfactory cells as a model. Two molecular mechanisms for cell fate diversification are investigated. One of these mechanisms acts cell-intrinsically to create the three major olfactory cell types of *C. elegans* (Chapter 2), and the other involves a lateral cell-cell interaction that distinguishes the left and right homologs of a particular olfactory cell type (Chapters 3 and 4). This introduction will first review some of the molecular mechanisms used to generate cell diversity during development, with emphasis on the role of the Notch signaling pathway in lateral cell interactions. The next section

discusses what is known about cell fate allocation in vertebrate, *Drosophila*, and nematode olfactory systems. The final section discusses the generation of left/right asymmetries during development, particularly in the nervous system.

Molecular mechanisms of Cell Fate Diversification

Asymmetric Cell Division

Developing embryos make use of a variety of cell-intrinsic and -extrinsic mechanisms of cell fate diversification. A fertilized oocyte, the first cell in an organism's developmental lineage, has no neighbors available for inductive interactions. The initial breaking of symmetry in the organism therefore often involves a cell-intrinsic diversification mechanism. The first cell division after fertilization in *C. elegans* and in mice is molecularly asymmetric. Presumably, proteins that determine cell fate are enriched in one part of the cell and thus become incorporated into only one of the daughter cells after mitosis (Piotrowska and Zernicka-Goetz, 2001; Guo and Kemphues, 1996).

Asymmetric cell division is important not only in the first cell division, but also later in development, when the nervous system is forming. For example, the HAM-1 protein is asymmetrically distributed in certain *C. elegans* neuroblasts and is required for the two daughter cells to take on distinct cell fates (Guenther and Garriga, 1996). The molecular mechanisms that mediate asymmetric cell division have been most thoroughly

studied in the fly nervous system and in the first cell division in *C. elegans*. Remarkably, in both systems a conserved protein complex consisting of two PDZ-domain containing proteins and an atypical protein kinase C is segregated to one of two dividing cells and is required for asymmetric cell fate allocation (reviewed in Doe and Bowerman, 2001).

This PDZ protein complex is also required for maintaining cell polarity in mammalian epithelial cells. Although the nature of the protein determinants that segregate to the cell opposite from the PDZ-complex containing cells is different in the first cell division of *C. elegans* and in neuroblast cell divisions in flies, the remarkable conservation of this complex suggests that asymmetric cell division is an ancient process mediated by a few, similar molecular mechanisms.

Cell-cell signaling and the Notch pathway

Compared to asymmetric cell division, cell-extrinsic fate diversification mechanisms that rely on cell-cell signaling are more varied. Several classes of ligand/receptor pairs are used during development to relay information from one cell to the nucleus of another, ultimately altering the transcriptional profile of the recipient cell (reviewed in Edlund and Jessell, 1999). These signals can be membrane associated or secreted and can act locally or at a distance. Most of these signaling systems function in many different developmental contexts and are conserved throughout the animal kingdom. The most common ligand families used in this way include Hedgehog, Wnt,

TGF- β , Delta, retinoic acid, EGF and FGF. The ultimate fate adopted by a particular cell depends on the particular combination of signals it receives, the order in which signals are received, and the intrinsic factors with which the cell is endowed.

Cell interactions can be inductive or lateral. Inductive signaling is unidirectional: one cell sends a signal and another receives it. As a result, the outcome of an inductive signaling interaction in a normal embryo is almost always invariant. Lateral signaling differ from inductive interactions in that the specific polarity of their outcome can not be predicted. In lateral interactions cells with equivalent developmental potentials communicate with one another so that each eventually adopts a unique fate. This interaction is sometimes characterized as a "competition" between the interacting cells for a particular fate. One example of this type of signaling occurs in the *Drosophila* epidermis, which consists of a sheet of cells with equal potential to become sensory organ precursor (SOP) cells (reviewed in Bray, 1998). Cells in the epidermis compete with one another through lateral signaling, so that only one cell in a field of epidermal neighbors takes on the SOP cell fate. Because the SOP goes on to form a sensory bristle, this mechanism ensures equal spacing of these bristles in the *Drosophila* epidermis.

All lateral signaling processes that have so far been characterized at the molecular level make use of the Notch signaling pathway (Kimble and Simpson, 1997). Notch proteins are transmembrane receptors characterized by EGF repeats in their extra-cellular domain and ankyrin repeats intracellularly. Notch receptors are activated by Delta

ligands, which are transmembrane proteins with a small intracellular domain, one or more extracellular EGF repeat and an extracellular Delta family-specific DSL domain.

Transduction of the Notch signal from the receptor to the nucleus is relatively simple compared to other developmental signal transduction pathways. Activation of Notch by Delta leads to cleavage of the Notch intracellular domain, which then translocates to the nucleus where it interacts with, and alters the activity of, a *Suppressor of hairless* type transcription factor. Notch signaling functions not only in lateral signaling phenomena, but also in unidirectional signaling, sometimes as a result of a bias imposed upon it by the Numb or Fringe proteins, as described below.

In order to achieve the perfect coordination characteristic of lateral signaling decisions, Notch signaling incorporates a feedback loop to amplify small stochastic differences in the signaling state of each cell. This feedback allows the initially equivalent cells to eventually develop a unidirectional relationship. The mechanism of Notch-mediated lateral signaling has been elegantly dissected in the AC/VU decision that occurs in the *C. elegans* gonad. The two cells involved in this interaction, Z1.ppp and Z4.aaa, make a stochastic, coordinated decision that allows one cell to adopt an anchor cell (AC) fate and the other cell to adopt a ventral uterine precursor cell (VU) fate (Kimble, 1981). This interaction requires the Notch family receptor *lin-12* (Greenwald et al., 1983). Seydoux and Greenwald (1989) used genetic mosaic analysis to show that *lin-12* activity is required in the VU cell to allow it to receive an inductive signal from the

AC cell. If *lin-12* was mutant in one of the two AC/VU cells, the mutant cell always adopted the AC fate, demonstrating that it was required to receive a signal that specified VU (Seydoux and Greenwald, 1989). In addition to its autonomous effect, loss of *lin-12* had a non-autonomous effect on the other cell, forcing it to adopt the VU fate. This result demonstrates that *lin-12* is involved in a feedback loop that re-enforces the VU fate in the cell that receives the signal, and inhibits it in the other cell.

Insight into the *lin-12* feedback loop in the AC/VU decision was provided by observing the behavior of fusion proteins of *lin-12* with LacZ reporter and the Delta ligand *lag-2* with LacZ (Wilkinson et al., 1994). This analysis revealed that the two interacting cells both expressed a low level of each protein at the beginning of the cell interaction. As the interaction proceeded, however, the Delta ligand began to disappear in the presumptive VU cell and was more strongly expressed in the presumptive AC cell. The Notch protein had a complementary distribution pattern, disappearing from AC and becoming stronger in VU. AC/VU feedback, therefore, probably functions through the control of ligand and receptor abundance, most likely at the transcriptional level. These data are consistent with a model in which a stochastic asymmetry of Notch activation is amplified by a feedback loop which promotes Notch transcription and inhibits Delta transcription. This process ultimately results in one cell that expresses only Notch and one cell that expresses only Delta, creating a situation where only unidirectional signaling

is possible. Presumably, once the cells have reached these states, Notch sends a signal to the nucleus that executes the VU cell fate.

Chapters 3 and 4 of this thesis describe a novel lateral signaling interaction between two *C. elegans* olfactory neurons that allows them to adopt distinct fates. This interaction does not seem to involve traditional Notch signaling proteins, but instead requires a MAPK signaling module. Nonetheless, the mechanistic framework of the Notch lateral signaling pathway serves as a useful model for understanding the functions of new molecules implicated in the AWC lateral signaling decision. Given the remarkable conservation of other cell fate diversification mechanisms, it is likely that elucidating the details of this new lateral signaling interaction will provide insight into cell fate diversification processes in other systems.

Signal Transduction by MAPK modules

Each developmental signal uses a unique signal transduction pathway to relay information from the cell membrane to the nucleus. Whereas the transduction pathways for most signals are specialized for a particular class of ligand and receptor, the EGF and FGF molecules feed into a common signal transduction cassette: the MAPK module. MAPK pathways can be downstream of many types of ligands and receptors (reviewed in Garrington and Johnson, 1999). For example, the EGF and FGF signals are transduced by receptor tyrosine kinases, whereas the mating pathway in yeast is activated by a

seven-transmembrane receptor, although both activate MAPK modules. In addition to growth factors, MAPKs can be activated by hormones, cytokines, high osmolarity, and cellular stresses, like UV radiation. The cascade often activates a transcriptional switch by phosphorylating a transcription factor, but can also affect cytoplasmic targets like the cytoskeleton.

The core MAPK module consists of three kinases (Garrington and Johnson, 1999). MAPKs are serine/threonine kinases that are phosphorylated and activated by MAPKKs. MAPKKs are typically dual specificity kinases that are activated by the serine/threonine MAPKKKs. MAPKs are divided into three major sequence classes, ERK, JNK, and P38, that are activated by unique sets of MAPKKs. All three MAPK classes have been implicated in developmental processes. However, ERKs have been more strongly associated with developmental processes, whereas JNKs and P38s have been more closely associated with responses to cytokines and cellular stresses.

MAPK modules are well-suited to developmental processes because of their ability to convert graded stimuli into switch-like responses. In most cases, unstable cell fates would be detrimental to the embryo, making all-or-none responses to cell-cell signals desirable. The ERK MAP kinase cascade in *Xenopus* oocytes exhibits ultrasensitivity as a consequence of the requirement for dual phosphorylation of the MAPKK and MAPK, as well as internal feedback loops within the cascade (Ferrell, 1996; Ferrell and Machleder, 1998). More recently, ultrasensitivity has been

demonstrated for activation of JNK by progesterone or hyperosmotic stimuli in *Xenopus* oocytes (Bagowski, 2001). JNK activity in a particular cell is bistable: either it is completely active or completely inactive, it can not exist in an intermediate state. Moreover, JNK activity exhibits a property called hysteresis, meaning that once a stimulus has been received and JNK has entered an activated state, it can maintain that state even after the stimulus has been removed. These properties make MAPK signaling modules ideal for mediating all-or-none developmental responses.

Cell Fate Diversity in Olfactory Systems

Organization of the mammalian olfactory system

Mammals can sense and distinguish between hundreds of chemicals in their environment. This sensory complexity is achieved by populating the olfactory epithelium with one of the richest array of cell types in the body. Although all olfactory neurons are morphologically similar, with ciliated endings on their dendrites and axons that project to the olfactory bulb, each transcribes only one olfactory receptor, allowing it to respond to a specific set of chemicals (Buck and Axel, 1991; Malnic et al., 1999). Olfactory receptors are members of the G-protein-coupled seven transmembrane receptor superfamily (Buck and Axel, 1991). In rodents, the olfactory receptor family consists of approximately one thousand members, making it the largest gene family. Olfactory receptor expression is confined to cells in one of four zones in the olfactory epithelium

(Ressler et al., 1993; Vassar et al., 1993). Each cell randomly selects a single receptor to express from the subset of receptors assigned to that zone. Remarkably, each cell expresses only a single allele of the chosen receptor (Chess et al., 1994), doubling the potential diversity of cell types in the olfactory epithelium.

In addition to determining which chemicals a cell can sense, the receptor also influences where in the brain the cell projects its axon, thus determining the perceived quality of the odorant it senses (Mombaerts et al., 1996). Although cells expressing a particular receptor are scattered randomly throughout one zone in the olfactory epithelium, the axons of all of the cells expressing a particular receptor converge on one of two bilaterally symmetrical glomeruli in the olfactory bulb (Ressler et al., 1994; Vassar et al., 1994). Navigating olfactory axons seem to follow a direct path towards their glomerulus and once there require a critical number of similar neighbors to maintain their connections (Ebrahimi and Chess, 2000). The map of glomerular locations is stereotyped from animal to animal. In other words, a glomerulus containing axons from cells expressing a particular receptor will usually occur in the same position relative to the neighboring glomeruli. Swapping the chromosomal location of receptor coding regions alters the axonal projection of the cells expressing them, demonstrating that it is the receptor itself and not other aspects of olfactory cell fate that determines axon pathfinding (Wang et al., 1998; Mombaerts et al., 1996).

The specification of cell fates in the vertebrate olfactory epithelium remains one of the most fascinating mysteries of developmental biology. Virtually nothing is known about how the zonal organization of the epithelium is specified, how each cell chooses a single receptor to express, how allelic exclusion is accomplished, or how the receptor specifies the cell's axonal projection. The inefficiency of forward genetics in mice has made these problems difficult to tackle. It is likely that insights into the molecular underpinnings of these processes will come from more genetically tractable model organisms.

Organization of the Drosophila olfactory system

Drosophila sense volatile chemicals with two organs: the antenna and the maxillary palp. A family of G-protein-coupled seven transmembrane receptors likely to encode *Drosophila* olfactory receptors has recently been identified (Clyne et al., 1999b; Gao and Chess, 1999; Vosshall et al., 1999). In contrast to the hundreds of likely receptors present in the mouse and *C. elegans* genomes, the fly genome contains only 57 candidate olfactory receptors, as well as a similar number of mixed olfactory/gustatory receptors (Scott et al., 2001). Although no mutations have yet been described in these genes, one receptor has been shown electrophysiologically to be activated by a specific set of volatile chemicals (Wetzel et al., 2001; Stortkuhl and Kettler, 2001).

Each *Drosophila* odorant receptor is expressed in a specific pattern either in the antenna, the maxillary palp, or both, and does not appear to be expressed anywhere else in the adult fly (Vosshall et al., 2000). This predictable arrangement of cells expressing a given receptor in the fly is different from the pattern of cell types in the mammalian olfactory bulb, where cells expressing a particular receptor appear to be scattered randomly within a particular zone. Like mammalian olfactory neurons, however, each *Drosophila* olfactory neuron probably expresses one or two receptors. Furthermore, the neurons expressing a particular receptor typically project to two stereotyped bilaterally-symmetric glomeruli in the antenna lobe of the fly brain (Vosshall et al., 2000; Gao et al., 2000). These results indicate remarkable similarity of the organization of the olfactory systems of flies and mammals.

Using a behavioral genetic screen, a mutant in the POU-domain transcription factor *Acj6* was found to alter olfactory receptor expression in the fly (Clyne et al., 1999a). Electrophysiological analysis of individual neurons in *acj6* mutants indicates that some neurons have either lost or changed their specificity for particular odorants. Accordingly, the expression of some receptors is diminished in the *acj6* mutant (Clyne et al., 1999b). The physiological transformation of some neurons suggests that other receptors must be expressed in ectopic patterns in *acj6*. *Acj6* is only the first identified transcription factor of what is likely to be a transcriptional network controlling the complex pattern of neuronal fates in the *Drosophila* sensory organs. Given the

organizational similarity between the mammalian and fly olfactory systems, it is likely that molecular clues to the control of mammalian olfactory neuron patterns will emerge from genetic studies in *Drosophila*.

Organization of the C. elegans olfactory system

Like mammals, nematodes can detect hundreds of chemicals and respond to their presence with specific behaviors. The *C. elegans* genome contains about 800 candidate seven transmembrane sensory receptors (Troemel et al., 1995). *C. elegans* possesses only about a dozen pairs of chemosensory cells, three of which are specifically olfactory (Bargmann and Horvitz, 1991; Bargmann et al., 1993). The small nervous system dictates that multiple receptors are expressed in each olfactory cell, rather than each receptor being segregated into separate cells, like the mammalian and fly receptors.

The invariant development of the *C. elegans* cell lineage makes possible the unequivocal identification of specific cell types. By ablating individual cells and assaying the behavior of operated animals, the sensory cells that respond specifically to volatile odorants have been defined (Bargmann et al., 1993; Troemel et al., 1997). Three pairs of bilaterally symmetrical olfactory neurons, designated AWA, AWB and AWC, are required for behavioral responses to volatile chemicals. A specific suite of distinct chemicals is sensed by each olfactory neuron. Expression of particular odorant receptors in AWA, AWB, and AWC is likely to underlie their specificity.

The three olfactory neuron pairs mediate different behaviors in response to the chemicals they sense. Activation of AWA or AWC causes animals to move towards the source of the chemical, whereas activation of AWB repels animals from the chemical source. These functional differences between the olfactory cell types is probably a reflection of the connections made by these neurons onto downstream interneurons. Unlike the mammalian olfactory system, the wiring of *C. elegans* olfactory axons is probably not dependent on the particular receptors expressed by that cell (Troemel et al., 1997).

In addition to their functional differences, *C. elegans* olfactory neurons can be identified by morphological and molecular differences. AWA, AWB and AWC share the general morphology of all sensory cells in the anterior nervous system, but possess several characteristics that indicate their unique identities. The tips of sensory dendrites consist of specialized endings called cilia, and each olfactory neuron type possesses a characteristic cilia morphology (Ward et al., 1975). AWA neurons have a filamentous cilium morphology, AWB cilia have a simple forked morphology, and AWC cilia have a membranous, fan-like morphology (Roayaie et al., 1998; Chapter 2). AWA and AWB have axons characteristic of most sensory neurons in the *C. elegans* head: they grow ventrally from the cell body, enter into a large circular neuropil called the nerve ring, and follow the nerve ring dorsally until they terminate at the dorsal midline, resulting in a roughly U-shaped morphology (White, 1986). The AWC axon has a similar trajectory

but continues past the dorsal midline, following the nerve ring back down the contralateral side, resulting in an S-shaped axon.

One olfactory receptor uniquely expressed in each olfactory cell type has been identified. *odr-10* was genetically identified as a receptor for the AWA-sensed chemical diacetyl (Sengupta et al., 1996). A fusion of the *odr-10* promoter to GFP is expressed exclusively in the AWA neuron pair. A reverse genetic approach has identified the orphan receptors *str-1* and *str-2* as candidate receptors expressed in the AWB and AWC sensory neurons, respectively (Troemel et al., 1997; Dwyer et al., 1998); Chapter 2, Chapter 3). GFP fusions to the regulatory regions of these receptors serve as molecular markers that facilitate identification of each neuron.

At the time that the work described in this thesis was begun, only one transcription factor was known to control the generation of olfactory cells in *C. elegans*. The nuclear hormone receptor transcription factor *odr-7* was identified as a gene required for AWA function (Sengupta et al., 1994). In *odr-7* mutants the AWA cells are generated and display roughly normal morphology, but fail to express the *odr-10* receptor (Sengupta et al., 1996). Chapter 2 of this thesis describes a new role for *odr-7*; not only is it required to promote *odr-10* expression, but it also represses expression of the AWC receptor *str-2* in the presumptive AWA cell. Chapter 2 focuses on the cloning and characterization of a second transcription factor involved in olfactory fate specification, the LIM homeodomain protein LIM-4. LIM-4 performs a function in AWB analogous to

ODR-7's function in AWA. In *lim-4* mutants AWB fails to express its endogenous receptor *str-1*, and expresses the AWC receptor *str-2* in its place. Analysis of *lim-4* mutants, and of animals ectopically expressing the LIM-4 protein, demonstrates that LIM-4 is both required and sufficient to impose many aspects of the AWB cell fate onto AWC-like precursor cells. These results suggest a model by which olfactory cell fates were diversified during evolution, endowing the animal with a more sophisticated behavioral repertoire.

In addition to the differences between the three major olfactory cell types, the AWC neurons possess an additional level of diversity. Chapter 3 describes the surprising finding that the left and right homologs of the AWC pair adopt distinct identities. The *str-2* receptor is expressed in only one of the two AWC cells, and in any given animal it is equally likely to be expressed on the left or the right. This further level of molecular diversity increases functional diversity, allowing each of the two AWC cells to sense different odorants (Wes and Bargmann, 2001). Chapter 3 reports on efforts to molecularly dissect the cell interaction between the left and right AWC neurons that allows each cell to take on a distinct fate. This study begins to define some of the features of this interaction, and initiates a genetic analysis of the molecules that mediate it. Specifically, axon outgrowth and calcium signaling are implicated in the cell interaction. Chapter 4 is a more in-depth analysis of a few of the molecules involved in the AWC interaction. *unc-43* encodes a calcium-dependent protein kinase and *nsy-1*

encodes a MAP kinase kinase kinase. This study demonstrates a novel link between the *unc-43* calcium signaling pathway and the *nsy-1* MAP kinase module, and shows that both are required cell-autonomously to implement asymmetric AWC cell fates.

The organization of the worm olfactory system appears superficially very different from that of the mouse or fly. Nonetheless, since little is known about the molecular mechanisms that pattern the mammalian and fly olfactory organs, it remains to be seen whether underlying analogies exist.

The Generation of Left/Right Asymmetry During Development

Left/Right axis determination in vertebrates

The left/right axis is the last of the three embryonic axes to develop asymmetry. Although externally most vertebrates appear symmetric, the shape and positioning of several internal organs are asymmetric. For example, the heart loops towards the left side, the liver is located on the right side, and the stomach and spleen are located on the left side. Morphological and cognitive left/right asymmetries also occur in the vertebrate nervous system and will be discussed below.

Research into the molecular mechanisms that generate left/right asymmetry has progressed rapidly over the past six years (reviewed in Capdevila et al., 2000). Two different models for the initial symmetry-breaking event have been proposed, based on genetic studies in mice and embryological manipulations in chick and frog. Left/right

asymmetry defects in classical and engineered mouse mutants result from mutations in microtubule motor proteins, implicating directed cytoskeletal movement in the symmetry-breaking event (Nonaka et al., 1998; Okada et al., 1999; Supp et al., 1997). Mutations in these motor proteins cause defects in the chiral motion of monocilia located in the mouse node. In wild type animals, ciliary motion results in directed leftward flow of the fluid above the node, and this flow is abrogated or slowed in the motor protein mutants (Nonaka et al., 1998; Okada et al., 1999). This observation has led to the proposal that nodal flow is responsible for asymmetrically localizing a molecular determinant to one side of the node, setting off a cascade that ultimately results in body asymmetry.

A radically different proposal for the generation of asymmetry has emerged from work in chick and frog. Levin and Mercola suggest that left/right asymmetry is established by the circumferential flow of a small molecule through a network of oriented gap junctions in the early blastoderm (Levin and Mercola, 1998; Levin and Mercola, 1999). The expression pattern of gap junction proteins, pharmacological and molecular interference with these proteins, and surgical disruption of the proposed field of circumferential flow all support the notion that gap junctional communication is required for the generation of left/right asymmetry. The proposed gap junctional communication event occurs before development of the node in chicks. The gap junctional communication and ciliary flow hypotheses can therefore only be reconciled if polarity

achieved during gap junctional flow is upstream of ciliary flow at the node, or if the two phenomenon participate in parallel pathways. Alternatively, it is possible that the initial events that break left/right symmetry in chicks and frogs is mechanistically different from the analogous event in mice.

Whether or not the initial symmetry breaking events are distinct in different species, asymmetry in all vertebrates seems to require asymmetric expression of the TGF- β family members *Nodal* and *lefty-1* in a small region just to the left of the node (Levin et al., 1995). This information is prevented from spreading across the midline by axial barriers, and is eventually relayed to the left lateral plate mesoderm (LPM), resulting in asymmetric expression of *Nodal* throughout the LPM. Asymmetric Nodal signaling controls the asymmetric expression of transcription factors, such as *Snail-related* and *Pitx2*, which ultimately determine the asymmetry of organs (Isaac et al., 1997; Logan et al., 1998).

Left/right axis determination in C. elegans

Like vertebrates, *C. elegans* displays several marked left/right asymmetries. The anterior lobe of the gonad is to the right of the intestine and the posterior lobe is to the left of the intestine. Several individual cells are located asymmetrically, including the excretory cell, the coelomocytes and a few neurons. The overall left/right asymmetry of *C. elegans* is arbitrarily designated as “dextral” handedness. Almost all nematode species

are dextral, suggesting that the development of handedness occurred early during nematode evolution. Remarkably, one species of nematode displaying sinistral handedness has recently been described, demonstrating that there is not necessarily an evolutionary advantage to a particular handedness (Felix, 1996).

The molecular control of left/right asymmetry in nematodes is still mysterious, but the cellular basis has begun to be described (Wood, 1991). The first cell division in *C. elegans* is asymmetric, generating a large anterior daughter (AB) and a smaller posterior daughter (P1), and establishing an anterior/posterior axis in the two-cell embryo. Subsequent division of the AB cell into ABa and ABp establishes the dorsal/ventral axis. Although the left and right sides of the embryo are naturally defined by the A/P and D/V axes, left/right polarity is not yet fixed at this stage: switching the positions of the two AB daughters in the four cell embryo switches the D/V axis without causing handedness reversal (Wood, 1991). Left/right asymmetry becomes apparent at the 6-cell stage, when the left daughters of ABa and ABp are situated slightly more anterior than their right daughters. This asymmetry is perpetuated as the embryo divides, ultimately resulting in the dextral body plan of the adult. Remarkably, by surgically pushing ABal and ABpl backwards relative to their sisters, so that now they are situated slightly posterior of ABar and ABpr, left/right polarity can be reversed, creating sinistral, but otherwise normal *C. elegans* (Wood, 1991). These results suggest that left/right

polarity is not programmed into the lineage at the six cell stage, but rather results from cell-cell interactions dependent on the A/P positions of the AB granddaughters.

The development of handedness in *C. elegans* is a cold-sensitive process (Wood et al., 1996). Animals subjected to cold pulses early in development sometimes develop sinistrally. *C. elegans* are sensitive to this cold shock for a brief period around the time of fertilization, demonstrating that the left/right axis is determined, perhaps by asymmetries in the egg shell, even before embryonic cell divisions begin. Removing the egg-shell with chitinase also results in left/right reversals, supporting the idea that egg shell polarity is the primary cause of left/right asymmetry in *C. elegans* (Wood et al., 1996). It is likely that intrinsic chirality of the egg shell constrains the embryo, causing the AB granddaughters to become skewed along the A/P axis relative to one another. Interestingly, handedness of the *C. elegans* internal organs, which is determined by the asymmetry of the AB granddaughters, can be genetically separated from cuticle chirality, suggesting that there are at least two independent mechanisms that determine handedness in *C. elegans* (Bergmann et al., 1998).

Invariant left/right asymmetries in the nervous system

Some brain functions in mammals, such as language and hand dominance, are asymmetrically oriented to either the left or right hemisphere. Although the vertebrate brain is morphologically grossly symmetrical, asymmetries between the left and right

hemispheres have been observed (e.g. Geschwind and Levitsky, 1968; Harris et al., 1996b). However, studies of human patients with *situs inversus totalis* (SI), a condition in which anatomical asymmetries are reversed, indicate that functional asymmetries do not necessarily correlate with overall anatomical handedness (Kennedy et al., 1999). Although SI patients exhibited reversal of some anatomical brain asymmetries, along with body cavity asymmetries, subjects still exhibited strong right-handedness and left-hemisphere language dominance. These results suggest that two distinct mechanisms determine at least some anatomical asymmetries in the brain and the cellular basis of certain functional asymmetries.

A molecular link between the pathway that mediates body asymmetry in vertebrates and brain asymmetry has been demonstrated in the zebrafish diencephalon. In addition to its asymmetric expression in the left lateral plate mesoderm, a Nodal ligand was found to be expressed asymmetrically in the epithalamus, a dorsal outpocketing of the diencephalon (Liang et al., 2000; Concha et al., 2000). The major components of the zebrafish epithalamus are the pineal organ, the parapineal organ, and the habenular nuclei (Wulliman, 1996). The pineal organ is a midline structure, but the parapineal organ is located asymmetrically to the left of the midline (Concha et al., 2000). The habenuli are paired nuclei on the left and right sides of the epithalamus that are connected to each other by a midline-crossing commissure. The habenular nucleus on the left side of the epithalamus extends notably more elaborate processes than the right habenular nucleus

(Concha et al., 2000). In Nodal signaling mutants the location of the parapineal and the more elaborate habenular nucleus is randomized, indicating that at least some brain asymmetries make use of the same left/right axis determination mechanism as the rest of the body.

The *C. elegans* nervous system is also roughly symmetric, but several cellular asymmetries are apparent. Presumably these asymmetries make use of the same system that determines left/right asymmetry of the gonad and intestine. Most obviously, some cells, such as the head neuron RIS, have no homolog on the contralateral side (White, 1986). Another example of developmental asymmetry in the nervous system is provided by the Q neuroblasts, which begin as equivalent left/right pairs at the same A/P location, but then migrate in opposite directions and give rise to different neurons (e.g. Harris et al., 1996a). The *C. elegans* ventral nerve cord, which consists of left and right tracts, provides an example of morphological asymmetry; the right tract consists of substantially more axons than the left tract.

A more subtle invariant left/right asymmetry occurs in the ASE chemosensory neurons. Although the left and right homologs of the ASE pair occupy the same AP position, exhibit the same axon and dendrite morphologies, and are specialized to sense water-soluble chemoattractants, the two cells are molecularly and functionally distinct. A genomic scan of guanylyl cyclase expression patterns found that two cyclases, *gcy-6* and *gcy-7*, are expressed exclusively in the left ASE neuron, whereas *gcy-5* is expressed

exclusively in the right ASE (Yu et al., 1997). The LIM homeobox gene *lim-6* is also expressed asymmetrically in ASEL and prevents symmetric *gcy-5* expression (Hobert et al., 1999). Guanylyl cyclases play important roles in sensory signal transduction, suggesting that the molecular asymmetry represented by their expression patterns may underlie functional asymmetry. Indeed, ASEL and ASER mediate chemotaxis towards different chemicals (Pierce-Shimomura et al., 2001).

Stochastic left/right asymmetries in the nervous system

In addition to the invariant brain asymmetries described above, a few instances of left/right asymmetries with randomized laterality have been described in invertebrates. Unlike the morphogenetic asymmetries that require polar organ development, such as looping of the heart or gut, these asymmetries seem to rely on communication across the midline by relatively mature neurons.

The leech nerve cord is a generally symmetric structure, but certain neuropeptide-containing cells called RAS and CAS are located asymmetrically to the left or right of the midline. Neuropeptide-immunoreactive cells alternate on the left and right sides in each adjacent segment. Post-mitotic ablation of one of the left/right homologous neurons that give rise to the CAS and RAS cells forces expression of neuropeptides in the remaining cell, over-riding the A/P coordination of alternating segments (Martindale and Shankland,

1990). This result suggests that left and right homologs compete through a lateral signaling interaction for the neuropeptide-immunoreactive cell fate.

Lobster claws provide another fascinating example of stochastic left/right asymmetry in the nervous system (reviewed in Govind, 1992). Adult lobsters almost always possess two morphologically distinct claws: a large crusher claw and a smaller cutter claw. Each claw type is located on the left and right sides with equal frequency. If a lobster is raised in the laboratory in the absence of tactile substrates during a specific stage of larval development, it develops two cutter claws, suggesting that development of the crusher claw requires neuronal activity. If one claw of these tactilely-deprived lobsters is exercised with a paint brush for just three minutes a day, it always develops into the crusher claw. However, if both claws are exercised equally, both claws develop into cutters. This demonstrates that it is not activity *per se* that is required for lobster claw development, but rather a difference in the activity of the two developing claws. This difference presumably arises stochastically during normal development, resulting in the stochastic laterality of the claws. The observation that the event specifying the fate of the two claws is determined by activity suggests that lateral signaling occurs in fairly mature neurons equipped with neuronal signaling molecules. There is no obvious relationship between neuronal activity and the well-characterized Notch pathway, suggesting that a novel mechanism determines lobster claw asymmetry.

This thesis describes another stochastic left/right asymmetry that occurs in the nervous system of *C. elegans* (Chapters 3 and 4). Like the ASE neurons, the morphologically indistinguishable AWC olfactory neuron pair express a molecular marker asymmetrically. Half of a population of animals expresses the seven-transmembrane olfactory receptor *str-2* in the left AWC and half expresses it in the right AWC. As in the invariant ASE asymmetry, *str-2* asymmetry in AWC correlates with the ability of each cell to sense different chemicals (Wes and Bargmann, 2001). The lateral signaling interaction that mediates AWC asymmetry seems to require normal axon pathfinding (Chapter 3). Thus, like the leech and lobster interactions, AWC lateral signaling interactions probably occur in functional post-mitotic neurons, after axon outgrowth. The AWC interaction does not seem to involve classical Notch signaling molecules, but does require a calcium channel and a calcium-dependent kinase to execute the lateral signaling decision (Chapter 3). These molecules are typically associated with neuronal function, and this is the first evidence that they affect cell fates.

A relationship between invariant and stochastic left/right asymmetries?

Capdevila et al. (2000) propose that the handedness manifest in the vertebrate body cavity evolved only after individual organ asymmetries. According to this hypothesis, asymmetric morphogenesis of individual organs arose before handedness, resulting in randomized laterality. Later in evolution, the Nodal-dependant pathway for

generating invariant left/right asymmetry was super-imposed on individual organ asymmetries, establishing the globally coordinated handedness of the modern vertebrate body plan. This model makes the prediction that asymmetry and handedness should be genetically separable.

Asymmetry and laterality were separated in this way in studies of the asymmetric migration of ventral epidermal blast cells in *C. elegans* called Pn cells (Delattre and Felix, 2001). At hatching, the 12 Pn cells exist as left/right pairs aligned along the A/P axis. During the L1 larval stage, the two cells of a pair rotate around each other, so that one ends up more anterior than the other. For the most posterior pair of Pn cells, designated P11 and P12, the handedness of rotation is highly biased: the left cell becomes the anterior cell in approximately 85% of animals. When the neighboring Y cell was ablated, P11/P12 migration was randomized, suggesting that a signal from the Y cell biases the outcome of an otherwise random morphogenetic process. The polarity of the P11/P12 migration is reversed in some other nematode species, providing support for the hypothesis that bias was superimposed on a randomized pattern during evolution. Moreover, four of the other five pairs of Pn cells in *C. elegans* exhibit no bias, suggesting that random migration evolved first, and that biasing of the P11/P12 migration is a more recent phenomenon.

Although Capdevila et al.'s proposal that asymmetry precedes invariant laterality was formulated specifically to explain the laterality of morphogenetic asymmetries, such

as the looping of the heart, an analogous process may have occurred with asymmetries generated through lateral communication across the midline. In other words, some invariant asymmetries, particularly in the nervous system, may have begun as stochastic asymmetries generated through a lateral signaling process between cells on opposite sides of the midline, similar to the generation of asymmetry in the AWC neurons. For example, the invariant left/right asymmetry of the ASE sensory neurons in *C. elegans* could have arisen as a stochastic asymmetry that employed the same lateral signaling mechanism as AWC, and was only later biased by signals from the left/right axis.

This two-step mechanism is also a plausible explanation for parapineal asymmetry in the zebrafish diencephalon. In the absence of the Nodal signals that determine left/right asymmetry, the parapineal organ remains asymmetric, but displays randomized laterality (Concha et al., 2000). In other words, in half of zebrafish embryos defective for Nodal signaling the parapineal is located to the left side of the midline, and in the other half it is located to the right. It remains to be determined whether the random asymmetry of the parapineal unmasked by removing Nodal signaling is a result of a stochastic morphogenetic event (e.g. migration of the organ from the midline to one side or the other), or a lateral signaling mechanism mediated by communication across the midline.

The best characterized signaling pathway mediating lateral signaling involves Delta family ligands and Notch family receptors (reviewed in Kimble and Simpson,

1997). Although Notch signaling has the potential to be unbiased, molecular biasing systems sometimes impose an invariant outcome. For example, a Delta ligand can be asymmetrically expressed, or an asymmetric cell division can bias the outcome. In the *Drosophila* nervous system the protein Numb, which is asymmetrically segregated into certain cells by an intrinsic mechanism, interferes with Notch signaling by binding to the intracellular domain of the Notch receptor. This interaction negatively regulates the Notch receptor and biases signaling between the two cells, causing an invariant outcome (Guo et al., 1996; Spana and Doe, 1996). Fringe family proteins appear to bias and modulate Notch signaling at limb compartment borders in flies and vertebrates (Panin et al., 1997; Laufer et al., 1997). Fringe proteins encode glycosyltransferases that modify the Notch receptor in the golgi by elongating *O*-linked glycosylations, altering the receptor's response to Delta ligands (Moloney et al., 2000). Numb and Fringe provide examples of the types of molecular interactions that could have evolved to convert stochastic asymmetries mediated by lateral signaling into invariant ones.

There are so far no proven examples of stochastic left/right asymmetries mediated by lateral interactions across the midline that have been made invariant by the superimposition of biasing mechanisms. Proving this hypothesis will require the genetic separation of asymmetry and handedness. This separation would also serve as the first step in dissecting the molecular nature of the lateral signals and biasing mechanisms.

References

Bagowski, C. P., Ferrell, J. E., Jr. (2001). Bistability of the JNK cascade. *Current Biology* 11, 1176-1182.

Bargmann, C. I., Hartwig, E., and Horvitz, H. R. (1993). Odorant-selective genes and neurons mediate olfaction in *C. elegans*. *Cell* 74, 515-527.

Bargmann, C. I., and Horvitz, H. R. (1991). Chemosensory neurons with overlapping functions direct chemotaxis to multiple chemicals in *C. elegans*. *Neuron* 7, 729-742.

Bergmann, D. C., Crew, J. R., Kramer, J. M., and Wood, W. B. (1998). Cuticle chirality and body handedness in *Caenorhabditis elegans*. *Dev Genet* 23, 164-174.

Bray, S. (1998). Notch signalling in *Drosophila*: three ways to use a pathway. *Semin Cell Dev Biol* 9, 591-597.

Buck, L., and Axel, R. (1991). A novel multigene family may encode odorant receptors: a molecular basis for odor recognition. *Cell* 65, 175-187.

Capdevila, J., Vogan, K. J., Tabin, C. J., and Izpisua Belmonte, J. C. (2000). Mechanisms of left-right determination in vertebrates. *Cell* 101, 9-21.

Chess, A., Simon, I., Cedar, H., and Axel, R. (1994). Allelic inactivation regulates olfactory receptor gene expression. *Cell* 78, 823-834.

Clyne, P. J., Certel, S. J., de Bruyne, M., Zaslavsky, L., Johnson, W. A., and Carlson, J. R. (1999a). The odor specificities of a subset of olfactory receptor neurons are governed by Acj6, a POU-domain transcription factor. *Neuron* 22, 339-347.

Clyne, P. J., Warr, C. G., Freeman, M. R., Lessing, D., Kim, J., and Carlson, J. R. (1999b). A novel family of divergent seven-transmembrane proteins: candidate odorant receptors in *Drosophila*. *Neuron* 22, 327-338.

Concha, M. L., Burdine, R. D., Russell, C., Schier, A. F., and Wilson, S. W. (2000). A nodal signaling pathway regulates the laterality of neuroanatomical asymmetries in the zebrafish forebrain. *Neuron* 28, 399-409.

Delattre, M., and Felix, M. A. (2001). Development and evolution of a variable left-right asymmetry in nematodes: the handedness of P11/P12 migration. *Dev Biol* 232, 362-371.

Doe, C. Q., and Bowerman, B. (2001). Asymmetric cell division: fly neuroblast meets worm zygote. *Curr Opin Cell Biol* 13, 68-75.

Dwyer, N. D., Troemel, E. R., Sengupta, P., and Bargmann, C. I. (1998). Odorant receptor localization to olfactory cilia is mediated by ODR-4, a novel membrane-associated protein. *Cell* 93, 455-466.

Ebrahimi, F. A., and Chess, A. (2000). Olfactory neurons are interdependent in maintaining axonal projections. *Curr Biol* 10, 219-222.

Edlund, T., and Jessell, T. M. (1999). Progression from extrinsic to intrinsic signaling in cell fate specification: a view from the nervous system. *Cell* 96, 211-224.

Felix, M.-A., Sternberg, P., De Ley, P. (1996). Sinistral nematode population. *Nature* 381, 122.

Ferrell, J. E., Jr. (1996). Tripping the switch fantastic: how a protein kinase cascade can convert graded inputs into switch-like outputs. *Trends Biochem Sci* 21, 460-466.

Ferrell, J. E., Jr., and Machleder, E. M. (1998). The biochemical basis of an all-or-none cell fate switch in *Xenopus* oocytes. *Science* 280, 895-898.

Gao, Q., and Chess, A. (1999). Identification of candidate *Drosophila* olfactory receptors from genomic DNA sequence. *Genomics* 60, 31-39.

Gao, Q., Yuan, B., and Chess, A. (2000). Convergent projections of *Drosophila* olfactory neurons to specific glomeruli in the antennal lobe. *Nat Neurosci* 3, 780-785.

Garrington, T. P., and Johnson, G. L. (1999). Organization and regulation of mitogen-activated protein kinase signaling pathways. *Curr Opin Cell Biol* 11, 211-218.

Geschwind, N., and Levitsky, W. (1968). Human brain: left-right asymmetries in temporal speech region. *Science* 161, 186-187.

Govind, C. K. (1992). Claw asymmetry in lobsters: case study in developmental neuroethology. *J Neurobiol* 23, 1423-1445.

Greenwald, I. S., Sternberg, P. W., and Horvitz, H. R. (1983). The *lin-12* locus specifies cell fates in *Caenorhabditis elegans*. *Cell* 34, 435-444.

Guenther, C., and Garriga, G. (1996). Asymmetric distribution of the *C. elegans* HAM-1 protein in neuroblasts enables daughter cells to adopt distinct fates. *Development* 122, 3509-3518.

Guo, M., Jan, L. Y., and Jan, Y. N. (1996). Control of daughter cell fates during asymmetric division: interaction of Numb and Notch. *Neuron* 17, 27-41.

Guo, S., and Kemphues, K. J. (1996). Molecular genetics of asymmetric cleavage in the early *Caenorhabditis elegans* embryo. *Curr Opin Genet Dev* 6, 408-415.

Harris, J., Honigberg, L., Robinson, N., and Kenyon, C. (1996a). Neuronal cell migration in *C. elegans*: regulation of Hox gene expression and cell position. *Development* 122, 3117-3131.

Harris, J. A., Guglielmotti, V., and Bentivoglio, M. (1996b). Diencephalic asymmetries. *Neurosci Biobehav Rev* 20, 637-643.

Hobert, O., Tessmar, K., and Ruvkun, G. (1999). The *Caenorhabditis elegans* *lim-6* LIM homeobox gene regulates neurite outgrowth and function of particular GABAergic neurons. *Development* 126, 1547-1562.

Isaac, A., Sargent, M. G., and Cooke, J. (1997). Control of vertebrate left-right asymmetry by a *snail*-related zinc finger gene. *Science* 275, 1301-1304.

Kennedy, D. N., O'Craven, K. M., Ticho, B. S., Goldstein, A. M., Makris, N., and Henson, J. W. (1999). Structural and functional brain asymmetries in *human situs inversus totalis*. *Neurology* 53, 1260-1265.

Kimble, J. (1981). Alterations in cell lineage following laser ablation of cells in the somatic gonad of *Caenorhabditis elegans*. *Dev Biol* 87, 286-300.

Kimble, J., and Simpson, P. (1997). The LIN-12/Notch signaling pathway and its regulation. *Annu Rev Cell Dev Biol* 13, 333-361.

Laufer, E., Dahn, R., Orozco, O. E., Yeo, C. Y., Pisenti, J., Henrique, D., Abbott, U. K., Fallon, J. F., and Tabin, C. (1997). Expression of Radical fringe in limb-bud ectoderm regulates apical ectodermal ridge formation. *Nature* 386, 366-373.

Levin, M., Johnson, R. L., Stern, C. D., Kuehn, M., and Tabin, C. (1995). A molecular pathway determining left-right asymmetry in chick embryogenesis. *Cell* 82, 803-814.

Levin, M., and Mercola, M. (1998). Gap junctions are involved in the early generation of left-right asymmetry. *Dev Biol* 203, 90-105.

Levin, M., and Mercola, M. (1999). Gap junction-mediated transfer of left-right patterning signals in the early chick blastoderm is upstream of Shh asymmetry in the node. *Development* 126, 4703-4714.

- Liang, J. O., Etheridge, A., Hantsoo, L., Rubinstein, A. L., Nowak, S. J., Izpisua Belmonte, J. C., and Halpern, M. E. (2000). Asymmetric nodal signaling in the zebrafish diencephalon positions the pineal organ. *Development* 127, 5101-5112.
- Logan, M., Pagan-Westphal, S. M., Smith, D. M., Paganessi, L., and Tabin, C. J. (1998). The transcription factor Pitx2 mediates situs-specific morphogenesis in response to left-right asymmetric signals. *Cell* 94, 307-317.
- Malnic, B., Hirono, J., Sato, T., and Buck, L. B. (1999). Combinatorial receptor codes for odors. *Cell* 96, 713-723.
- Martindale, M. Q., and Shankland, M. (1990). Neuronal competition determines the spatial pattern of neuropeptide expression by identified neurons of the leech. *Dev Biol* 139, 210-226.
- Moloney, D. J., Panin, V. M., Johnston, S. H., Chen, J., Shao, L., Wilson, R., Wang, Y., Stanley, P., Irvine, K. D., Haltiwanger, R. S., and Vogt, T. F. (2000). Fringe is a glycosyltransferase that modifies Notch. *Nature* 406, 369-375.
- Mombaerts, P., Wang, F., Dulac, C., Chao, S. K., Nemes, A., Mendelsohn, M., Edmondson, J., and Axel, R. (1996). Visualizing an olfactory sensory map. *Cell* 87, 675-686.
- Nonaka, S., Tanaka, Y., Okada, Y., Takeda, S., Harada, A., Kanai, Y., Kido, M., and Hirokawa, N. (1998). Randomization of left-right asymmetry due to loss of nodal cilia

generating leftward flow of extraembryonic fluid in mice lacking KIF3B motor protein. *Cell* 95, 829-837.

Okada, Y., Nonaka, S., Tanaka, Y., Saijoh, Y., Hamada, H., and Hirokawa, N. (1999). Abnormal nodal flow precedes *situs inversus* in *iv* and *inv* mice. *Mol Cell* 4, 459-468.

Panin, V. M., Papayannopoulos, V., Wilson, R., and Irvine, K. D. (1997). Fringe modulates Notch-ligand interactions. *Nature* 387, 908-912.

Pierce-Shimomura, J. T., Faumont, S., Gaston, M. R., Pearson, B. J., and Lockery, S. R. (2001). The homeobox gene *lim-6* is required for distinct chemosensory representations in *C. elegans*. *Nature* 410, 694-698.

Piotrowska, K., and Zernicka-Goetz, M. (2001). Role for sperm in spatial patterning of the early mouse embryo. *Nature* 409, 517-521.

Ressler, K. J., Sullivan, S. L., and Buck, L. B. (1993). A zonal organization of odorant receptor gene expression in the olfactory epithelium. *Cell* 73, 597-609.

Ressler, K. J., Sullivan, S. L., and Buck, L. B. (1994). Information coding in the olfactory system: evidence for a stereotyped and highly organized epitope map in the olfactory bulb. *Cell* 79, 1245-1255.

Roayaie, K., Crump, J. G., Sagasti, A., and Bargmann, C. I. (1998). The G alpha protein ODR-3 mediates olfactory and nociceptive function and controls cilium morphogenesis in *C. elegans* olfactory neurons. *Neuron* 20, 55-67.

Scott, K., Brady, R., Jr., Cravchik, A., Morozov, P., Rzhetsky, A., Zuker, C., and Axel, R. (2001). A chemosensory gene family encoding candidate gustatory and olfactory receptors in *Drosophila*. *Cell* 104, 661-673.

Sengupta, P., Chou, J. H., and Bargmann, C. I. (1996). *odr-10* encodes a seven transmembrane domain olfactory receptor required for responses to the odorant diacetyl. *Cell* 84, 899-909.

Sengupta, P., Colbert, H. A., and Bargmann, C. I. (1994). The *C. elegans* gene *odr-7* encodes an olfactory-specific member of the nuclear receptor superfamily. *Cell* 79, 971-980.

Seydoux, G., and Greenwald, I. (1989). Cell autonomy of *lin-12* function in a cell fate decision in *C. elegans*. *Cell* 57, 1237-1245.

Spana, E. P., and Doe, C. Q. (1996). Numb antagonizes Notch signaling to specify sibling neuron cell fates. *Neuron* 17, 21-26.

Stortkuhl, K. F., and Kettler, R. (2001). From the Cover: Functional analysis of an olfactory receptor in *Drosophila melanogaster*. *Proc Natl Acad Sci U S A* 98, 9381-9385.

Supp, D. M., Witte, D. P., Potter, S. S., and Brueckner, M. (1997). Mutation of an axonemal dynein affects left-right asymmetry in *inversus viscerum* mice. *Nature* 389, 963-966.

Troemel, E. R., Chou, J. H., Dwyer, N. D., Colbert, H. A., and Bargmann, C. I. (1995). Divergent seven transmembrane receptors are candidate chemosensory receptors in *C. elegans*. *Cell* 83, 207-218.

Troemel, E. R., Kimmel, B. E., and Bargmann, C. I. (1997). Reprogramming chemotaxis responses: sensory neurons define olfactory preferences in *C. elegans*. *Cell* 91, 161-169.

Vassar, R., Chao, S. K., Sitcheran, R., Nunez, J. M., Vosshall, L. B., and Axel, R. (1994). Topographic organization of sensory projections to the olfactory bulb. *Cell* 79, 981-991.

Vassar, R., Ngai, J., and Axel, R. (1993). Spatial segregation of odorant receptor expression in the mammalian olfactory epithelium. *Cell* 74, 309-318.

Vosshall, L. B., Amrein, H., Morozov, P. S., Rzhetsky, A., and Axel, R. (1999). A spatial map of olfactory receptor expression in the *Drosophila* antenna. *Cell* 96, 725-736.

Vosshall, L. B., Wong, A. M., and Axel, R. (2000). An olfactory sensory map in the fly brain. *Cell* 102, 147-159.

Wang, F., Nemes, A., Mendelsohn, M., and Axel, R. (1998). Odorant receptors govern the formation of a precise topographic map. *Cell* 93, 47-60.

Ward, S., Thomson, N., White, J. G., and Brenner, S. (1975). Electron microscopical reconstruction of the anterior sensory anatomy of the nematode *Caenorhabditis elegans*. *J Comp Neurol* 160, 313-337.

Wes, P. D., and Bargmann, C. I. (2001). *C. elegans* odour discrimination requires asymmetric diversity in olfactory neurons. *Nature* 410, 698-701.

Wetzel, C. H., Behrendt, H. J., Gisselmann, G., Stortkuhl, K. F., Hovemann, B., and Hatt, H. (2001). From the Cover: Functional expression and characterization of a *Drosophila* odorant receptor in a heterologous cell system. *Proc Natl Acad Sci U S A* 98, 9377-9380.

White, J. G., Southgate, E., Thomson, J. N., Brenner, S. (1986). The structure of the nervous system of the nematode *Caenorhaditis elegans*. *Phil Trans R Soc Lond B* 314, 1-340.

Wilkinson, H. A., Fitzgerald, K., and Greenwald, I. (1994). Reciprocal changes in expression of the receptor *lin-12* and its ligand *lag-2* prior to commitment in a *C. elegans* cell fate decision. *Cell* 79, 1187-1198.

Wood, W. B. (1991). Evidence from reversal of handedness in *C. elegans* embryos for early cell interactions determining cell fates. *Nature* 349, 536-538.

Wood, W. B., Bergmann, D., and Florance, A. (1996). Maternal effect of low temperature on handedness determination in *C. elegans* embryos. *Dev Genet* 19, 222-230.

Wulliman, M. F., Rupp, B., and Reichert, H. (1996). Neuroanatomy of the Zebrafish Brain: A Topological Atlas (Basel, Birkhauser Verlag).

Yu, S., Avery, L., Baude, E., and Garbers, D. L. (1997). Guanylyl cyclase expression in specific sensory neurons: a new family of chemosensory receptors. *Proc Natl Acad Sci U S A* 94, 3384-3387.

Chapter 2

Alternative olfactory fates are specified by the LIM homeobox gene *lim-4*

(Published in Genes and Development, July 15, 1999, 13: 1794-1806)

Alternative olfactory neuron fates are specified by the LIM homeobox gene *lim-4*

Alvaro Sagasti,¹ Oliver Hobert,^{2,3} Emily R. Troemel,¹ Gary Ruvkun,² and Cornelia I. Bargmann^{1,4}

¹Howard Hughes Medical Institute, Department of Anatomy and Department of Biochemistry and Biophysics, University of California, San Francisco, California 94143-0452 USA, ²Department of Molecular Biology, Massachusetts General Hospital, Boston, Massachusetts 02114 USA

The *Caenorhabditis elegans* AWA, AWB, and AWC olfactory neurons are each required for the recognition of a specific subset of volatile odorants. *lim-4* mutants express an AWC reporter gene inappropriately in the AWB olfactory neurons and fail to express an AWB reporter gene. The AWB cells are morphologically transformed toward an AWC fate in *lim-4* mutants, adopting cilia and axon morphologies characteristic of AWC. AWB function is also transformed in these mutants: Rather than mediating the repulsive behavioral responses appropriate for AWB, the AWB neurons mediate attractive responses, like AWC. *LIM-4* is a predicted LIM homeobox gene that is expressed in AWB and a few other head neurons. Ectopic expression of *LIM-4* in the AWC neuron pair is sufficient to force those cells to adopt an AWB fate. The AWA nuclear hormone receptor ODR-7 described previously also represses AWC genes, as well as inducing AWA genes. We propose that the *LIM-4* and ODR-7 transcription factors function to diversify *C. elegans* olfactory neuron identities, driving them from an AWC-like state into alternative fates.

[Key Words: Olfactory neuron; cell fate specification; LIM homeobox gene; *C. elegans*]

Received May 12, 1999; revised version accepted June 4, 1999.

Olfactory neurons in worms, flies, and mice fall into a few structural classes, defined by characteristic cilia and axon morphologies. At a finer level, however, the diversity of signaling molecules, and especially of olfactory receptors, divides the olfactory neurons into many functionally distinct subtypes (for review, see Buck 1996). In the nematode *Caenorhabditis elegans*, the olfactory neurons reside in the amphids, a bilateral pair of sensory organs in the head of the animal that contain twelve sensory neurons each (White et al. 1986). The amphid sensory neurons extend dendrites to the tip of the nose, where specialized ciliated endings interact with the animal's environment and send their axons into the nerve ring, a major neuropil in which synaptic connections are made. Each bilateral pair of amphid neurons has a particular function in the sensation of pheromones, temperature, mechanical stimulation, soluble chemicals, or volatile chemicals. Three pairs of neurons—AWA, AWB, and AWC—are required for olfaction, the detection of volatile odorants. The AWA and AWC neurons are required for chemotaxis toward distinct subsets of attractive odorants (Bargmann et al. 1993), whereas the AWB

neurons are required for a repulsive behavioral response to at least one odorant (Troemel et al. 1997). Despite their shared olfactory function, the AWA, AWB, and AWC neurons are not closely related by cell lineage.

The AWA, AWB, and AWC olfactory neurons express overlapping but distinct sets of signal-transduction molecules that contribute to each cell's unique identity. Chemotaxis to AWA-sensed odorants requires the G protein α subunit ODR-3 (Roayaie et al. 1998) and the predicted cation channel subunit OSM-9 (Colbert et al. 1997), which is related to TRP channels and the VR1 capsaicin receptor. Responses to AWC- and AWB-sensed odorants require ODR-3 and the TAX-2/TAX-4 cGMP-gated ion channel (Coburn and Bargmann 1996; Komatsu et al. 1996). *C. elegans* has a large number of seven transmembrane domain proteins expressed in sensory neurons that may function as chemoreceptors (Troemel et al. 1995). One of these genes, *odr-10*, has been shown to function in AWA as a receptor for the volatile odorant diacetyl (Sengupta et al. 1996; Zhang et al. 1997). Two additional *odr-10*-like genes have upstream promoter sequences that direct expression of GFP to other olfactory neurons, suggesting that they also encode olfactory receptors. The *str-1* gene is expressed in the AWB neuron pair, whereas the *str-2* gene is expressed asymmetrically in one of the two AWC olfactory neurons (Troemel et al. 1997; E.R. Troemel and C.I. Bargmann, in prep.). These

³Present address: Department of Biochemistry and Molecular Biophysics, Columbia University, College of Physicians and Surgeons, New York, New York 10032 USA.

⁴Corresponding author.

E-MAIL cori@itsa.ucsf.edu; FAX (415) 476-3493.

putative receptors are useful both for investigating cell function and as markers of cell fate.

Little is known in any organism about how the specific identities of olfactory neurons are determined. Only two genes that participate in this process, *odr-7* in *C. elegans* and *acj6* in *Drosophila*, have been identified. The *odr-7* nuclear hormone receptor has been implicated in the specification of AWA olfactory neuron identity in *C. elegans* (Sengupta et al. 1994). ODR-7 is expressed exclusively in the AWA neurons, is required for their function, and is required for full expression of the AWA-specific ODR-10 receptor (Sengupta et al. 1996). It therefore acts to promote the unique differentiated features of the AWA neuron. A similar function in *Drosophila* olfactory neurons may be provided by the *acj6* POU homeobox gene (Clyne et al. 1999a,b). In *acj6* mutants, some behavioral responses to odorants are lost, the electrophysiological responses of certain olfactory cells are altered, and the expression of several putative olfactory receptors is abolished.

Sensory neuron specification in *C. elegans* has been studied best in the mechanosensory system. A battery of transcription factors acts combinatorially to ensure that six neurons develop as touch receptor neurons (Mitani et al. 1993). At the core of this mechanosensory transcriptional program is the *mec-3* gene, which is required for the neurons to exhibit the final differentiated features of touch receptors. *mec-3* belongs to the LIM homeobox class of transcription factors (Way and Chalfie 1988; Freyd et al. 1990). These genes contain two metal-binding domains used for protein-protein interactions (LIM domains) and a DNA-binding homeodomain. Seven genes of this class have been found in the *C. elegans* genome and four of these now correspond to genetically defined mutants (Way and Chalfie 1988; Freyd et al. 1990; Hobert et al. 1997, 1999). All LIM homeobox genes are first expressed in post-mitotic neurons and are required for late aspects of neuron cell fate, such as axon pathfinding and neurotransmitter expression. Cells with mutant LIM homeobox genes therefore usually exhibit phenotypes that mimic loss of certain cell types. For example, the *ttx-3* and *lin-11* genes are required for the function of interneurons that act in different parts of the thermosensory circuit (Hobert et al. 1997, 1998b). Mutations in these genes result in phenotypes that resemble ablation of those interneurons (Mori and Ohshima 1995). Studies of LIM homeobox gene function in vertebrates and *Drosophila* have also implicated these genes in controlling various late aspects of cell fates. For instance, two vertebrate LIM homeobox genes, *lhx3* and *lhx4*, as well as their *Drosophila* homolog, *lim3*, are required to maintain proper axon trajectories in a subset of motor neurons and to repress improper axon trajectories characteristic of different motor neuron classes (Sharma et al. 1998; Thor et al. 1999).

To investigate how the unique features of olfactory neurons are determined, we performed a screen for altered expression of *str-2::GFP*, a reporter gene normally expressed in one of the two AWC olfactory neurons. Mutations in a LIM homeobox gene, *lim-4*, were found to

cause ectopic expression of *str-2::GFP* in the AWB neurons. Molecular, morphological, and functional analyses indicate that in this mutant, AWB neurons are strongly transformed into AWC neurons. Moreover, expression of LIM-4 in AWC is sufficient to force AWC neurons to adopt an AWB fate. LIM-4 thus acts as a molecular switch that distinguishes between alternative sensory neuron fates. We suggest that the LIM-4 and ODR-7 transcription factors function to drive neurons in the *C. elegans* amphid from an AWC-like fate into alternative olfactory neuron fates.

Results

The LIM homeobox gene lim-4 affects olfactory receptor expression, movement, and foraging behavior

A 4-kb region upstream of the putative seven transmembrane domain olfactory receptor STR-2 directs expression of GFP to a single AWC olfactory neuron (E.R. Troemel and C.I. Bargmann, in prep.). To study the mechanisms by which AWC cell fate is confined to a single neuron, we isolated mutant animals with altered expression of the *str-2::GFP* transgene (see Materials and Methods). Three mutants recovered from the screen expressed GFP in both AWB olfactory neurons as well as the normal AWC neuron (Fig. 1A,B). Conversely, expression of the AWB-specific marker gene *str-1::GFP* was severely reduced in these mutants (Fig. 1D,E). GFP markers for six other amphid sensory neuron cell types (ADLL/R, ADFL/R, ASER, ASEL, ASIL/R, and AWAL/R) were expressed normally, indicating that the mutants have a selective defect in sensory gene expression.

The three mutants failed to complement each other and formed an allelic series of increasingly defective *str-2::GFP* expression (Table 1). In the weaker mutant (*ky395*), a substantial fraction of animals expressed *str-2::GFP* in only one AWB neuron, whereas in the more severe mutants, most animals expressed GFP in both AWB neurons. When only one AWB neuron expressed *str-2::GFP*, the GFP-expressing AWB neuron was sometimes on the same side as the GFP-expressing AWC neuron and sometimes on the opposite side. All three alleles were slightly semidominant for their *str-2::GFP* misexpression phenotype and were more severe in hermaphrodites than males (data not shown). The mutants also moved in a coily manner (Fig. 3E-F, below), and exhibited defects in foraging behavior, as manifested by aberrant head movements (McIntire et al. 1993).

The most severe allele in this complementation group (*ky403*) was mapped to a small region on the left arm of the X chromosome. Rescue of the *str-2::GFP* expression phenotype was obtained with a cosmid containing the LIM homeobox gene *lim-4* (Fig. 2), and the coily movement phenotype was rescued with a LIM-4 transgene tagged at its 3' end with GFP (Fig. 3E-G). To confirm the identification of *lim-4*, the coding region was sequenced in the *lim-4* mutants and mutations were found in all three alleles (Fig. 2). The weakest allele, *lim-4(ky395)*, was associated with a missense mutation in a well-con-

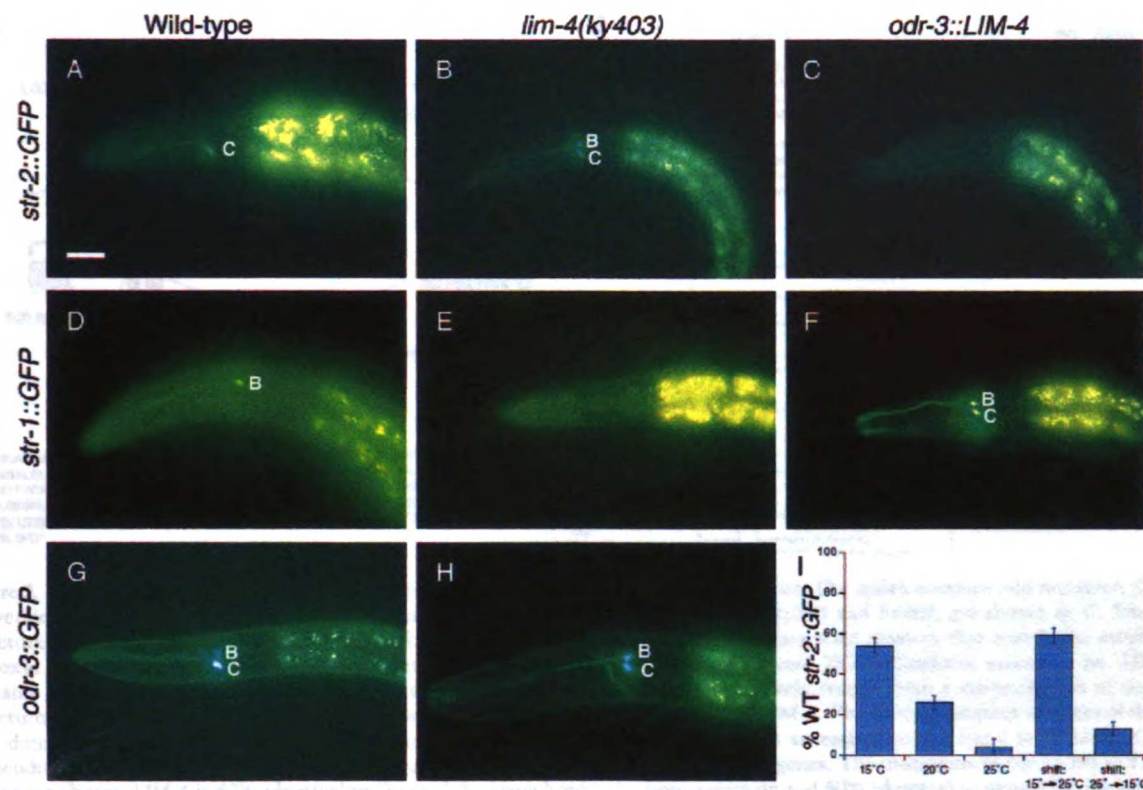


Figure 1. LIM-4 controls expression of putative receptor and signaling genes and is required early to repress *str-2::GFP* expression. (A) *str-2::GFP* is expressed in a single AWC neuron in wild-type animals. (B) *lim-4* mutants express *str-2::GFP* in AWC and AWB. (C) Transgenic animals carrying the *odr-3::LIM-4* transgene do not express *str-2::GFP* in either cell. (D) *str-1::GFP* is expressed in the AWB neurons in wild-type animals. (E) In *lim-4* mutants, *str-1::GFP* expression is severely reduced. (F) Transgenic animals expressing *odr-3::LIM-4* express *str-1::GFP* in both AWC and AWB. (G) In wild-type animals, *odr-3::GFP* fluoresces more brightly in AWC than in AWB. (H) In *lim-4* mutants, the *odr-3::GFP* signal is equally bright in AWB and AWC. Quantitative analysis of these phenotypes is presented in Tables 1 and 2, except for *str-2::GFP* in an *odr-3::LIM-4* strain (no GFP expression in 84% of animals, $n = 80$). Anterior is left and dorsal is up in all panels. Scale bar, 40 μ m and applies to A–H. (I) LIM-4 is required early in development to repress *str-2::GFP* in AWB. The y axis indicates the percentage of animals that express *str-2::GFP* in its wild-type pattern, in a single AWC neuron. Animals grown at different temperatures have different penetrances for the *str-2::GFP* misexpression phenotype (first three columns). Animals were shifted from one temperature to another at the L1 larval stage and assayed as adults. Temperature-shifted animals exhibited the phenotype characteristic of the temperature they experienced during the embryonic and L1 stages (last two columns; shifts are indicated by arrows). Error bars, standard error of the proportion.

served homeodomain residue. *lim-4(ky402)* had a mutation in the splice acceptor site before the fifth exon, which contains portions of the second LIM domain and the beginning of the homeodomain. The most severe

lim-4 allele (*ky403*) had a stop codon within the DNA recognition helix of the homeodomain that would be predicted to disrupt the DNA-binding activity of the LIM-4 protein. All experiments were performed with the *ky403* allele unless otherwise noted.

lim-4 is most similar to the *Drosophila arrowhead* gene (Curtiss and Heilig 1997) and the vertebrate *L3/Lhx7* and *Lhx6* genes (Fig. 2C,D) (Matsumoto et al. 1996; Grigoriou et al. 1998). Although these genes were presumably derived from a common ancestor, their degree of identity to each other is lower than that observed within LIM homeodomain protein subclasses, suggesting a greater divergence of function. Both *arrowhead* and *L3* are expressed in subsets of neurons of the central nervous system (Matsumoto et al. 1996; Curtiss and Heilig 1997).

The weakest *lim-4* allele (*ky395*) was temperature sensitive for its *str-2::GFP* misexpression phenotype (Table

Table 1. *str-2::GFP* expression in *lim-4* mutant alleles

Strain	Percent <i>str-2::GFP</i> expression			No. ^a
	AWC	AWC + 1 AWB	AWC + 2 AWB	
Wild type, 20°C	100	0	0	>1000
<i>lim-4(ky403)</i> , 20°C	0	10	90	223
<i>lim-4(ky402)</i> , 20°C	4	15	81	209
<i>lim-4(ky395)</i> , 25°C	4	35	60	116
<i>lim-4(ky395)</i> , 20°C	30	43	27	241
<i>lim-4(ky395)</i> , 15°C	54	32	14	162

^aNo. of animals scored.

IC
TUM
RAF

IA UNIV
IA UNIV

BR
H

IA UNIV
IA UNIV

IC
Franc

BRAR

IA UNIV
IA UNIV

IRRA
m. f. m.

IC

IA UNIV
IA UNIV

IC
Franc

BRAR

IA UNIV
IA UNIV



[Faint, mostly illegible text, likely bleed-through from the reverse side of the page. The text is arranged in several columns and appears to be a dense block of writing.]

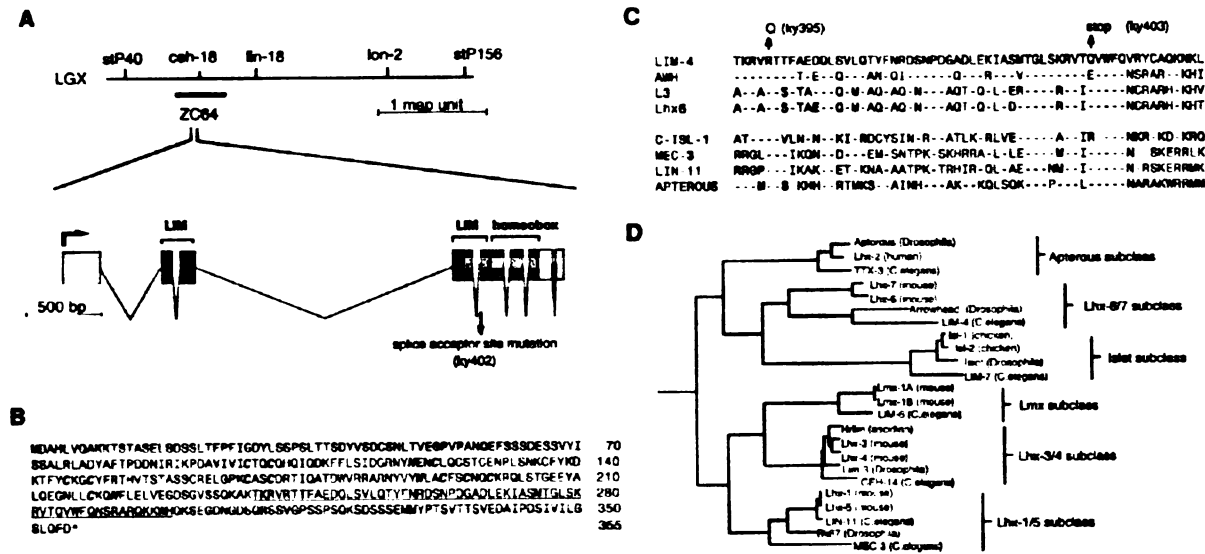


Figure 2. *lim-4* gene structure. (A) Genetic map and genomic structure of the *lim-4* locus. The splice acceptor site mutation (G to A conversion) in the *ky402* allele is shown. Mutations in the other two *lim-4* alleles, *ky395* and *ky403*, are shown in C. The gene structure was confirmed by isolating a cDNA by PCR from a mixed-stage cDNA library with primers that match the amino and carboxyl terminus of the predicted ZC64.4 gene. The predicted ZC64.4 gene on cosmid ZC64 [GenBank accession no. U39740] contains a 17-amino-acid insertion at amino acid position 289. This insertion most likely results from a misprediction of the gene structure, as we could not detect it in cDNAs that we isolated. (B) Protein sequence of LIM-4. The Zn-coordinating residues of the two LIM domains are in bold and italics. The homeobox is underlined. The GenBank accession no. for *lim-4* is U72348. (C) The homeodomain of LIM-4 aligned with the homeodomains of seven other LIM homeobox genes. The mutations in the *ky395* and *ky403* alleles are shown. LIM-4 is 67% identical to *Drosophila* Arrowhead in its homeodomain and 50% identical to mouse L3. Broken lines indicate amino acid identities. (D) Phylogenetic relationship of LIM homeodomain proteins. The analysis was performed with individual homeodomains, with the pileup, distances, and grow-tree algorithms of the GCG software package. Only a limited number of vertebrate representatives from each subgroup are shown.

1). The proportion of animals expressing *str-2::GFP* in its wild-type pattern in this allele ranged from 54% at 15°C to 4% at 25°C. However, the defect in *str-1::GFP* expression was not affected by temperature in the *lim-4(ky395)* allele (at 15°C, 66% of *ky395* animals had defective *str-1::GFP* expression, $n = 99$; and at 25°C, 69% of animals had defective expression, $n = 112$). At high temperature, there must therefore be some *lim-4(ky395)* animals in which the cells that normally develop into AWB express neither the AWB nor the AWC marker gene. We made use of the *lim-4(ky395)* allele's temperature sensitivity for the *str-2::GFP* expression phenotype to determine when during development LIM-4 performs this function. Animals carrying the *str-2::GFP* reporter were grown at 15°C or 25°C, shifted to the other temperature during the L1 larval stage, and scored for GFP expression as young adults, 2 or 3 days later. Temperature-shifted animals exhibited the phenotype characteristic of the temperature they experienced during the embryonic and L1 stages (Fig. 11). LIM-4 was therefore required in the AWB neurons for a discrete interval of early development to repress the AWC fate, and was not needed later in life to perform this function.

LIM-4 is expressed in head neurons and regulates its own expression in AWB

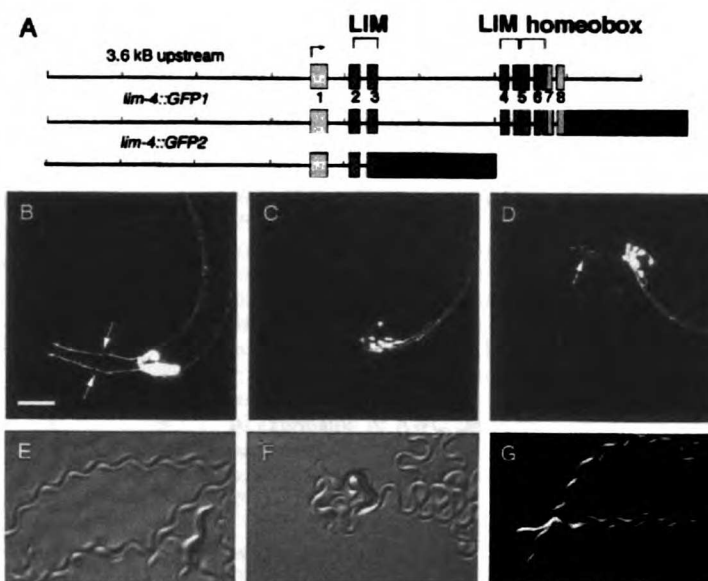
The expression pattern of LIM-4 was determined with

two GFP fusion genes, one that included 3.6 kb of upstream sequence, all exons and introns, and had GFP fused to the carboxyl terminus (*lim-4::GFP1*), and one fusion gene that truncated the protein after the third exon (*lim-4::GFP2*) (Fig. 3A). In larvae and adults, *lim-4::GFP1* expression was confined to neurons in the worm's anterior ganglia (Fig. 3B); embryonic expression was not examined in detail. Expression from both transgenes was observed in the AWB neurons but not in other sensory neurons. *lim-4::GFP1* was also expressed in one RMEV motor neuron, two RMD motor neurons (RMDL and RMDR), and the RID, RIV, SAA and SIA interneurons. *lim-4::GFP2* was expressed in the same neurons, except for RID and RMEV. Expression in the GABAergic RMEV motor neurons, which control head movement, is consistent with the mutants' foraging defect (McIntire et al. 1993). Because the functions of the interneurons and motor neurons expressing LIM-4 are poorly understood, lack of LIM-4 function in any of these cells could be responsible for the coily movement of *lim-4* mutants.

To ask whether LIM-4 regulates its own expression, the short *lim-4::GFP2* transgene was examined in the *lim-4(ky403)* mutant. In *lim-4* mutants, *lim-4::GFP2* expression was abolished in the AWB neurons (Fig. 3C,D), but unaffected in the other *lim-4::GFP2*-expressing cells. The *lim-4::GFP2* fusion gene also revealed defects in

10
11
12
13
14
15
16
17
18
19
20
21
22
23
24
25
26
27
28
29
30
31
32
33
34
35
36
37
38
39
40
41
42
43
44
45
46
47
48
49
50
51
52
53
54
55
56
57
58
59
60
61
62
63
64
65
66
67
68
69
70
71
72
73
74
75
76
77
78
79
80
81
82
83
84
85
86
87
88
89
90
91
92
93
94
95
96
97
98
99
100

Figure 3. *lim-4* is expressed in anterior neurons. (A) Two GFP fusion genes used to analyze LIM-4 expression. *lim-4::GFP1* is a fusion of GFP to the end of the last amino acid in LIM-4, *lim-4::GFP2* truncates the gene after the third exon. *lim-4::GFP2* was integrated into the genome to minimize mosaicism. (B) *lim-4::GFP2* expression in wild-type animals is confined to the anterior ganglia. *lim-4::GFP2* is expressed in the two AWB neurons, which send dendrites to the tip of the nose (arrows), two of six RMD neurons (RMDL and RMDR), the RIV neuron, four SAA neurons, and four SIA neurons. *lim-4::GFP1* is expressed in all the same cells as well as RMEV and RID (not shown). (C,D) In *lim-4* mutants, AWB expression is eliminated, as is most evident by the absence of sensory dendrites. Sometimes ectopic sprouting of anterior processes from the SAA axons is visible in *lim-4* mutants (D, arrow), these processes are normally unbranched. Anterior is left and dorsal is up in B–D. Scale bar, 20 μ m, applies to B–D. (E–G) The full-length *lim-4::GFP1* construct is capable of rescuing the *lim-4* movement defect. Wild-type animals move in a characteristic manner, leaving regular, shallow sinusoidal tracks (E). *lim-4* animals move in a coily manner, leaving exaggerated high amplitude tracks (F). This movement defect is rescued with a full-length *lim-4::GFP1* transgene (G). The adult worms shown are ~1 mm long.



neurite morphology in *lim-4* mutants. For example, the SAA neurons often sent thick sprouting processes into the head in place of their normal unbranched processes (Fig. 3D). Ectopic axon sprouting and misrouted axon trajectories are common defects in LIM homeobox mutants (Way and Chalfie 1988; Lundgren et al. 1995; Hobert et al. 1997, 1998b, 1999; Sharma et al. 1998).

The repulsive olfactory neuron AWB is transformed into the attractive olfactory neuron AWC in *lim-4* mutants

To determine the extent to which the AWB neurons were transformed towards the AWC cell fate, we characterized several aspects of AWB fate in the *lim-4(ky403)* mutant. As noted above, expression of the AWB-specific marker *str-1::GFP* was severely reduced or absent in the *lim-4(ky403)* mutant (Fig. 1D,E; Table 2). AWC and AWB neurons share most of their signal transduction components, but the ODR-3 G α protein is expressed at notably different levels in AWC and AWB. In wild-type animals, an *odr-3::GFP* reporter is expressed most intensely in AWC, more weakly in AWB, and very faintly in the AWA, ADF, and ASH neurons (Roayaie et al. 1998). In *lim-4* animals, however, *odr-3::GFP* expression was usually equally bright in AWB and AWC (Fig. 1G,H; Table 2).



The cilia and axons of the AWB and AWC sensory neurons are strikingly different (Fig. 4A). Cilia are specialized structures at the tips of sensory dendrites that encounter environmental stimuli. AWB cells have a

simple two-pronged cilium morphology reminiscent of a tuning fork, whereas AWC neurons have more elaborate, fan-like cilia. In *lim-4* mutants, the AWB neurons often have a fan-like cilium morphology, like AWC (Fig. 4B–D; Table 2). The other notable difference in the morphology of AWB and AWC neurons is their axon trajectory. The AWB neurons extend a U-shaped axon that terminates at the dorsal midline, in which it makes contact with its homolog from the contralateral side. The AWC neurons have a similar initial trajectory, but then extend past the dorsal midline to the contralateral side of the nerve ring, resulting in an S-shaped axon. In *lim-4* mutants, 30% of the AWB axons continue past the dorsal midline, forming an S shape like the AWC neurons (Fig. 4F,G; Table 2).

Another distinction between AWB and AWC cells is their abilities to take up certain fluorescent lipophilic dyes. It is not known what morphological or molecular aspects of the cells' identity determine this property. In wild-type animals soaked in DiD or DiO, six pairs of amphid neurons, including AWB but not AWC, take up the dye (Fig. 5A–C). In *lim-4* mutants, however, neither AWB nor AWC cells fill with dye, consistent with an AWB-to-AWC change in cell fate (Fig. 5D–F; Table 2).

The most profound physiological difference between the fates of AWB and AWC neurons is their function during behavior—the AWB neurons mediate repulsion from a subset of volatile odorants, whereas the AWC neurons mediate attraction to a different subset of odorants. These differences in neuron function may result from the distinct patterns of synaptic wiring characteristic of AWB and AWC (White et al. 1986). To ask whether the AWB neurons have changed their behavioral

Table 2. Cell fate transformations caused by mutations in *lim-4* and ectopic expression of *LIM-4*

Strain	Phenotype (%)			No.*
	<i>str-1::GFP^b</i>			
	no GFP	AWB	AWB + AWC	
Wild type	0	100	0	>1000
<i>lim-4(ky403)</i>	100	0	0	206
<i>odr-3::LIM-4^c</i>	0	5	95 ^d	93
	<i>odr-3::GFP^e</i>			
	AWB ≥ AWC		AWC > AWB	
	AWB	AWC		
Wild type	14	86	73	
<i>lim-4(ky403)</i>	97	3	79	
	cilia morphology ^f			
				
	AWB	AWC		
Wild type AWB	0	100	106	
Wild type AWC	98	2	96	
<i>lim-4(ky403)</i> AWB	85	15	68	
<i>odr-3::LIM-4</i> AWC	14	86	78	
	axon morphology ^g			
	both S-shape	AWB - U-shape AWC - S-shape	both U-shape	
	AWB	AWC		
Wild type	0	100	34	
<i>lim-4(ky403)</i>	30	70	33	
<i>odr-3::LIM-4</i>	6	60	32	
	dye filling ^h			
	no cells	AWB	AWB + AWC	
	AWB	AWC		
Wild type	6	94	81	
<i>lim-4(ky403)</i>	97	3	98	
<i>odr-3::LIM-4</i>	0	6	79	

*No. of animals scored for *str-1::GFP* and *odr-3::GFP* expression, and number of neurons scored for cilia, axons, and dye-filling.

^bGFP was scored as present if fluorescence was visible in the cell bodies and processes, dim GFP only in the cell body was considered "off."

^c*lim-4 str-1::GFP* with extrachromosomal *odr-3::LIM-4 rol-6*.

^d23% expressed GFP in one ectopic cell; 77% in two ectopic cells.

^eFor each animal, the relative intensities of GFP expression in the AWB and AWC neurons was compared. (AWB ≥ AWC) GFP expression in AWB was as intense or more intense than in AWC.

^f(Wild type) *str-1::GFP* and *str-2::GFP* were scored for AWB and AWC, respectively. (*lim-4*) *lim-4 str-2::GFP* was scored using animals in which only one neuron expressed *str-2::GFP*. (*odr-3::LIM-4*) *lim-4 lin-15* with extrachromosomal *odr-3::LIM-4 str-1::GFP lin-15*.

^gDetermined in mosaics with GFP expressed in two cells on one side. (Wild type) *str-2::GFP* with extrachromosomal *str-1::GFP rol-6* (*lim-4*) *lim-4 odr-10 lin-15* with extrachromosomal *str-2::GFP str-2::odr-10 lin-15* (The *odr-10* strain was used in this experiment simply because it was available and should not affect the results.) (*odr-3::LIM-4*) *lim-4 lin-15* with extrachromosomal *odr-3::LIM-4 str-1::GFP lin-15*.

^hDetermined by filling with DiD and comparing to GFP expression. (Wild type) *str-1::GFP str-2::GFP*. (*lim-4*) *lim-4 str-2::GFP*. (*odr-3::LIM-4*) *lim-4 lin-15* with extrachromosomal *odr-3::LIM-4 str-1::GFP lin-15*.

function in *lim-4* mutants, we expressed the ODR-10 diacetyl receptor in these cells. In wild-type animals, ODR-10 expressed in AWB under the *str-1* promoter mediates repulsion from diacetyl (Troemel et al. 1997; Fig. 6G). We used single animal behavioral assays to ask whether ODR-10 expression in AWB mediates attraction or repulsion in a *lim-4* mutant.

Despite their coily movement, *lim-4* animals were able to chemotax towards diacetyl with the endogenous *odr-10* gene expressed in AWA (Fig. 6A). The *odr-10(ky225)* null mutation abolished this attraction (Fig. 6B). Expression of ODR-10 in AWB in *lim-4 odr-10* double mutants was accomplished by placing ODR-10 under the control of the *str-2* promoter. In wild-type animals, this transgene expresses ODR-10 exclusively in a single AWC neuron, but in *lim-4* mutants it is expressed in one AWC neuron and both AWB neurons. The *str-2::ODR-10* transgene restored diacetyl chemotaxis to both *odr-10* and *lim-4 odr-10* animals (Fig. 6C,E). ODR-10 expression in AWC could therefore mediate chemotaxis towards diacetyl, and in *lim-4* mutants this effect was enhanced by its simultaneous expression in AWB ($P < 0.001$).

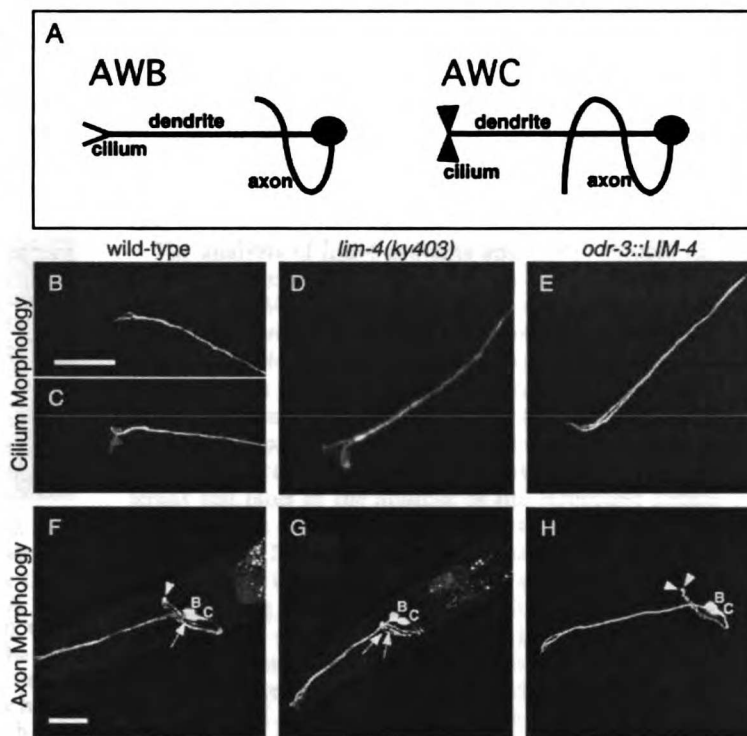
To probe the specific function of the transformed AWB neuron in *lim-4* mutants, the AWC neuron expressing ODR-10 was killed with a laser so that the only remaining ODR-10-expressing cells were the transformed AWB neurons. Although their attractive response was reduced, these animals were able to chemotax towards diacetyl (Fig. 6D). In contrast, killing the ODR-10-expressing AWC in wild-type *str-2::ODR-10* animals abolished diacetyl chemotaxis (Fig. 6F). These results indicate that the AWB neurons in a *lim-4* mutant can mediate attractive olfactory behaviors rather than repulsive ones.

LIM-4 is sufficient to repress the AWC cell fate and promote the AWB cell fate

LIM-4 is required to repress AWC fate and promote AWB fate in the AWB neurons. To ask whether it is also sufficient to perform these functions, *LIM-4* was expressed ectopically in the AWC neurons. The *lim-4* cDNA was placed under the control of the *odr-3* promoter, which is expressed in AWB, AWC, and faintly in AWA, ADF, and ASH (Roayaie et al. 1998). Expression of *odr-3::LIM-4* caused ectopic expression of the AWB-specific *str-1::GFP* marker and repression of *str-2::GFP* in the AWC neurons (Fig. 1C,F; Table 2). The *odr-3::LIM-4* transgene was also able to rescue AWB defects in a *lim-4(ky403)* mutant, as assessed by its *str-1::GFP* and *str-2::GFP* expression phenotypes, but it did not rescue coily movement (Fig. 1C,F; data not shown). Thus, *LIM-4* acts in sensory neurons, and probably acts cell autonomously within AWB or AWC to promote the AWB cell fate and repress the AWC cell fate. The AWA, ADF, and ASH neurons, which should also express a low level of *LIM-4* from this transgene, did not express detectable *str-1::GFP*.

The morphology and dye-filling properties of the AWC neurons were also transformed in *odr-3::LIM-4*-expressing animals. Cilium morphology in AWC neurons changed from the typical fan-like AWC structure to the

Figure 4. LIM-4 controls the morphology of sensory cilia and axons. (A) Diagrams illustrating the wild-type morphologies of AWB and AWC neurons. Cilia are specialized sensory structures at the tips of dendrites. An AWB cilium is a simple two-pronged structure, resembling a tuning fork, whereas an AWC cilium is more membranous or fan-like. The U-shaped AWB axon extends into the nerve ring and stops at the dorsal midline. The S-shaped AWC axon continues past the dorsal midline to a ventral position on the contralateral side of the nerve ring. (B–E) Confocal Z-series projections of AWC and AWB cilia. Wild-type cilium morphologies of AWB (B) and AWC (C), visualized with *str-1::GFP* and *str-2::GFP*, respectively. (D) An AWB cilium in a *lim-4(ky403)* mutant, visualized with *str-2::GFP*, resembles the fan-like AWC cilia. (E) An *odr-3::LIM-4*-expressing animal visualized with *str-1::GFP*; both cilia exhibit the simple tuning fork morphology of AWB. (F–H) Confocal Z-series projections of GFP-expressing AWC and AWB neurons. Mosaic animals in which the neurons on only one side of the animal expressed GFP were chosen to simplify analysis of axon trajectories. (F) In animals with wild-type axon morphologies, the AWB axon stops at the ventral midline (arrowhead), whereas the AWC axon continues ventrally past the midline (arrow). This picture is of a *lim-4* mutant expressing *str-2::GFP* displaying the wild-type axon morphologies for AWB and AWC. Wild-type animals expressing *str-1::GFP* and *str-2::GFP* exhibited an identical phenotype 100% of the time (Table 2). (G) A *lim-4(ky403)* mutant expressing *str-2::GFP*; both AWB and AWC axons exhibit the longer S-shaped AWC axon morphology (arrows). (H) An *odr-3::LIM-4*-expressing animals with *str-1::GFP*; both AWB and AWC axons stop at the midline (arrowheads). Quantitative analysis of these phenotypes is presented in Table 2. Anterior is left and dorsal is up in all panels. Scale bars, 20 μ m. Bar in B applies to B–E; bar in F applies to F–H.



tuning fork appearance characteristic of AWB (Fig. 4E; Table 2). Similarly, the *odr-3::LIM-4* transgene caused the longer S-shaped axon of AWC to adopt the U-shaped morphology appropriate for the AWB axon (Fig. 4H; Table 2). The lipophilic dye-filling properties of the AWC cell were also transformed by ectopic LIM-4 expression. In *odr-3::LIM-4* animals exposed to DiI, both AWB and AWC neurons took up dye, like normal AWB neurons (Fig. 5G–I; Table 2). Transformation of AWC into AWB by the *odr-3::LIM-4* transgene was therefore complete by several criteria, indicating that LIM-4 can repress an AWC fate and promote an AWB fate in the AWC neuron.

ODR-7 promotes the AWA olfactory neuron cell fate and represses the AWC fate, making AWA unresponsive to LIM-4

ODR-7 is a protein homologous to nuclear hormone receptors that is expressed exclusively in the AWA olfactory neurons. A null mutation in *odr-7* causes defects in chemotaxis toward all AWA-sensed odorants and re-

duces expression of the AWA olfactory receptor ODR-10 (Sengupta et al. 1994, 1996). We observed that ODR-7 is also required to repress *str-2::GFP* expression in AWA, but does not affect *str-1::GFP* expression (Fig. 7A,B). In the *odr-7(ky4)* null mutant, 97% of the worms expressed *str-2::GFP* ectopically in at least one AWA neuron ($n = 150$). In the mild *odr-7(ky55)* missense mutation, however, *str-2::GFP* expression was restricted to AWC.

Because AWA was transformed toward an AWC fate in *odr-7* mutants, it might have become sensitive to LIM-4's ability to transform AWC neurons into AWB neurons. As noted above, *odr-3::LIM-4* was not able to induce expression of the AWB marker *str-1::GFP* in AWA in a wild-type background, even though ODR-3 is expressed in AWA at a low level. However, *odr-7(ky4)* *str-1::GFP* animals carrying the *odr-3::LIM-4* transgene expressed GFP in AWC, AWB, and AWA (Fig. 7C; 41% of the time three cells on one side expressed GFP, $n = 86$). Reducing ODR-7 activity in the AWA neurons thus makes them susceptible to LIM-4 activity and reveals an underlying potential to produce AWC- or AWB-like cell fates.

Discussion

LIM-4 is a cell fate switch

LIM-4 plays a crucial role in determining the fate of the AWB olfactory neurons: It promotes the appropriate AWB cell fate while repressing an inappropriate AWC fate. In *lim-4* mutants, AWB adopts many molecular, morphological, and functional characteristics of AWC. Conversely, ectopic expression of *LIM-4* from the *odr-3* promoter is sufficient to cause the AWC cells to take on several morphological and molecular aspects of the AWB fate.

The analysis of *lim-4* mutants and *LIM-4* ectopic expressors suggests that *LIM-4* acts as a binary cell fate switch in AWB and AWC. Cells without functional *LIM-4* take on an AWC fate, whereas cells with *LIM-4* are repressed for the AWC fate and take on the AWB fate. This role as a cell fate switch is so far unique for a LIM homeobox gene in *C. elegans*. As measured by a variety of cell fate markers and anatomical criteria, the neurons that express *ttx-3*, *lin-11*, or *lim-6* have not adopted different cell fates in the absence of the respective gene's function, but are functionally defective (Hobert et al. 1997, 1998b, 1999). The neurite-sprouting defects of the SAA neurons in *lim-4* mutant animals resemble the neurite-sprouting defects observed in other LIM homeobox gene mutant animals. *LIM-4* may thus be performing different functions in different cells. In the SAA neurons it may be acting more like the LIM homeobox genes characterized previously, whereas in AWB, *LIM-4* performs a novel function, repressing one cell fate while promoting another cell fate.

The only other *C. elegans* LIM homeobox mutant that is suspected of undergoing a cell fate transformation is *mec-3*, in which the ALM neurons display characteristics of the BDU neurons (Way and Chalfic 1988). How-

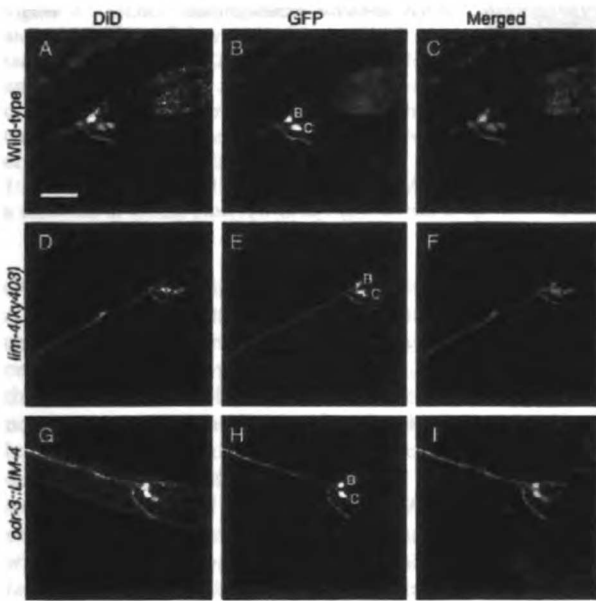
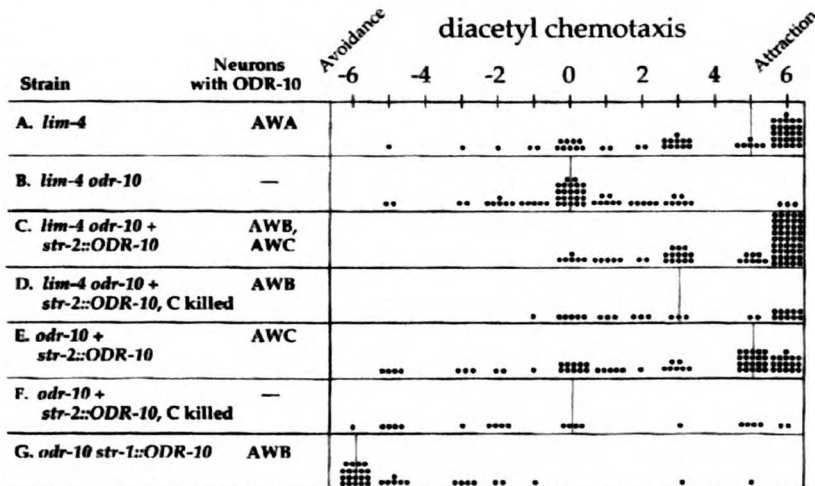


Figure 5. *LIM-4* controls dye-filling properties of AWB and AWC. Confocal sections of worms expressing GFP in AWB and AWC neurons, soaked in the fluorescent lipophilic dye DiD. GFP is visualized with FITC wavelength filters (A,D,G), and DiD is visualized with TRITC wavelength filters (B,E,H). GFP was false-colored green, DiD was false-colored red and the images were merged (C,F,I); yellow indicates areas of overlap. In all cases, the more dorsal GFP-expressing cell is AWB and the more ventral cell is AWC. In wild-type dye-filled animals with *str-1::GFP* and *str-2::GFP* (A-C), only AWB fills with dye. In *lim-4* mutant animals with *str-2::GFP* (D-F), neither cell fills with dye. In transgenic worms expressing *odr-3::LIM-4* and *str-1::GFP* (G-I), both cells fill with dye. Quantitative analysis of these phenotypes is presented in Table 2. Anterior is left and dorsal is up in all panels. Scale bar, 20 μ m in A-I.

Figure 6. AWB mediates attractive chemosensory behaviors in *lim-4*. Graphic representation of single worm chemotaxis assays: Strains and neurons in those strains that express ODR-10 are at left, and assay results are at right. -6 indicates complete repulsion from diacetyl, 0 indicates indifference, and +6 indicates attraction. Each dot represents the chemotaxis score for a single worm, and vertical lines indicate the median score. All strains tested also carried a mutation in the *lin-15* marker and were rescued with an extrachromosomal *lin-15* gene. Assays were performed with (A) *lim-4(ky403)* mutants, (B) *lim-4 odr-10(ky225)* double mutants, (C) *lim-4 odr-10* animals with extrachromosomal *str-2::ODR-10* and *str-2::GFP* (only animals expressing GFP in AWC and AWB were assayed), (D) the same strain as in C following laser ablation of the GFP-expressing AWC neuron, (E) an *odr-10* strain wild-type for *LIM-4*, expressing the *str-2::ODR-10* and *str-2::GFP* transgenes, and F the same strain as in E following laser ablation of the GFP-expressing AWC neuron. (G) Data from a *str-1::ODR-10* strain in a wild-type background, reproduced from Troemel et al. (1997) for comparison. Data were analyzed with a Mann-Whitney rank sum test, and significant differences ($P \leq 0.002$) were observed between D and G, B and C, B and D, D and F, and C and E. D and E were not significantly different ($P = 0.499$).



1
2
3
4
5
6
7
8
9
10
11
12
13
14
15
16
17
18
19
20
21
22
23
24
25
26
27
28
29
30
31
32
33
34
35
36
37
38
39
40
41
42
43
44
45
46
47
48
49
50
51
52
53
54
55
56
57
58
59
60
61
62
63
64
65
66
67
68
69
70
71
72
73
74
75
76
77
78
79
80
81
82
83
84
85
86
87
88
89
90
91
92
93
94
95
96
97
98
99
100

Figure 7. ODR-7 distinguishes between AWA and AWC-like cell fates. (A) An *odr-7(ky4)* mutant expresses *str-2::GFP* ectopically in AWA and in the appropriate AWC cell. (B) Expression of the AWB-specific *str-1::GFP* marker is not altered in an *odr-7* mutant. (C) Ectopic expression of LIM-4 from the *odr-3* promoter causes *str-1::GFP* to be expressed ectopically in both AWA and AWC, as well as the normal AWB cells in an *odr-7* mutant. (C) A projection of a confocal Z-series. Anterior is left and dorsal is up in A–C. Scale bars, 40 μ m. Bar in A applies to A–B; bar in C applies to C.



ever, *mec-3* is not known to be sufficient for a BDU to ALM transformation. Because ALM and BDU are sister cells, a mutation in *mec-3* transforms an asymmetric cell division into a symmetric division. This differs from the situation with LIM-4 because the AWB and AWC neurons are not related to each other by lineage yet are both responsive to the same transcription factor. LIM-4 does not appear to affect the AWB cell lineage as AWB's sister cell ADF, and its lineal cousin ASE, develop normally in *lim-4* mutants. Thus, whereas the principle by which MEC-3 distinguishes between BDU and ALM cell fates is dictated by lineage, LIM-4 distinguishes between AWC and AWB within a hierarchy of cell function.

Analogous roles for LIM homeobox genes as switches for at least one aspect of motor neuron fate, the axon trajectory, have been reported recently for vertebrate and fly LIM homeobox genes. Cell fates within the vertebrate spinal cord are likely specified by the unique combination of LIM homeobox genes they express (Tsuchida et al. 1994). Mutants in the two redundant LIM homeobox genes *lhx3* and *lhx4* together cause the misrouting of a subpopulation of spinal cord axons (Sharma et al. 1998). Ectopic expression of LHX3 causes the reciprocal transformation in spinal cord axon trajectory. A similar function has been shown for *lim3*, the *Drosophila* homolog of these spinal cord LIM homeobox genes (Thor et al. 1999). In a *lim3* mutant, a subpopulation of motor neurons develop projections onto inappropriate muscles, and ectopic expression of LIM3 causes the reciprocal defects in motor neuron projection. Like LIM-4 these LIM homeobox genes act as binary cell fate switches, distinguishing between two alternative cell fates. The completeness of the AWB to AWC transformation in *lim-4* establishes that multiple aspects of cell fate, not just the axon trajectory, can be transformed by this class of genes.

All LIM homeobox genes are expressed throughout the life of the animal, leading to the hypothesis that these genes act continuously to maintain proper cell identity (Hobert and Ruvkun 1998a). Our experiment with a temperature-sensitive allele of LIM-4 suggests that this is not true for at least one of its functions. LIM-4 is required acutely to repress *str-2::GFP* expression in AWB during a discrete period of early development and not later in the life of the animal. Thus, the repression of AWC fate by LIM-4 is an irreversible decision made soon after neuron birth. None of the *lim-4* alleles were temperature-sensitive for their *str-1::GFP* expression phenotypes, so it was not possible to test whether LIM-4 is similarly required acutely to promote the AWB fate or

continuously to maintain it. It is possible that LIM homeobox genes have different temporal requirements for different aspects of their function.

LIM-4 controls the behavioral output of olfactory neurons

Perhaps the most striking aspect of AWB's transformation into AWC in *lim-4* mutants is its change in neuronal function. In wild-type animals, odorant stimulation of AWB and AWC leads to opposite behavioral responses. When activated by an odorant, AWC directs worms to move toward it, whereas activation of AWB causes worms to move away from the odorant. Previous studies in *C. elegans* suggest that the nature of the behavioral response to an odorant is defined by the sensory neuron and not by olfactory receptors (Troemel et al. 1997). Specifically, the ODR-10 diacetyl receptor mediates attractive behaviors in its native neuron AWA and repulsive behaviors when placed in AWB (Sengupta et al. 1996; Troemel et al. 1997). We show here that ODR-10 is functional in AWC as well, in which it mediates attractive behaviors. Strikingly, ODR-10 can also function in AWB cells lacking *lim-4* function, but these transformed neurons now mediate attractive responses, demonstrating that AWB in *lim-4* forms active, functional connections.

All three pairs of olfactory neurons in *C. elegans*—AWA, AWB, and AWC—express candidate-seven transmembrane domain olfactory receptors and share components of their signal transduction pathways, notably the G-protein α subunit ODR-3 (Roayaie et al. 1998). AWB and AWC require many of the same components for odorant sensation, including a cGMP-gated channel (Coburn and Bargmann 1996; Komatsu et al. 1996). The differences in the responses generated by activation of these neurons might therefore lie in their patterns of connectivity to downstream interneurons. According to electron microscope reconstructions of the *C. elegans* nerve ring, AWB and AWC have nearly exclusive sets of downstream targets (White et al. 1986). AWC forms synapses primarily onto the interneurons A1Y, A1B, and A1A, whereas AWB forms connections primarily onto A1Z and the sensory neuron ADF. LIM-4 might act upstream of the genes that are required for choosing appropriate synapses, repressing those that determine AWC's pattern of connectivity and activating those that determine AWB's connectivity.

A model for the specification of olfactory cell fates

ODR-7 is a predicted nuclear hormone receptor required

1
2
3
4
5
6
7
8
9
10
11
12
13
14
15
16
17
18
19
20
21
22
23
24
25
26
27
28
29
30
31
32
33
34
35
36
37
38
39
40
41
42
43
44
45
46
47
48
49
50
51
52
53
54
55
56
57
58
59
60
61
62
63
64
65
66
67
68
69
70
71
72
73
74
75
76
77
78
79
80
81
82
83
84
85
86
87
88
89
90
91
92
93
94
95
96
97
98
99
100

for the proper specification of the AWA olfactory neurons (Sengupta et al. 1994). In an *odr-7* mutant, AWA fails to express the diacetyl receptor ODR-10 (Sengupta et al. 1996), and we show here that it ectopically expresses the putative AWC receptor STR-2. *odr-7* and *lim-4* thus act analogously, as repressors of AWC cell fate and promoters of the AWA and AWB fates, respectively. In the *acj6* POU-domain gene mutant of *Drosophila*, the odorant specificities of certain olfactory neurons have changed, suggesting an analogous alteration in cell fates (Clyne et al. 1999a,b).

Although the *odr-3* promoter is expressed in the AWA, ADF, and ASH neurons, those cells were not affected by *odr-3::LIM-4* expression in wild-type animals. Only the AWB and AWC neurons seem to be capable of responding to LIM-4's AWB-promoting activity. The two AWC neurons can be thought of as two distinct cell types, as only one of the two AWC cells expresses *str-2::GFP* (E.R. Troemel and C.I. Bargmann, unpubl.). The AWB neurons in *lim-4* mutants adopt only one of those two fates, or possibly both at once, as both express *str-2::GFP*. The further subdivision of AWC's cell fate must therefore be determined by a separate factor acting in parallel to LIM-4, or by environmental cues present at AWC's cell position. Thus, there seems to be a specific group of cells responsive to LIM-4, including AWB and the two AWCs. Because AWA neurons in the *odr-7* mutant have become more AWC-like, we reasoned that they may now be part of this LIM-4-responsive group. We found that an *odr-7*-defective AWA neuron can express AWB markers if it also expresses LIM-4.

These results suggest a model for the specification of olfactory neuron identities in the *C. elegans* amphid (Fig. 8). *lim-4* and *odr-7* mutants reveal a common AWC-like developmental potential in the olfactory neurons AWA and AWB, which are not closely related to AWC or each other by lineage. This potential could be specified by an olfactory neuron fate determinant that is generated through the cell lineage, or induced by the embryonic environment, in three separate cells, AWA, AWB, and AWC. Without further modification, all of these cells can take on some of the characteristics of AWC. Modification of the AWC-like state in AWA and AWB is achieved by the transcription factors ODR-7 and LIM-4, either by themselves or in cooperation with other unidentified factors. It is these factors that allow the three olfactory neurons to establish their unique patterns of gene expression, their cell morphologies, and perhaps their synaptic connectivities, ultimately determining the behavioral outputs mediated by each cell. We speculate that the AWC-like fate may serve as an olfactory ground state on which the other neuronal fates can be elaborated. If this is true, the AWC-like fate could be a basic blueprint for making an olfactory cell, to which evolution can make alterations that diversify the animal's repertoire of responses to volatile chemicals. Intriguingly, the head of the skin-penetrating nematode parasite *Strongyloides stercoralis* has been reconstructed from electron microscope sections and only one neuron has the structural features of an olfactory cell (Ashton et

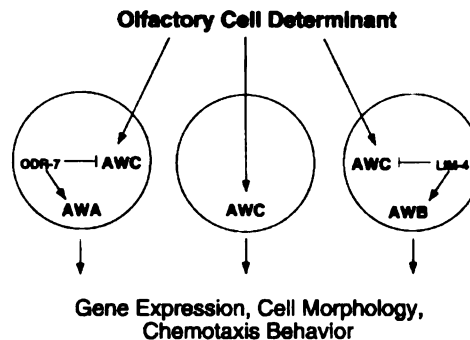


Figure 8. A model for olfactory cell fate specification in *C. elegans*. Analysis of *lim-4* and *odr-7* mutants suggests that a common cell fate specification pathway operates in AWA, AWB, and AWC, despite the fact that these neurons are not related by lineage. A common olfactory cell fate determinant may specify generic features of these three olfactory cells. In the absence of ODR-7 and LIM-4, these cells will develop like AWC, a potential olfactory default state. Modification of this fate in AWA and AWB is accomplished by ODR-7 and LIM-4, either by themselves or in cooperation with other factors. These factors direct the three olfactory neurons to adopt distinct gene expression patterns, cell morphologies, and behavioral functions.

al. 1995). It may be interesting to determine whether this cell most closely resembles *C. elegans* AWC. A possible role for AWC as a cellular module is likely just one example of a general strategy used during evolution to transform a simple organ with a few cell types into a complex multifunctional organ.

Materials and methods

Strain maintenance

Wild-type strains were *C. elegans* variety Bristol, strain N2. Strains were maintained by standard methods (Brenner 1974).

Isolation of mutants, mapping, and cloning *lim-4*

str-2::GFP(ky1s140); rol-6(e187) worms were mutagenized with EMS according to standard protocols and screened for ectopic expression of GFP under a fluorescence dissecting scope in the F₂ generation (Anderson 1995). The three *lim-4* alleles were outcrossed once to a *str-2::GFP* strain and at least twice to N2. *lim-4(ky403)* was mapped with respect to Tc1 transposable element polymorphisms in the DP13 strain (Williams 1995). Mapping localized the mutant to the X chromosome between the *stP40* and *stP156* polymorphisms. Rescue of the *str-2::GFP* misexpression phenotype was observed in three independent lines injected with the cosmid ZC64 at 10 µg/ml. The *lim-4* genomic coding sequence in the three mutants was amplified by PCR in two pieces and PCR products were sequenced directly. Lesions were confirmed by sequencing a second independently amplified PCR product.

Germ-line transformation

Transgenic strains were created according to methods described previously (Mello and Fire 1995). Transgenic animals used for

behavioral assays were generated in a *lin-15(n765)* background and rescued with a *lin-15* pJM23 coinjection marker at 50 µg/ml. These strains were maintained by picking non-Multivulva worms. Other transgenic lines were made with the dominant pRF4 *rol-6(su1006)* coinjection marker at 50 µg/ml, and maintained by picking Roller animals. The *odr-3::LIM-4* transgene was injected at 100 µg/ml, and all other transgenes were injected at 50 µg/ml. In all cases in which phenotypes were quantified in extrachromosomal array-bearing lines, at least five lines exhibited the same qualitative phenotype and the strongest was chosen for quantitation.

Transgenes and cDNA

The *str-2::GFP(kyIs140)*, *str-1::GFP(kyIs104)*, and *odr-3::GFP(kyIs126)* transgenes were integrated strains described previously [Troemel et al. 1997; Dwyer et al. 1998; Roayaie et al. 1998].

Six GFP marker strains were crossed into *lim-4(ky403)* to determine the specificity of the mutant's phenotype. The ASI, ADL, and ADF GFP marker transgenes were fusions of GFP to promoters of putative seven-transmembrane domain proteins (ASI = M7.13, ADL = F47C12.5, ADF = T08G3.3; Y. Zhang, E.R. Troemel, J. Hao, and C.I. Bargmann, unpubl.). The ASI and ADL strains were integrated and the ADF strain was extrachromosomal. For AWA, an integrated *odr-10::GFP(kyIs37)* transgene was used [Sengupta et al. 1996]. For ASEL and ASER extrachromosomal fusions with promoters of the guanylyl cyclase, genes *gcy-5* and *gcy-6* were used [Yu et al. 1997]. The ADF, ADL, ASEL, and ASER markers were crossed into *lim-4(ky403)* and hemizygous F₁ males were scored. For the ASI and AWA markers, homozygous *lim-4; GFP* strains were generated.

lim-4 cDNA The cDNA was isolated by PCR from a mixed-stage cDNA library with primers that match the amino and carboxyl terminus of the predicted ZC64.4 gene. The predicted gene structure of ZC64.4 (GenBank accession no. U39740) was confirmed with one exception. ZC64.4 was predicted to contain a 17-amino-acid insertion at amino acid position 289. This insertion most likely results from a misprediction of the gene structure because we could not detect it in cDNAs that were isolated. Moreover, the insertion is in the middle of the homeodomain, which would be highly unusual.

lim-4::GFP2[mgIs19] A 4.5-kb fragment containing 3.6 kb 5' to the predicted ATG start codon and the first three *lim-4* exons was amplified from genomic DNA and cloned into the GFP reporter gene vector *pPD95.75* generously provided by A. Fire (Carnegie Institute, Baltimore, MD). Transgenic lines were generated by injecting 50 µg/ml *lim-4::GFP2* and 100 µg/ml pRF4 DNA into wild-type worms. The extrachromosomal DNA was integrated by use of a Stratalinker 1800 UV light source at 300 J/m².

lim-4::GFP1 A total of 2682 bp containing the remaining introns and exons of the *lim-4* gene were added to the *lim-4::GFP2* fusion. GFP was fused to the last amino acid of the *lim-4* coding sequence.

odr-3::LIM-4 The pD95.77 expression plasmid, generously provided by A. Fire, was digested with *MscI* and *EcoRI* to remove GFP, and the *EcoRI* overhang was blunted. The *lim-4* cDNA was amplified by PCR with primers bearing blunt restriction site, digested, and ligated into the vector. The PCR

product was sequenced to ensure that no errors were introduced. An *EcoRV* fragment of the *odr-3* promoter [Roayaie et al. 1998] was cloned into the *SmaI* site in the vector.

str-2::ODR-10 Amplification of the *str-2* coding region was done by PCR at 3.7 kb upstream. *PstI* and *BamHI* sites engineered into the PCR primers were used to insert the amplified product into a vector containing an *odr-10* cDNA [Sengupta et al. 1996].

Dye-filling

Worms were placed in 4 µl of a DiD solution (10 mg/ml DiD dissolved in DMSO) diluted in 1 ml of M9 buffer with food, incubated for 12 to 16 hr, and allowed to recover for 4 to 6 hr on a fresh seeded plate before examination with TRITC fluorescence filters. GFP markers for AWB and AWC cells were included to facilitate cell identifications.

Temperature shifts

To synchronize populations of mutant animals, L4 larval stage animals were placed at 15°C or 25°C and then disintegrated as gravid adults in a bleach solution (40% bleach, 0.4 M NaOH), leaving a synchronized population of eggs. Animals were shifted between temperatures at the L1 larval stage and assayed as young adults, 48 to 72 hr later.

Single worm chemotaxis assays and laser ablations

Single worm assays were performed as described previously [Troemel et al. 1997]. Briefly, a healthy adult worm was placed at the center of a square agarose plate, two 1 µl point sources of the odorant (diacetyl diluted 1:1000 in ethanol) were spotted at one end of the plate and two 1 µl spots of the diluent (ethanol) were placed at the other end of the plate. The animal's tracks were observed after 1 hr. Plates were divided into six zones with assigned values from -3, for the zone farthest from the odorant, to +3, for the zone closest to the odorant. Assays were scored by summing the scores for the zones through which the worm traveled. For example, a worm that moved directly toward the odorant passed through zones 1, 2, and 3 and received the maximum score of 6. Conversely, worms that were completely repulsed by the odorant received a score of -6. Worms unable to sense the odorant moved randomly and averaged a score of 0. Results were analyzed with a Mann Whitney rank sum test.

Laser ablations were performed in the L1 or L2 larval stages as described previously [Bargmann and Avery 1995]. Animals used for laser ablation carried both the *str-2::ODR-10* and the *str-2::GFP* transgenes. Only animals that expressed GFP in the appropriate cells were used in behavioral assays. The transgene-bearing AWC cell was identified for ablation by the presence of the *str-2::GFP* coinjection marker. To confirm that ablations were effective, animals were examined for *str-2::GFP* in the AWC cell after the assay. Only animals with no GFP expression in AWC were included.

Acknowledgments

We thank Shannon Grantner and Yongmei Zhang for excellent technical support; Joe Hao and Tim Yu for help with confocal microscopy; and Candace Chi, Gage Crump, Sue Kirch, Noelle

L'Etoile, David Tobin, and Fan Wang for comments on the manuscript and discussions about experiments. We are grateful to Alan Coulson and the Sanger Centre for cosmids. This work was supported by grants from the Human Frontiers Science Program (to C.I.B.) and Hoechst AG to the Department of Molecular Biology, Massachusetts General Hospital (G.R.). A.S. is a Howard Hughes Medical Institute predoctoral fellow, O.H. was a Human Frontiers Science Program postdoctoral fellow, E.R.T. was a National Science Foundation predoctoral fellow, and C.I.B. is an Assistant Investigator of the Howard Hughes Medical Institute.

The publication costs of this article were defrayed in part by payment of page charges. This article must therefore be hereby marked 'advertisement' in accordance with 18 USC section 1734 solely to indicate this fact.

References

- Anderson, P. 1995. Mutagenesis. *Methods Cell Biol.* 48: 31–58.
- Ashton, F.T., V.M. Bhopale, A.E. Fine, and G.A. Schad. 1995. Sensory neuroanatomy of a skin-penetrating nematode parasite: *Strongyloides stercoralis*. I. Amphidial neurons. *J. Comp. Neurol.* 357: 281–295.
- Bargmann, C.I. and L. Avery. 1995. Laser killing of cells in *Caenorhabditis elegans*. *Methods Cell Biol.* 48: 225–250.
- Bargmann, C.I., E. Hartwig, and H.R. Horvitz. 1993. Odorant-selective genes and neurons mediate olfaction in *C. elegans*. *Cell* 74: 515–527.
- Brenner, S. 1974. The genetics of *Caenorhabditis elegans*. *Genetics* 77: 71–94.
- Buck, L.B. 1996. Information coding in the vertebrate olfactory system. *Annu. Rev. Neurosci.* 19: 517–544.
- Clyne, P.J., S.J. Certel, M. de Bruyne, L. Zaslavsky, W.A. Johnson, and J.R. Carlson. 1999a. The odor specificities of a subset of olfactory receptor neurons are governed by *Acj6*, a POU-domain transcription factor. *Neuron* 22: 339–347.
- Clyne, P.J., C.G. Warr, M.R. Freeman, D. Lessing, J. Kim, and J.R. Carlson. 1999b. A novel family of divergent seven-transmembrane proteins: Candidate odorant receptors in *Drosophila*. *Neuron* 22: 327–338.
- Coburn, C.M. and C.I. Bargmann. 1996. A putative cyclic nucleotide-gated channel is required for sensory development and function in *C. elegans*. *Neuron* 17: 695–706.
- Colbert, H.A., T.L. Smith, and C.I. Bargmann. 1997. OSM-9, a novel protein with structural similarity to channels, is required for olfaction, mechanosensation, and olfactory adaptation in *Caenorhabditis elegans*. *J. Neurosci.* 17: 8259–8269.
- Curtiss, J. and J.S. Heilig. 1997. Arrowhead encodes a LIM homeodomain protein that distinguishes subsets of *Drosophila* imaginal cells. *Dev. Biol.* 190: 129–141.
- Dwyer, N.D., E.R. Troemel, P. Sengupta, and C.I. Bargmann. 1998. Odorant receptor localization to olfactory cilia is mediated by ODR-4, a novel membrane-associated protein. *Cell* 93: 455–466.
- Freyd, G., S.K. Kim, and H.R. Horvitz. 1990. Novel cysteine-rich motif and homeodomain in the product of the *Caenorhabditis elegans* cell lineage gene *lin-11*. *Nature* 344: 876–879.
- Grigoriou, M., A.S. Tucker, P.T. Sharpe, and V. Pachnis. 1998. Expression and regulation of *Lhx6* and *Lhx7*, a novel subfamily of LIM homeodomain encoding genes, suggests a role in mammalian head development. *Development* 125: 2063–2074.
- Hobert, O., I. Mori, Y. Yamashita, H. Honda, Y. Ohshima, Y. Liu, and G. Ruvkun. 1997. Regulation of interneuron function in the *C. elegans* thermoregulatory pathway by the *ttx-3* LIM homeobox gene. *Neuron* 19: 345–357.
- Hobert, O. and G. Ruvkun. 1998a. A common theme for LIM homeobox gene function across phylogeny? *Biol. Bul.* 195: 377–381.
- Hobert, O., T. D'Alberti, Y. Liu, and G. Ruvkun. 1998b. Control of neural development and function in a thermoregulatory network by the LIM homeobox gene *lin-11*. *J. Neurosci.* 18: 2084–2096.
- Hobert, O., K. Tessmar, and G. Ruvkun. 1999. The *Caenorhabditis elegans* *lim-6* LIM homeobox gene regulates neurite outgrowth and function of particular GABAergic neurons. *Development* 126: 1547–1562.
- Komatsu, H., I. Mori, J.S. Rhee, N. Akaike, and Y. Ohshima. 1996. Mutations in a cyclic nucleotide-gated channel lead to abnormal thermosensation and chemosensation in *C. elegans*. *Neuron* 17: 707–718.
- Lundgren, S.E., C.A. Callahan, S. Thor, and J.B. Thomas. 1995. Control of neuronal pathway selection by the *Drosophila* LIM homeodomain gene *apterous*. *Development* 121: 1769–1773.
- Matsumoto, K., T. Tanaka, T. Furuyama, Y. Kashihara, N. Ishii, M. Tohyama, J. Kitanaka, M. Takemura, T. Mori, and A. Wanaka. 1996. Differential expression of LIM-homeodomain genes in the embryonic murine brain. *Neurosci. Lett.* 211: 147–150.
- McIntire, S.L., E. Jorgensen, J. Kaplan, and H.R. Horvitz. 1993. The GABAergic nervous system of *Caenorhabditis elegans*. *Nature* 364: 337–341.
- Mello, C. and A. Fire. 1995. DNA transformation. *Methods Cell Biol.* 48: 451–482.
- Mitani, S., H. Du, D.H. Hall, M. Driscoll, and M. Chalfie. 1993. Combinatorial control of touch receptor neuron expression in *Caenorhabditis elegans*. *Development* 119: 773–783.
- Mori, I. and Y. Ohshima. 1995. Neural regulation of thermotaxis in *Caenorhabditis elegans*. *Nature* 376: 344–348.
- Roayaie, K., J.G. Crump, A. Sagasti, and C.I. Bargmann. 1998. The G alpha protein ODR-3 mediates olfactory and nociceptive function and controls cilium morphogenesis in *C. elegans* olfactory neurons. *Neuron* 20: 55–67.
- Sengupta, P., H.A. Colbert, and C.I. Bargmann. 1994. The *C. elegans* gene *odr-7* encodes an olfactory-specific member of the nuclear receptor superfamily. *Cell* 79: 971–980.
- Sengupta, P., J.H. Chou, and C.I. Bargmann. 1996. *odr-10* encodes a seven transmembrane domain olfactory receptor required for responses to the odorant diacetyl. *Cell* 84: 899–909.
- Sharma, K., H.Z. Sheng, K. Lettieri, H. Li, A. Karavanov, S. Potter, H. Westphal, and S.L. Pfaff. 1998. LIM homeodomain factors *Lhx3* and *Lhx4* assign subtype identities for motor neurons. *Cell* 95: 817–828.
- Thor, S., S.G. Andersson, A. Tomlinson, and J.B. Thomas. 1999. A LIM-homeodomain combinatorial code for motor-neuron pathway selection. *Nature* 397: 76–80.
- Troemel, E.R., J.H. Chou, N.D. Dwyer, H.A. Colbert, and C.I. Bargmann. 1995. Divergent seven transmembrane receptors are candidate chemosensory receptors in *C. elegans*. *Cell* 83: 207–218.
- Troemel, E.R., B.E. Kimmel, and C.I. Bargmann. 1997. Reprogramming chemotaxis responses: Sensory neurons define olfactory preferences in *C. elegans*. *Cell* 91: 161–169.
- Tsuchida, T., M. Ensini, S.B. Morton, M. Baldassarre, T. Edlund, T.M. Jessell, and S.L. Pfaff. 1994. Topographic organization of embryonic motor neurons defined by expression of LIM homeobox genes. *Cell* 79: 957–970.

- Way, J.C. and M. Chalfie. 1988. *mec-3*, a homeobox-containing gene that specifies differentiation of the touch receptor neurons in *C. elegans*. *Cell* **54**: 5-16.
- White, J.G., E. Southgate, J.N. Thomson, and S. Brenner 1986. The structure of the nervous system of the nematode *Caenorhabditis elegans*. *Phil. Trans. R. Soc. Lond. B* **314**: 1-340.
- Williams, B.D. 1995. Genetic mapping with polymorphic sequence-tagged sites. *Methods Cell. Biol.* **48**: 31-58.
- Yu, S., L. Avery, E. Baude, and D.L. Garbers. 1997. Guanylyl cyclase expression in specific neurons: A new family of chemosensory receptors. *Proc. Natl. Acad. Sci.* **94**: 3384-3387.
- Zhang, Y., J.H. Chou, J. Bradley, C.I. Bargmann, and K. Zinn. 1997. The *Caenorhabditis elegans* seven-transmembrane protein ODR-10 functions as an odorant receptor in mammalian cells. *Proc. Natl. Acad. Sci.* **94**: 12162-12167.

Chapter 3

Lateral signaling mediated by axon contact and calcium entry regulates asymmetric odorant receptor expression in *C. elegans*

(Published in Cell, November 12, 1999, 99: 387-398)

Lateral Signaling Mediated by Axon Contact and Calcium Entry Regulates Asymmetric Odorant Receptor Expression in *C. elegans*

Emily R. Troemel,[†] Alvaro Sagasti,[†]
and Cornelia I. Bargmann*

Howard Hughes Medical Institute
Programs in Developmental Biology, Neuroscience,
and Genetics

Department of Anatomy and
Department of Biochemistry and Biophysics
The University of California
San Francisco, California 94143-0452

Summary

C. elegans detects several odorants with the bilaterally symmetric pair of AWC olfactory neurons. A stochastic, coordinated decision ensures that the candidate odorant receptor gene *str-2* is expressed in only one AWC neuron in each animal—either the left or the right neuron, but never both. An interaction between the two AWC neurons generates asymmetric *str-2* expression in a process that requires normal axon guidance and probably AWC axon contact. This interaction induces *str-2* expression by reducing calcium signaling through a voltage-dependent Ca²⁺ channel and the CaM kinase II UNC-43. CaMKII activity acts as a switch in the initial decision to express *str-2*; thus, calcium signals can define distinct cell types during neuronal development. A cGMP signaling pathway that is used in olfaction maintains *str-2* expression after the initial decision has been made.

Introduction

The developing nervous system generates an enormous variety of neurons whose functions depend on distinct patterns of gene expression. In the olfactory system, the functional properties of individual sensory neurons are determined by the odorant receptor genes that they express. In both vertebrates and invertebrates, odorant receptors are encoded by large families of G protein-coupled receptors (Buck and Axel, 1991; Troemel et al., 1995; Clyne et al., 1999; Vosshall et al., 1999). The genome of the nematode *Caenorhabditis elegans* contains about 1000 potential seven-transmembrane domain receptor genes, many of which are likely to encode chemosensory receptors (Bargmann, 1998). One of these receptors is ODR-10, a receptor for the odorant diacetyl (Sengupta et al., 1996). The correct pattern of odorant receptor gene expression is necessary to dictate the correct behavioral response to odorants. Expression of ODR-10 in its normal context in the AWA olfactory neurons allows the animal to chemotax to diacetyl, but misexpression of ODR-10 in the AWB olfactory neurons causes the animal to avoid diacetyl (Troemel et al., 1997). In mammals, the expression of the correct

receptor gene is critical not only for a neuron's olfactory function but also for its projection to its target in the olfactory bulb (Mombaerts et al., 1996). An individual olfactory neuron in mammals probably expresses only one of a thousand receptor genes (Buck and Axel, 1991; Chess et al., 1994; Malnic et al., 1999).

Chemosensory receptor expression in *C. elegans* is highly stereotyped. The major chemosensory organs of *C. elegans* are the amphids, a bilaterally symmetric pair of sensory structures on the left and right sides of the head. The 22 amphid chemosensory neurons fall into 11 morphological classes, with one member of each class in the left and right amphids. Each class of amphid neurons expresses a particular set of receptor genes. Thirty-eight different candidate receptors from several large gene families have been shown to be expressed in specific subsets of chemosensory neurons (Troemel et al., 1995; E. R. T. et al., unpublished data). A single class of sensory neurons can express at least six receptor genes, allowing the large diversity of chemosensory receptors to be distributed in a small number of neurons. In most cases, a chemosensory receptor gene is expressed in both the left and right members of a class of neurons. For example, *odr-10* and the candidate receptors *srd-1*, *str-1*, *str-3*, and *sra-6* all have a bilaterally symmetric expression pattern. However, the two neurons in a class may not always be equivalent: in the ASE neurons, two receptor guanylyl cyclases are expressed only in ASEL, while one guanylyl cyclase is expressed only in ASER (Yu et al., 1997).

Three bilateral pairs of amphid olfactory neurons, called AWA, AWB, and AWC, are required for the detection of volatile odorants. AWA and AWC detect different groups of attractive odorants, whereas AWB detects repulsive odorants (Bargmann et al., 1993; Troemel et al., 1997). The appropriate regulation of odorant receptor genes requires the nuclear receptor transcription factor ODR-7, which acts in the AWA neurons, and the LIM-homeodomain transcription factor LIM-4, which acts in the AWB neurons (Sengupta et al., 1994; Sagasti et al., 1999). Mutations in *odr-7* and *lim-4* transform the sensory neurons in which they are expressed toward an AWC-like fate. Thus, the ODR-7 and LIM-4 proteins act to diversify odorant receptor expression and olfactory neuron fates.

Here, we describe an additional level of receptor gene regulation that further increases olfactory neuron diversity. The candidate receptor *str-2* is asymmetrically expressed in only one of the two AWC neurons. Unlike previous examples of stereotyped left/right asymmetry in *C. elegans*, *str-2* expression is stochastic: half of the animals in a population express *str-2* in AWCL, and the other half express it in AWCR. Asymmetric *str-2* expression arises from an interaction between the two AWC neurons that appears to require axon contact. *str-2* asymmetry is regulated by calcium entry and the calcium/calmodulin-dependent CaM kinase II, and it is maintained by cGMP signaling. Thus, molecules that affect neuronal activity can cause equivalent olfactory cells to differentiate into distinct cell types.

*To whom correspondence should be addressed (e-mail: corie.itsa.ucsf.edu).

[†] These authors contributed equally to this work.

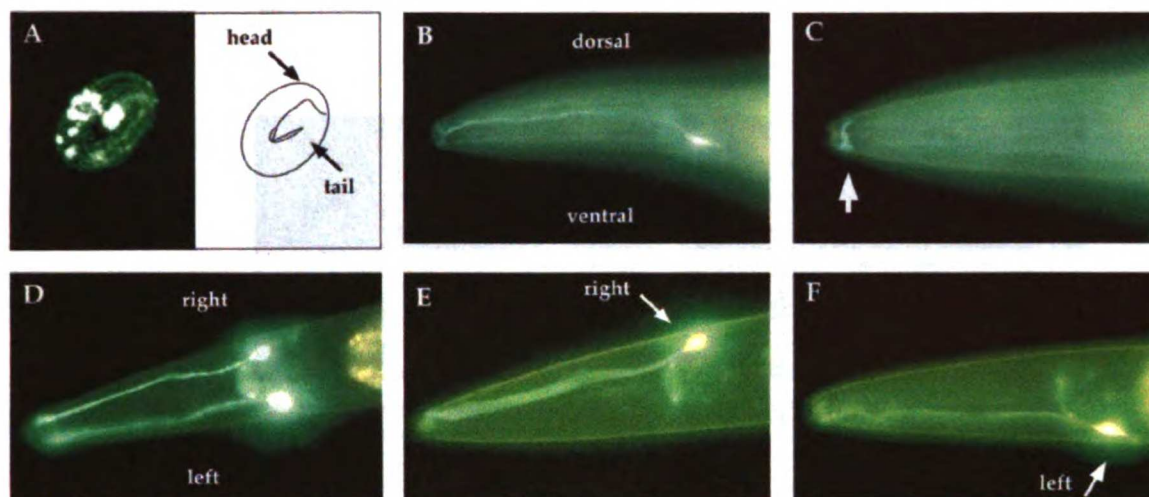


Figure 1. *str-2* Encodes a Candidate Odorant Receptor that Is Asymmetrically Expressed in the AWC Olfactory Neurons

(A) A *str-2::GFP* fusion is first expressed in about ten cells in the late embryo. The *str-2::GFP* fusion contains 3.7 kb of upstream region and the first seven amino acids fused to GFP. Nonspecific GFP expression is also seen in the posterior gut. Figure shows a confocal z series image collapsed into one plane.

(B) *str-2::GFP* drives strong expression in an AWC neuron of an adult.

(C) A GFP-tagged full-length STR-2::*str-2::GFP* fusion protein localizes to the AWC cilia of an adult.

(D) All animals with an integrated *str-1::GFP* transgene express GFP in both AWC neurons.

(E and F) About half of the animals with an integrated *str-2::GFP* transgene express GFP in the right AWC neuron, and the other half express GFP in the left AWC neuron.

(B and C) Lateral views. Anterior is left; dorsal is up. (D–F) Dorsal views. Anterior is left; right is up.

Results

str-2, a Candidate Odorant Receptor, Is Asymmetrically Expressed in the AWC Neurons

str-2 is a predicted seven-transmembrane domain protein with sequence similarity to the diacetyl receptor *odr-10*. To ask whether *str-2* might encode an odorant receptor, the expression patterns of *str-2::GFP* fusion genes were examined. A transgene with the *str-2* promoter fused to GFP (*str-2::GFP*) was first expressed in the late embryo, where GFP expression could be detected in approximately ten cells (Figure 1A). Expression became more restricted after hatching and by late L1 was present strongly in AWC olfactory neurons and faintly in the ASI chemosensory neurons (Figures 1B and 2B). Other odorant receptors such as ODR-10 are localized to the cilia of olfactory neurons, where odorant detection occurs. To ask whether STR-2 also localizes to the cilia, GFP was fused to its C terminus to create a fluorescently tagged STR-2 protein (STR-2::*GFP*; Dwyer et al., 1998). The STR-2::*GFP* fusion gene was expressed strongly in the AWC cilia of transgenic animals, with faint expression in the cell body that was excluded from the nucleus (Figure 1C). Expression in the AWC olfactory neurons and localization to their cilia suggest that STR-2 could be a receptor for an attractive odorant.

C. elegans chemosensory neurons, including the olfactory neurons AWA, AWB, and AWC, exist as bilaterally symmetric pairs. GFP fusions to the receptor genes ODR-10 and STR-1 are expressed in the AWA and AWB neurons, respectively, in both the left and right neurons

of the pair. For example, in a transgenic strain containing a *str-1::GFP* fusion, 100% of the animals in a population express GFP in both AWB left (AWBL) and AWB right (AWBR) (Figure 1D). By contrast, we found that *str-2::GFP* expression in the AWC neurons is bilaterally asymmetric. In a strain with a *str-2::GFP* transgene integrated on chromosome I (*kyls140*), 42% of the animals expressed GFP solely in AWCL, and the other 58% of the animals expressed GFP solely in AWCR ($n = 198$, Figures 1E and 1F). No animals expressed GFP in both AWC neurons. Therefore, *str-2::GFP* appears to be stochastically expressed in AWCL or AWCR, but it is invariably restricted to just one of the two neurons.

The potential to express the *str-2::GFP* fusion genes reveals a difference between the two AWC neurons. *str-2::GFP* expression is asymmetric regardless of the chromosomal location of the *str-2::GFP* transgene. Four independent *str-2::GFP* strains with the transgenes integrated on chromosomes I, IV, V, or X expressed GFP in just one AWC neuron, with about half of the animals in a population expressing GFP in AWCL and the other half expressing GFP in AWCR (see Experimental Procedures). Asymmetric expression was observed in both homozygous and heterozygous integrants, as well as animals bearing extrachromosomal arrays of *str-2::GFP*. These *str-2::GFP* integrants were used to monitor *str-2* expression in all experiments; subsequent references to *str-2* expression refer to *str-2::GFP* expression.

Although asymmetric regulation only requires the *str-2* promoter, the STR-2::*GFP* translational fusion was also expressed asymmetrically, with transgenic animals showing expression only in the AWCL cilia, or the AWCR cilia, but never in both. The *str-2* promoter could also

ULL
Fru
RA

UNIA UNI
UNIA UNI

BRA
H
UNIA UNI
UNIA UNI

LIC
Franc
RAR

UNIA UNIVER
UNIA UNIVER

BRA
n. Fran
M

UNIA UNI
UNIA UNI

LIC
Franc
RARI

UNIA UNIVER
UNIA UNI



Vertical text on the left side, possibly bleed-through or a stamp, including the word "UNIVERSITY" and some illegible characters.

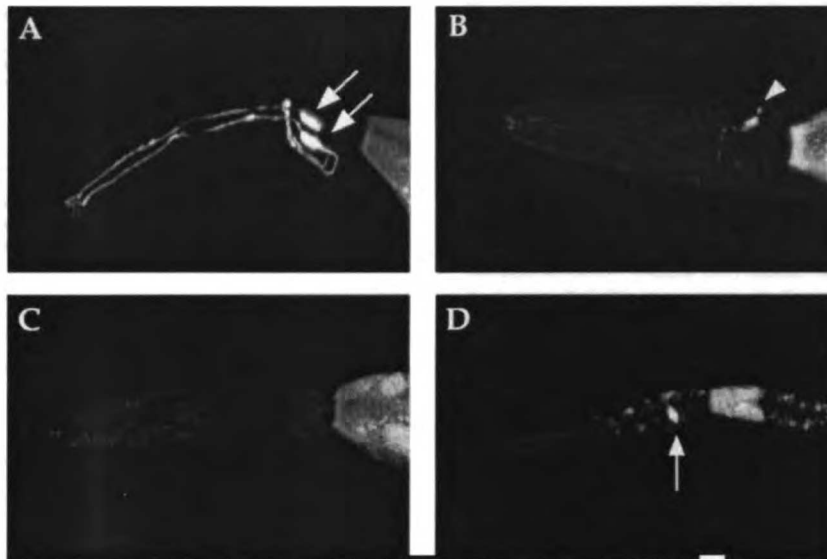


Figure 2. Ca^{2+} and cGMP Signaling Regulate *str-2::GFP* Expression

(A) *str-2::GFP* is expressed in both AWC neurons in an *unc-36* mutant animal.
 (B) *str-2::GFP* is expressed in neither AWC neuron in an *unc-43(gf)* mutant animal. Arrowhead indicates faint ASI expression.
 (C) *str-2::GFP* is not expressed in an *odr-1* adult animal.
 (D) *str-2::GFP* is expressed in one AWC neuron in an *odr-1* L1 animal.
 Images are a confocal z series collapsed into one plane; anterior is left, and dorsal is up.

confer asymmetric expression onto other genes. A *str-2::ODR-10::GFP* fusion was expressed and localized to the AWC cilia in an asymmetric fashion similar to *str-2* (in an extrachromosomal array line, 35% of transgenic animals expressed GFP in AWCL, 56% in AWCR, and 9% did not express GFP, $n = 179$), whereas ODR-10 expression under its own promoter is symmetric in the two AWA neurons. Furthermore, animals with both the *str-2::GFP* transgene and the *str-2::ODR-10-GFP* translational fusion gene always expressed both transgenes in the same AWC neuron. Although the *str-2* promoter reveals an intrinsic difference between the two AWC neurons, the expression of the endogenous *str-2* RNA and protein have not been determined. Transgenes do not necessarily recapitulate the precise expression of endogenous genes, so it is most conservative to consider *str-2::GFP* expression simply as a marker for one AWC neuron. We will refer to a *str-2*-expressing AWC cell as AWC^{ON} , and a non-*str-2*-expressing AWC cell as AWC^{OFF} .

The stochastic nature of *str-2* expression is reminiscent of other developmental events in which cells that are initially equivalent achieve distinct cell fates by lateral signaling. In many systems, including *C. elegans*, lateral signaling is mediated by a pathway involving the Notch receptor. To ask whether Notch signaling regulates the decision for an AWC neuron to express *str-2*, expression of the *str-2::GFP* transgene was examined in several mutants affecting the Notch pathway. *C. elegans* has two Notch homologs, *glp-1* and *lin-12* (Yochem et al., 1988; Austin and Kimble, 1989; Yochem and Greenwald, 1989). *str-2* expression in the AWC neurons

was asymmetric, with a wild-type ratio of AWCL and AWCR cells, in *lin-12* loss-of-function (*lf*) and gain-of-function (*gf*) mutants, *glp-1* null mutants, *glp-1(ts)* mutants, and in a mutant for the Notch ligand, *lag-2* (see Experimental Procedures). These results suggest that Notch signaling is not required for *str-2* asymmetry. It is possible that *glp-1* and *lin-12* are required but redundant for this decision; *glp-1 lin-12* double mutants were not examined because they arrest before the stage when *str-2* is first upregulated in AWC.

The Basal State for *str-2* Expression in a Single AWC Neuron Is Off

To determine whether *str-2* is expressed in an AWC neuron in the absence of its contralateral partner, we killed precursors of either AWCL or AWCR early in development. The operated adult animals were then examined for *str-2* expression in the surviving AWC neuron. The two AWC neurons derive from different cell lineages that separate at the eight cell stage. The AWCL precursor (ABplpaa) and the AWCR precursor (ABprpaa) were laser killed in embryos at about the 50-cell stage. At this point in development, each precursor cell gives rise to 15 cells, including AWC. When either the AWCL or the AWCR precursor was killed, the remaining AWC neuron failed to express *str-2* (Table 1). Control cell ablations confirmed that killing AWC precursors resulted in elimination of the expected cells (see Experimental Procedures). These results suggest that an AWC neuron requires a signal from the other AWC neuron or a closely related cell in order to express *str-2*. In the absence of

IC
Fran

RAI

IA UNIV
IA UNIV

ERA

IC

Franc

RAR

IA UNIVER
IA UNIVER

1881

IA UNIVER
IA UNIVER

IC

Franc

RAR



IC
Franc
RAR
IA UNIVER
IA UNIVER

1881

IA UNIVER
IA UNIVER

IC

Franc
RAR

Table 1. Effects of Embryo and L1 Cell Ablations on *str-2* Expression in AWC

Embryonic Ablations	Percentage with <i>str-2::GFP</i> on		No. of Animals
	AWCL	AWCR	
Mock kill	47	53	n = 17
Kill AWC precursor*	0	N/A	n = 11
Kill AWC precursor*	N/A	0	n = 17
Kill AWC precursor* in <i>unc-36</i>	100*	N/A	n = 3

L1 Ablations		
AWC Killed	Percentage with <i>str-2::GFP</i> in Remaining Neuron	
AWC ^{ON}	0	AWCR, n = 36 AWCL, n = 29
AWC ^{OFF}	100	AWCR, n = 4 AWCL, n = 4

* AWC precursor is AB_{prpa}; AWCL precursor is AB_{pipa}.
* Statistically different from control, p = 0.003.

its contralateral partner or a closely related cell, the basal state for *str-2* expression in an AWC neuron is off.

To ask whether cell signaling was required to maintain the AWC^{ON} and AWC^{OFF} fates, AWC neurons were killed in the L1 stage after *str-2* expression resolved to a single AWC neuron. When AWC^{ON} was killed in L1 after strong *str-2* expression appeared, the other AWC did not express *str-2* in the adult (Table 1). Similarly, if AWC^{OFF} was killed after *str-2* was strongly expressed in AWC^{ON}, expression of *str-2* in AWC^{ON} did not change (Table 1). Thus, the state of *str-2* expression is stable once AWC^{ON} and AWC^{OFF} are generated in the L1 stage. The decision to express *str-2* must be made at some time between the 50-cell stage and the late L1 stage.

Ca²⁺ Signaling Inhibits *str-2* Expression

A genetic screen was performed to identify mutants defective in *str-2* asymmetry. This screen yielded ten mutations in seven complementation groups that led to *str-2* expression in both AWC neurons (Table 2). New alleles of the previously identified genes *unc-2*, *unc-36*, *unc-43*, and *unc-44* were identified. *unc-2* and *unc-36* encode $\alpha 1$ and $\alpha 2$ subunits of a voltage-gated calcium

Table 2. Neuronal Symmetry Mutants (*nsy*)

Mutants	Percentage with 2 AWC ^{ON}	n
<i>unc-2(ky390)</i> X	80	94
<i>unc-2(ky385)</i> X	70	229
<i>unc-36(ky386)</i> III	77	78
<i>unc-43(ky384)</i> IV	88	29
<i>unc-44(ky384)</i> IV	23	168
<i>nsy-1(ky397)</i> II	100	34
<i>nsy-1(ky400)</i> II	98	55
<i>nsy-2(ky388)</i> III	68	62
<i>nsy-3(ky389)</i> V	96	107
<i>nsy-3(ky389)</i> +	30	60
<i>nsy-3(ky399)</i> V	92	301
<i>nsy-3(ky399)</i> +	51	130

(Ca²⁺) channel, respectively (Schafer and Kenyon, 1995; Lee et al., 1997); *unc-43* encodes the calcium/calmodulin-dependent protein kinase CaMKII (Reiner et al., 1999); *unc-44* encodes a *C. elegans* homolog of ankyrin (Otsuka et al., 1995). These four *unc* genes are widely expressed in the nervous system. All of the *unc* mutants from our screen exhibited uncoordinated movement and appeared similar to previously identified loss-of-function mutations in these genes. Indeed, canonical loss-of-function alleles of each gene also affected *str-2* asymmetry (Table 3 and below). The three remaining complementation groups may define novel genes required to establish or maintain *str-2* asymmetry. These genes have tentatively been named neuronal symmetry (*nsy*) genes. *nsy-1(ky397, ky400)* and *nsy-2(ky388)* mutations are fully recessive, whereas both alleles of *nsy-3(ky389, ky399)* are semidominant (Table 2). *nsy-1* mutants are coordinated but egg-laying defective; *nsy-2* and *nsy-3* mutants exhibit superficially normal movement and egg laying. The *unc-44* mutant showed a distinctive defect in which 0, 1, or 2 AWC neurons could express *str-2* (Table 3); in all other mutants at least one AWC neuron expressed GFP. Based on the number of alleles isolated per gene, this screen is not saturated and additional genes that affect *str-2* asymmetry are likely to exist.

Three genes identified in the genetic screen affect calcium signaling. To confirm the results of the screen, *str-2* expression was examined in the canonical *unc-2(e55)* and *unc-36(e251)* loss-of-function alleles. In both cases, many animals expressed *str-2* in both AWC neurons (Table 3 and Figure 2A). *unc-2(e55)* had a milder defect, perhaps because it is a partial loss-of-function mutation. These results indicate that the *unc-2* and *unc-36* Ca²⁺ channel subunits are required to repress *str-2* and define the AWC^{OFF} neuron.

The Ca²⁺ and calmodulin-dependent kinase CaMKII converts an increase in Ca²⁺ levels into protein phosphorylation of many targets (Braun and Schulman, 1995); *unc-43* encodes a *C. elegans* CaMKII homolog that is expressed in neurons (Reiner et al., 1999). A loss-of-function allele of *unc-43* was identified in the screen for animals with two AWC^{ON} cells. Expression of *str-2* was examined in both null *unc-43(lf)* mutants and *unc-43(gf)* mutants that are predicted to have calcium-independent kinase activity. These experiments revealed that *unc-43* acts as a switch for *str-2* expression. *str-2* was expressed in both cells in an *unc-43(lf)* background, and it was often expressed in neither cell in an *unc-43(gf)* background (Table 3 and Figure 2B). Thus, the level of *unc-43* CaMKII activity can determine whether a cell adopts the AWC^{ON} or AWC^{OFF} fate. This result suggests that regulation of *unc-43* CaMKII is central to asymmetric *str-2* expression.

The presence of two AWC^{ON} cells in Ca²⁺ signaling mutants could result from altered signaling between AWC neurons or from a cell-intrinsic change in AWC that makes *str-2* expression independent of the normal inducing signal. If the calcium signaling molecules act within the AWC neurons, they could affect either the signaling or the responding cell in the interaction. To begin to distinguish between these models, ablations of AWC precursors were performed in an *unc-36* background (Table 1). In three animals in which the AWC

Table 3. Genes Required for Asymmetric Expression of *str-2*

Strain	Percentage of Animals			n
	2 AWC ^{off}	1 AWC ^{on} 1 AWC ^{off}	2 AWC ^{on}	
Wild type	0	100	0	500
Axon guidance mutants				
<i>unc-76(e911)</i>	43	57	0	114
<i>sax-5(ky118)</i>	52	47	1	79
<i>vab-3(e648)</i>	51	47	2	126
<i>sax-3(ky123)</i>	56	44	0	126
Axon guidance/cytoskeleton mutants				
<i>unc-33(e204)</i>	14	59	27	195
<i>unc-44(e362)*</i>	21	62	18	195
Ca²⁺ signaling mutants				
<i>unc-2(e55)*</i>	13	39	48	158
<i>unc-36(e251)*</i>	0	3	97	121
<i>unc-43(n1186)*</i>	3	5	92	101
<i>unc-43(n498gf)</i>	80	20	0	133
<i>unc-43(gf); unc-36</i>	65	25	10	166
<i>egl-2(n693gf)</i>	0	1	99	166
Olfactory signaling mutants				
<i>odr-3(n1605)</i>	0	100	0	150
<i>odr-1(n1933)</i>	100	0	0	150
<i>daf-11(sa195), 15°C</i>	100	0	0	150
<i>daf-11, L1/L2, 15°C</i>	0	100	0	98
<i>odr-1, L1/L2</i>	21	79	0	114
<i>tax-4(p678)</i>	13	81(56)	6	162
<i>tax-2(p689)</i>	4	80(10)	16	69
<i>odr-1; tax-4</i>	100	0	0	126
<i>odr-1; tax-4 L1/L2</i>	4	96	0	140

All animals were scored at 20°C, except *daf-11* animals, which were scored at 15°C to allow non-dauer development. Animals were scored as adults, unless otherwise indicated. Numbers in parentheses for *tax-2* and *tax-4* are percentages of animals that have 1 AWC^{on} with dim expression. Asterisks indicate genes also identified in screen for 2 AWC^{on} animals.

precursor was killed, the remaining AWC cell expressed *str-2*. This result suggests that *unc-36* affects *str-2* expression in an isolated AWC neuron, so that in *unc-36* mutants AWC^{on} can be generated without the normal inducing signal. In one model, the normal AWC signaling event might inhibit Ca²⁺ signaling and CaMKII in one AWC neuron, resulting in the AWC^{on} fate.

unc-43/CaMKII could be either a target or a regulator of the *unc-2* and *unc-36* Ca²⁺ channel subunits. If Ca²⁺ entry through the channel increases *unc-43* kinase activity, then the *unc-43(gf)* mutation should be epistatic to the *unc-36(lf)* phenotype. Conversely, if *unc-43* kinase regulates Ca²⁺ channel activity, Ca²⁺ channel mutations should be epistatic to *unc-43(gf)*. Double mutant analysis indicates that *unc-43(gf)* is epistatic to *unc-36*, suggesting that Ca²⁺ entering through the *unc-2* and *unc-36* channels stimulates *unc-43* to inhibit *str-2* expression in one neuron (Table 3).

The voltage-activated Ca²⁺ channel encoded by *unc-2/36* is related to channels that are regulated by membrane potential. To ask whether neuronal excitability regulates *str-2* expression, the *str-2* reporter gene was examined in *egl-2(n693)* mutants. *egl-2(n693)* encodes an ERG-type potassium channel that opens at a lower voltage than the wild-type channel, resulting in defects in AWC function, egg laying, and other behaviors (Weinshenker et al., 1999). In *egl-2(n693)* mutants, *str-2* was expressed in both AWC neurons (Table 3). Reduced excitability of the AWC neurons in *egl-2(n693)* mutants might prevent the voltage-dependent Ca²⁺ channel from opening, thereby affecting *str-2* expression.

Ca²⁺ signaling is specifically required for *str-2* asymmetry and not globally required for left-right asymmetry. The ASEL and ASER neurons exhibit asymmetric expression of three guanylyl cyclase genes, including *gcy-5*, which is always expressed in ASER (Yu et al., 1997). *gcy-5* was asymmetrically expressed only in ASER in both *unc-43(lf)* (n = 45) and *unc-43(gf)* (n = 50) mutants.

str-2 Expression Is Altered in Axon Guidance Mutants

The AWC cell bodies are distant from one another, but their axons contact one another at several points in the circumferential nerve ring (Figures 3A-3C) (White et al., 1986). Therefore, if the decision to express *str-2* is made through cell-cell interactions between AWCL and AWCR, a likely place for this communication to occur is at the AWC axons. To ask whether axon contact is required for the decision to express *str-2*, expression of *str-2* was examined in four different axon guidance mutants: *unc-76*, *sax-5*, *vab-3*, and *sax-3*. These mutants all display premature axon termination of chemosensory axons in the nerve ring (Hedgecock et al., 1985; Zallen et al., 1998, 1999). In all four mutants, many animals had no *str-2* expression in AWC (Table 3 and Figure 3E). As expected from previous results, all four mutants exhibited premature termination of the AWC axons (Figure 3D and data not shown). These results suggest that normal axon guidance, perhaps to allow contact between the two AWC axons, is required for asymmetric expression of *str-2*. Since AWC^{off} is the default state,

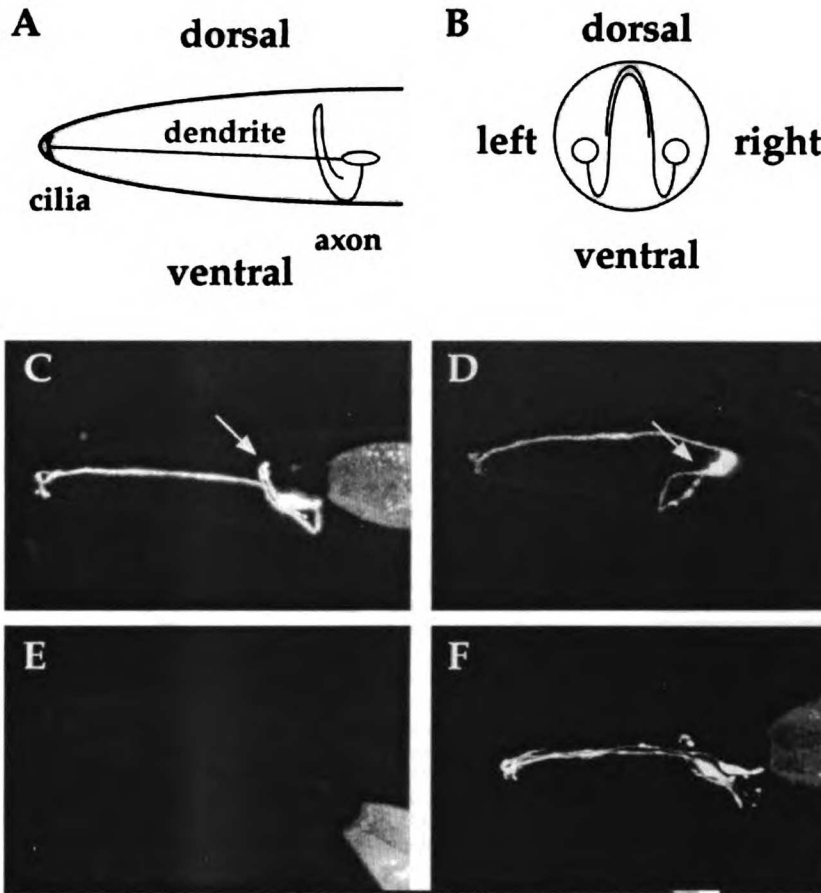


Figure 3. Axon Guidance Mutants Are Defective in *str-2* Asymmetry

(A) A lateral diagram showing the morphology of one AWC neuron.

(B) A cross-sectional diagram of both AWC axons. The two neurons are in contact in the dorsal half of their trajectory and synapse on each other.

(C) A lateral view of the AWC neuron as visualized by *str-2::GFP* expression. The axon projects dorsally past the cell body and then wraps around the contralateral side. Arrow indicates the dorsal midline.

(D) *str-2::GFP* expression in an *unc-76* mutant animal. The AWC axon often terminates prematurely (arrow) and fails to reach the dorsal midline.

(E) *str-2::GFP* is not expressed in this *unc-76* mutant animal.

(F) *str-2::GFP* can be expressed in both AWC neurons in *unc-33* mutants.

(C)–(F) are confocal z series images collapsed into a single plane; anterior is left, and dorsal is up.

contact with the contralateral AWC neuron may induce *str-2* expression and the AWC^{ON} fate.

The genetic screen for *str-2* expression in both AWC neurons yielded one allele of the axon guidance gene *unc-44* (Hedgecock et al., 1985). *str-2* was expressed in either 0, 1, or 2 AWC cells in *unc-44* mutants (Tables 2 and 3). A similar effect was observed in *unc-33* mutants, which share many phenotypes with *unc-44* (Hedgecock et al., 1985) (Table 3 and Figure 3F). *unc-44* encodes a *C. elegans* ankyrin, which may have a general role in regulating cell polarity and the cytoskeleton (Otsuka et al., 1995). In addition to axon guidance defects, both *unc-33* and *unc-44* mutants have abnormal microtubule structures in sensory cilia (Hedgecock et al., 1985). The defective *str-2* expression in these mutants could result

from a combination of altered axon guidance, altered cilia, and other consequences of cytoskeletal defects.

The AWC neurons make several synapses onto one another in the nerve ring (White et al., 1986). Mutants with defects in synaptic transmission were examined for *str-2* expression. *snt-1*, *unc-104*, and *unc-13* are genes that are required for chemical neurotransmission: *snt-1* encodes a synaptotagmin homolog, *unc-104* encodes a kinesin-related protein that transports vesicles to synapses, and *unc-13* encodes a novel conserved protein that regulates synaptic release (Hall and Hedgecock, 1991; Maruyama and Brenner, 1991; Nonet et al., 1993). *unc-7* encodes a membrane protein that is a possible gap junction component (Starich et al., 1993). In all four mutants, asymmetry of *str-2* was unaffected (see Experi-

ll
Fra
RA



IA UNIV
IA UNI



RA

H



IA UNIV
IA UNI



IA UNIV
IA UNI



IC

Franc

RAR



IA UNIVER
IA UNIVER



IBRA

u Fra

M



IA UNIVER
IA UNIVER



IC

Franc

RAR



IA UNIVER
IA UNIVER



IA UNIVER
IA UNIVER

LIBRARY
UNIVERSITY OF
TORONTO
1827



mental Procedures). Therefore, although neuronal activity and axon contact play a role, classical fast synaptic transmission may not be involved in the decision to express *str-2*.

Olfactory Signaling Components Are Required to Maintain *str-2* Expression

Within olfactory neurons, the *unc-2/unc-36* Ca²⁺ channels could potentially respond to depolarization at the sensory cilia, depolarization at neuronal synapses, or G protein-mediated second messenger pathways. To explore these possibilities, *str-2* expression was examined in mutants that affect olfactory signal transduction. AWC olfactory signaling involves a cGMP second messenger and requires the Gi/Go-like G α protein ODR-3, the TAX-2/TAX-4 cGMP-gated channel, and the ODR-1 and DAF-11 guanylyl cyclases (Birnbay and Thomas, personal communication; N. L'Etoile and C. I. B., unpublished data; Coburn and Bargmann, 1996; Komatsu et al., 1996; Roayaie et al., 1998). *str-2* was not expressed in either of the AWC neurons in adult animals with mutations in the guanylyl cyclase genes *daf-11* and *odr-1* (Figure 2C and Table 3). Mutations in either the *tax-2* or *tax-4* subunit of the cyclic nucleotide-gated channel decreased overall levels of *str-2* expression and sometimes resulted in two AWC^{OFF} cells (Table 3). *tax-2/4* mutants occasionally expressed *str-2* in both AWC neurons, but one neuron was usually much fainter than the other, unlike Ca²⁺ signaling mutants, where two AWC neurons expressed *str-2* at equivalent levels. Thus, the *tax-2/4* channel mutants disrupt *str-2* expression in several ways, but they act chiefly to lower *str-2* expression.

The low but visible level of *str-2* expression in channel mutants contrasted with the guanylyl cyclase mutants in which no *str-2* expression could be detected. This result suggests that the guanylyl cyclases have slightly different functions from the *tax-2/4* channel, perhaps because cGMP regulates multiple targets. *tax-4; odr-1* double mutants did not express any *str-2* in the AWC neurons (Table 3), like *odr-1* mutants alone. *str-2* expression was normal in *odr-3* mutants (Table 3). Several other G α proteins are expressed in AWC and may play a role in olfaction (Jansen et al., 1999), so lack of a phenotype in *odr-3* mutants could be due to G protein redundancy.

The cGMP signal transduction mutants and the Ca²⁺ channel mutants had opposite effects on *str-2* expression, suggesting that these pathways act independently in AWC. Indeed, in *odr-1* mutants, *daf-11* mutants, *daf-11; odr-1* mutants, and *tax-4; odr-1* mutants, the initial decision to express *str-2* was mostly unaffected. *str-2* expression was present in one AWC neuron in the L1/L2 larval stage, but its expression disappeared later during the L2-L3 stage (Table 3 and Figure 2D). This phenotype is specific to the cGMP mutants, since other mutants that lack *str-2* expression, such as *unc-76* and *unc-43(gf)*, had reduced expression in both L1 stages and in adults. These results suggest that olfactory cGMP signaling is required to maintain *str-2* expression but is not required to create the initial asymmetry.

Double Mutant Analysis of Genes Required for *str-2* Expression

str-2::GFP expression appears to be regulated by genes that fall into four different categories: (1) axon guidance

mutants in which there are two AWC^{OFF} cells; (2) cytoskeleton/axon guidance mutants that can have two AWC^{OFF} cells or two AWC^{ON} cells; (3) Ca²⁺ signaling mutants in which there are two AWC^{ON} cells; and (4) cGMP signaling mutants that have two AWC^{OFF} cells after the L1 stage due to a defect in *str-2* maintenance. For most mutant classes, some animals exhibited the normal 1 AWC^{ON}/1 AWC^{OFF} pattern. To determine the relationship among these different pathways with regard to their effects on *str-2* expression, double mutants were made with genes from different pathways (Table 4 and Figure 4A) and examined for the frequency of the aberrant two AWC^{ON} and two AWC^{OFF} classes.

Ca²⁺ signaling mutants were epistatic to the axon guidance mutant *unc-76*, suggesting that the initial information provided by axon contact must be interpreted through the Ca²⁺ signaling pathway. These results are consistent with the laser killing experiment showing that AWC communication is not required for *str-2* expression in *unc-36* mutants. The cGMP pathway was epistatic to the Ca²⁺ signaling mutants, suggesting that the maintenance pathway is needed even when *str-2* expression comes on via abnormal Ca²⁺ signaling. The Ca²⁺ signaling mutants were epistatic to the mutants *unc-33/44*, which affect the cytoskeleton and axon guidance, but paradoxically the cytoskeletal mutants were epistatic to cGMP signaling mutants. A possible explanation for this result is that cytoskeletal factors act both in axon guidance and in another process. For example, they could act in axon guidance upstream of Ca²⁺ signaling to promote expression of *str-2* in one cell (leading to the two AWC^{OFF} phenotype) and also at a later step to inhibit *str-2* expression in one cell (leading to the two AWC^{ON} phenotype). This model is consistent with the pleiotropic effects of *unc-33* and *unc-44* on cell polarity, axon guidance, and cilium morphology.

Discussion

Lateral Signaling through Axon Contact and CaMKII Controls *str-2* Expression

The *C. elegans* candidate odorant receptor *str-2* is expressed in a stochastic, asymmetric fashion in the AWC olfactory neurons. An individual animal expresses *str-2* in either the left AWC or the right AWC neuron, but never in both. *str-2* is the only known odorant receptor that is expressed at high levels in AWC, so at this point it is unclear whether AWC^{OFF} expresses completely different receptors from AWC^{ON}, or whether the two cells share most receptors other than *str-2*. Laser ablations and genetic experiments suggest that both AWC^{OFF} and AWC^{ON} respond to attractive odors (data not shown).

A model for *str-2* regulation is proposed in Figure 4B. In the absence of cell signaling, the AWC neurons do not express *str-2* (Step 1). This *str-2*-negative state is probably maintained by Ca²⁺, which enters the cell through a voltage-gated Ca²⁺ channel and activates *unc-43*/CaMKII. During normal development, the axons of the two AWC neurons communicate either directly or via another axon in the nerve ring, and *str-2* expression is specified in one of the two cells. The initial signal for asymmetry between the two AWC neurons is unknown, but an essential aspect of their communication involves

Table 4. *str-2* Expression in Double Mutants

Strain	Percentage of Animals			n	
	2 AWC ^{OFF}	1 AWC ^{ON} 1 AWC ^{OFF}	2 AWC ^{ON}		
Wild type	N2	0	100	0	>500
Double mutants					
Axon guidance alone					
Axon guidance and Ca ²⁺	<i>unc-76</i>	43	57	0	114
	<i>unc-76; unc-2</i>	19	43	38	150
	<i>unc-76; unc-36</i>	10	23	67	136
	<i>unc-76; unc-43(lf)</i>	2	5	93	116
Axon guidance and cGMP					
	<i>unc-76; odr-1</i>	97	3	0	118
Ca²⁺ signaling alone					
	<i>unc-2</i>	13	39	48	158
	<i>unc-36</i>	0	3	97	121
	<i>unc-43(lf)</i>	3	5	92	101
Ca²⁺ signaling and cGMP					
	<i>unc-2; daf-11</i>	100	0	0	82
	<i>unc-36; daf-11</i>	98	2	2	131
	<i>unc-36; odr-1</i>	98	2	0	81
	<i>unc-43(lf); odr-1</i>	100	0	0	125
Ca²⁺ signaling and cytoskeleton					
	<i>unc-2; unc-33</i>	1	21	78	114
	<i>unc-2; unc-44</i>	1	40	59	81
	<i>unc-36; unc-33</i>	0	0	100	82
	<i>unc-36; unc-44</i>	1	5	94	121
cGMP signaling alone					
	<i>odr-1</i>	100	0	0	150
	<i>daf-11</i>	100	0	0	150
cGMP signaling and cytoskeleton					
	<i>odr-1; unc-33</i>	15	33	52	115
	<i>odr-1; unc-44</i>	17	38	45	196
	<i>daf-11; unc-33</i>	28	65	8	219
	<i>daf-11; unc-44</i>	23	58	19	150

Mutant alleles as in Table 2, except *unc-43(lf); odr-1(n1936)*. All animals scored at 20°C, except *daf-11* mutants, which were scored at 15°C to allow non-dauer development.

the *unc-2/36* calcium channel and *unc-43*/CaMKII. At some point one cell takes on the AWC^{OFF} fate (shown as the left cell in Figure 4B) and instructs the other cell to take on the AWC^{ON} fate (Step 2). The AWC^{ON} fate is then maintained by the cGMP signaling pathway (Step 3).

When one AWC precursor was killed early in development, the surviving AWC neuron always became AWC^{OFF}. This result indicates that a descendent of the ablated AWC precursor is required to induce *str-2* expression and the AWC^{ON} fate. AWC itself is the best candidate to be the descendent that provides this inductive signal, though it could be provided by a close relative of AWC. The two AWC axons contact one another in the nerve ring, whereas the AWC relatives are not closely associated with AWC (White et al., 1986). In mutants in which AWC axons terminate prematurely, *str-2* is often not expressed, suggesting that axon contact is required for AWC communication.

The decision to express *str-2* appears to be fixed by the end of the L1 stage, after expression is upregulated in AWC. Ablation of AWC^{ON} in the L1 stage did not cause AWC^{OFF} to express *str-2*, nor did ablation of AWC^{OFF} cause AWC^{ON} to turn off *str-2*. The ablations define a period between the 50-cell stage and the late L1 stage in which a stable pattern of *str-2* asymmetry is established. The course of *str-2::GFP* expression changes during that period: *str-2::GFP* is first expressed in a number of cells during late embryonic development and expression becomes progressively more restricted until only one AWC neuron shows expression in larvae.

The stochastic AWC interaction that establishes *str-2* expression is reminiscent of lateral signaling pathways, in which cells of equivalent potential interact with each other to generate two distinct cell fates. Lateral signaling

decisions usually involve the Notch signaling pathway, which has been implicated in a broad spectrum of cell fate decisions in animal development (Robey, 1997; Greenwald, 1998). While an involvement of Notch signaling in *str-2* asymmetry has not been definitively ruled out, *str-2* expression is not altered in many mutants of this pathway. Moreover, our direct mutant screens have not yet revealed any genes in the *C. elegans* Notch pathway. Regulation of *str-2* expression may therefore define a novel type of lateral signaling pathway.

The signaling pathway that induces *str-2* expression is different in several fundamental ways from known lateral signaling pathways. AWC signaling appears to take place in mature neurons that have already extended axons and made contacts with each other. Notch pathways usually act on undifferentiated precursor cells to prevent differentiation or to determine cell fate. Another unique property of the decision to express *str-2* is the central role of Ca²⁺ signaling. Analysis of *str-2* expression in CaMKII *unc-43(lf)* and *unc-43(gf)* mutants indicates that CaMKII acts as a switch for *str-2* expression, probably as a result of Ca²⁺ entering through the *unc-2/36* Ca²⁺ channel. Ca²⁺ signaling is required for each AWC cell to repress *str-2* and take on the AWC^{OFF} fate: ablation of an AWC precursor in *unc-36* Ca²⁺ channel mutants indicates that an isolated AWC neuron took on the AWC^{ON} fate instead of the normal AWC^{OFF} fate. These results and the analysis of double mutants suggest that signaling between AWC neurons inhibits Ca²⁺ signaling in the AWC^{ON} cell. Ca²⁺ signaling has well-established roles in synaptic transmission and neuronal plasticity; these results indicate that Ca²⁺ pathways can also act to diversify neuronal cell fates during development.

We have not yet identified the receptors or ligands

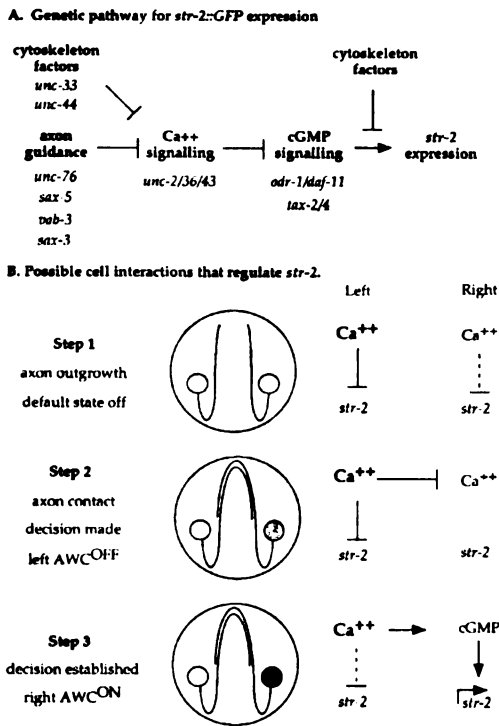


Figure 4. Model for *str-2* Regulation
(A) Epistasis based on double mutant analysis.
(B) Possible cell interactions involved in the choice to express *str-2* in a hypothetical example in which the right AWC neuron will become AWC^{ON} (see text for details).

that allow the AWC neurons to recognize and signal to each other. Examination of *C. elegans* neuroanatomy suggests that many neurons recognize their contralateral partner; most bilaterally symmetric neurons in the nerve ring terminate at the dorsal midline where they make a gap junction with the axon from their contralateral partner (White et al., 1986). The two AWC neurons make chemical synapses onto each other in the nerve ring, suggesting that they have an intrinsic affinity for each other among the 180 or so other axons in the neuropil. Molecules that mediate AWC self-recognition, which might include homophilic cell adhesion molecules, could initiate the signaling between the two AWC axons. Signaling should lower the activity of the CaMKII Ca²⁺ signaling pathway, which regulates *str-2* expression. Although there are synapses between the two AWC axons, genes involved in classical neurotransmission do not appear to be required for *str-2* asymmetry, suggesting that other forms of cell signaling are involved. Many peptide factors and cell adhesion pathways can regulate calcium signaling. Developing snail neurons display a large Ca²⁺ influx and change their Ca²⁺ setpoint in response to specific target contact (Zoran et al., 1993).

The initial asymmetry between AWC neurons could be generated by any process that is slightly variable between animals. The first AWC axon to arrive at the dorsal midline could become competent to induce the

AWC^{ON} fate in the contralateral AWC neuron. Alternatively, since Ca²⁺ signaling plays a role in the decision, differences in electrical activity might create a bias in CaMKII activity between the two AWC cells. The connections that the two AWC neurons make in the nerve ring are mostly symmetrical in adults, but there might be additional axons that make asymmetrical contacts in the embryo and contribute to AWC asymmetry.

In the final stages of lateral signaling, one cell's stochastic advantage is amplified into an irreversible decision. In Notch signaling, a small initial asymmetry in receptor-ligand expression is amplified by both positive and negative feedback loops to yield two distinct cell types. The *str-2* lateral signaling decision might use Ca²⁺ signaling to reinforce the decision. Neuronal activity downregulates the cell adhesion molecules apCAM (Mayford et al., 1992) and fasciclin II (Schuster et al., 1996); a related mechanism could allow Ca²⁺ feedback to amplify an asymmetric interaction mediated by adhesion molecules. Alternatively, Ca²⁺ may act downstream of all earlier signaling pathways to execute the *str-2* decision.

The screen for genes affecting *str-2* asymmetry yielded four known *unc* genes and three new *nsy* genes. The *nsy* genes appear to be less pleiotropic than the *unc* genes and may be more specific to the AWC cell fate decision. The *nsy* genes could encode the receptors or ligands involved in AWC interactions, transcription factors that regulate *str-2* expression downstream of CaMKII, or other signaling components. The dominant *nsy-3* mutations are particularly intriguing since many mutations in Notch, its ligand Delta, and the Enhancer of Split transcription factor have dominant phenotypes due to haploinsufficiency or altered function.

cGMP signaling appears to have a role in the maintenance of *str-2* expression. Direct observation and double mutant analysis suggest that cGMP signaling acts after Ca²⁺ signaling. In contrast to other mutants defective in the AWC^{ON} fate, the initial decision to express *str-2* asymmetrically appears to occur normally in cGMP signaling mutants, but expression is not maintained. It is possible that cGMP signaling also has an ancillary role in the decision to express *str-2*, since *tax-2/4(N)* mutants sometimes have two AWC^{ON} cells. cGMP levels are thought to be regulated by olfactory stimuli, so this pathway could link external olfactory cues to the regulation of gene expression within olfactory neurons. Overexpression of STR-2 or ODR-10 odorant receptors can affect *str-2* asymmetry (data not shown), but these results should be interpreted with caution, since inappropriate receptor expression could drive Ca²⁺, cGMP, or other signaling pathways to disrupt *str-2* asymmetry.

Interestingly, both the *unc-2* and *unc-36* Ca²⁺ channel subunits and the *tax-2/4* cGMP channel can be Ca²⁺ permeable yet appear to have opposite effects on *str-2* expression. These channels might function differently because of different subcellular localization in the cilia, axons, or cell body of AWC. It is also possible that they act in different cells, since the sites of action of these genes have not been determined. The Ca²⁺ channel and the cGMP channel may also be active at different times in development, so that one functions during the initial decision and the other predominates at later stages, during the maintenance of expression.

Does Calcium-Mediated Lateral Signaling Act in Other Systems?

Our studies of *str-2* expression show that alternative olfactory cell fates can be specified by calcium channels and CaM kinase. We speculate that Ca^{2+} signaling may act in other developmental systems where fine patterning occurs via neuronal interactions. Many regions of the nervous system contain dozens or hundreds of cell types that are distinguished by the expression of particular neurotransmitter receptors, channels, or neuropeptides. The signals that create this cellular diversity are mostly unknown; a few examples with interesting properties are described below.

In the R7 and R8 photoreceptor cells of *Drosophila*, cell interactions restrict and coordinate rhodopsin expression. The R7 cell can express either the rh3 or rh4 rhodopsin, while R8 can express either the rh5 or rh6 rhodopsin (Papatsenko et al., 1997; Chou et al., 1999). Neighboring R7/R8 pairs coordinately express rh3/rh5 or rh4/rh6, and an apparently random choice made by R7 instructs the choice made by the neighboring R8. Although the purpose of this regulation is unknown, the stochastic and coordinated nature of this phenomenon is reminiscent of *str-2* regulation and could involve a similar signaling pathway.

C. elegans has an overall left-right body plan; within this context, *str-2* expression creates an additional stochastic bilateral asymmetry. Other examples of stochastic bilateral asymmetry established through cell-cell interactions and activity occur in leeches and lobsters. In the leech nerve cord, individual AS neurons lie on alternate left and right sides of successive ganglia (Blair et al., 1990). An individual AS neuron develops from bilaterally paired embryonic homologs that likely interact through their axons to specify one to adopt the AS fate and the other the non-AS fate. Like the *str-2* decision, this patterning appears not to be predetermined, but rather specified through interactions among initially equivalent neurons during development. Lobsters provide another example of bilateral asymmetry that is both stochastic and activity regulated (Govind, 1992). Lobsters develop claws that are bilaterally asymmetric; one side forms as a major (crusher) claw, while the other side becomes a minor (cutter) claw, with the sidedness randomly chosen. Behavioral activity has been shown to be important during a critical period of development in which the more active side develops as a crusher. As with *str-2*, this decision seems to involve comparison of activity between two initially equivalent sides during a specific developmental period, which then results in bilateral asymmetry.

On a more speculative note, the lateral signaling mediated by axon contact that we observe for *str-2* expression has the potential to generate a precise arrangement of cells at a specific density defined by the axonal or dendritic arbor. In the mammalian retina, dozens of subclasses of bipolar cells, amacrine cells, and retinal ganglion cells appear to "tile" the retina so that dendrites for a given cell class cover the retina completely with minimal overlap (Wassle and Boycott, 1991; Grunert et al., 1994; Devries and Baylor, 1997; MacNeil and Masland, 1998). One way to generate this precise pattern would be a lateral signaling process whereby each cell's dendritic arbor signals to adjacent cells and drives them

into alternative fates. A regular, nonrandom spacing of cells has also been suggested to occur in the zebrafish olfactory epithelium (Baier et al., 1994).

Asymmetric expression of the *str-2* candidate odorant receptor reveals an intrinsic difference in the transcriptional program of the two AWC neurons. What is the significance of this regulation? One possibility is that it creates two independent AWC neurons that each have a distinct olfactory specificity. Alternatively, the asymmetric expression of receptors may allow for comparison of inputs between the two AWC neurons. Perhaps this organization increases discrimination between odors or creates a system for signal integration. Further understanding of this pathway could be provided by analysis of a *str-2* mutant, identification of a *str-2* ligand, or isolation of other AWC receptors and their ligands.

Experimental Procedures

Plasmid Construction

str-2 corresponds in part to the predicted gene C50C10.7, but cDNA clones of *str-2* isolated by RT-PCR had a 3' exon distinct from that predicted by the Genome Sequencing Consortium. The authentic STR-2 protein is 26% identical to *odr-10* at the amino acid level. A *str-2::GFP* fusion gene was prepared by using the polymerase chain reaction (PCR) to amplify 3.7 kb of sequence upstream of the predicted start site of *str-2* and the first seven amino acids of its coding region. A PstI site and a BamHI site engineered into the PCR primers were used to insert the amplified product into the GFP vector pPD95.75 (A. Fire et al., personal communication). The STR-2::GFP (C terminal tag) construct was prepared by using PCR to amplify 3.7 kb of sequence upstream of the predicted start site of *str-2* and the entire coding region except for the last six amino acids. A PstI site and a BamHI site engineered into the PCR primers were used to insert the amplified product into the GFP vector pPD95.75. The *str-2::ODR-10-GFP* fusion gene was generated by PCR using 3.7 kb upstream region without any of the *str-2* coding region. A PstI site and a BamHI site engineered into the PCR primers were used to insert the amplified product into a vector containing an *odr-10* cDNA fused to GFP at its carboxyl terminus (Sengupta et al., 1996).

Transgenic Strains

Germline transformation was carried out as described (Mello et al., 1991). The *lin-15* clone pJM23 (50 ng/ μ l) (Huang et al., 1994) and *str-2::GFP*, *str-2::ODR-10-GFP* or STR-2::GFP (50 ng/ μ l) were injected into *lin-15(n765)* animals. Transgenic animals were identified by rescue of the *lin-15(n765ts)* multivulval phenotype at 20°C. At least three independent lines were characterized for each transgene. Transgenes were integrated into *lin-15(n765ts)* by psoralen/UV mutagenesis. The *str-2::GFP* transgene was integrated onto chromosomes I, IV, V, and X to generate four independent integrated strains. All *str-2::GFP* integrated strains showed strong GFP expression in only one AWC neuron and weak expression in both ASI neurons. In the integrant on chromosome IV (*ky1s131*), 39% of the animals expressed GFP in AWCL and 61% in AWCR (n = 56); in the integrant on chromosome V (*ky1s137*), 52% of the animals expressed GFP in AWCL and 48% in AWCR (n = 21); in the integrant on the X chromosome (*ky1s138*), 51% of the animals expressed GFP in AWCL and 49% in AWCR (n = 221). Cell identification was based on the characteristic morphology and position of GFP-positive cell nuclei viewed by simultaneous fluorescence and Nomarski differential interference microscopy. Most crosses were performed with the integrant on chromosome I, *ky1s140*. A subset of mutants were analyzed with both *ky1s140* and the integrant on chromosome X, *ky1s138*, and yielded similar results in both strains.

Analysis of Candidate Mutations

Expression of *str-2::GFP* was examined in a *lin-12* loss-of-function mutant (*n676n930* at 25°C, n = 120) and two *lin-12* gain-of-function mutants (*n137n460* at 15°C, n = 160 and *n676n930* at 15°C, n =

117). A zygotic requirement for *glp-1* was examined in two mutants (*q339*, *n* = 36; *q175*, *n* = 52). A maternal requirement for *glp-1* was also examined with temperature shift experiments using the *glp-1* temperature-sensitive allele, *q224*. *glp-1* is essential for early embryonic inductive events, so shifts to the restrictive temperature were performed after this time period (*n* = 79). In all cases expression was normal (i.e., asymmetric expression in AWC, with about half the animals showing expression in AWCL and the other half in AWCR). Expression of *str-2::GFP* was also normal in four synaptic transmission mutants: *unc-13(e450)*, *n* = 50; *unc-104(e1265)*, *n* = 68; *snt-1(md172)*, *n* = 150; and *unc-7(e1390)*, *n* = 30. *str-2::GFP* expression was also examined in two mutants that affect downstream target neurons of AWC: asymmetric AWC expression was observed in *unc-86(rs46)* mutants (*n* = 196), which have defective AIZ interneurons, and in *txr-3(ks5)* mutants (*n* = 27), which have defective AIY interneurons.

Isolation of Mutations that Affect *str-2* Expression

str-2::GFP(ky15140); rol-6(e187) worms were mutagenized with EMS according to standard protocols and screened for ectopic expression of GFP under a fluorescence dissecting scope in the F2 generation (Anderson, 1995). From a screen of 9000 mutagenized genomes, ten independent mutants that fell into seven complementation groups were identified. Individual mutants expressed *str-2::GFP* in both AWC cells in 23%–100% of animals. Mutants were mapped with respect to Tc1 transposable element polymorphisms in the DP13 strain (Williams et al., 1992). Complementation testing was performed to identify alleles of previously characterized genes. The semidominant mutations *ky389* and *ky399* were tentatively assigned to the same gene because they mapped to the same region on the right arm of chromosome V and because animals heterozygous for both mutations have a *str-2* expression phenotype as severe as either homozygous mutant.

Laser Killing of AWC Neurons and AWC Precursors

AWC precursors were killed at approximately the 50-cell stage of embryogenesis. This stage was chosen because the founder cells could be identified relatively easily; later kills are substantially more difficult. Embryos were prepared by cutting *str-2::GFP* gravid adult hermaphrodites and transferring their embryos to a 5% agar pad in M9 solution. Cells were identified in embryos at the 28-cell stage, which were allowed to go through one more cell division before either ABpipaa (AWCL precursor) or ABprpaa (AWCR precursor) was irradiated with a laser beam. Embryos were then recovered on an NGM plate at 20°C and allowed to hatch and grow for 3 days. Killing ABpipaa leads to a loss of the left amphid socket cell, while killing ABprpaa leads to a loss of the right amphid socket cell. Socket cells are required for uptake of the fluorescent dye Dil, so the death of these cells was assessed by lack of dye filling. For example, in ABpipaa kills, if the left side failed to fill with Dil while the right side filled successfully, ABpipaa and therefore AWCL was considered to be killed, and AWCR was then examined for *str-2* expression. Occasionally, the ablation appeared to damage but not kill the precursor cell, because the operated animals lost socket cell function while retaining the ipsilateral AWC neuron. In those cases, GFP was observed in AWC on a side that failed to fill with Dil. None of these animals expressed *str-2::GFP* on the contralateral side, so these results do not affect the conclusion that the basal state for *str-2* expression in a single AWC is off. In most animals without *str-2::GFP* expression in AWC, faint ASI expression was still visible, indicating that the effect on *str-2::GFP* expression was specific to AWC.

To make sure that killing the AWC precursor did not cause major changes in amphid development, control kills were conducted in a strain expressing *tax-2Δ::GFP*. *tax-2Δ::GFP* is expressed in six chemosensory neurons, including AWC (Coburn and Bargmann, 1998). Based on the *tax-2Δ::GFP* expression pattern, killing one AWC precursor led to the death of expected cells, and not others (*n* = 7). The surviving AWC neuron on the contralateral side expressed *tax-2Δ::GFP*, indicating that it maintained its sensory fate after the other AWC neuron was killed.

Mock-killed animals were exposed to the same conditions as the successfully killed animals, but Dil filled both sides, indicating that

the kill was not successful. Killing AWC in the L1 stage was performed as described (Bargmann and Horvitz, 1991). Briefly, L1 animals were mounted on a 5% agar pad, the AWC neuron was identified by its characteristic morphology and position, or by the use of cell-specific GFP markers, and then laser irradiated.

Acknowledgments

We thank Amanda Kahn, Noelle L'Etolle, Shai Shaham, and Massimo Hilliard for comments on this manuscript, Iva Greenwald, Noelle L'Etolle, Alex Santos, and Erin Peckol for ideas and strains that facilitated this work, Jim Thomas for sharing results prior to publication, and Shannon Grantner for technical support. This work was supported by a grant from the American Cancer Society. E. R. T. was supported by a National Science Foundation predoctoral fellowship and a Chancellor's Fellowship. A. S. was supported by a Howard Hughes Medical Institute Predoctoral Fellowship, and C. I. B. is an Investigator of the Howard Hughes Medical Institute.

Received July 29, 1999; revised October 13, 1999.

References

- Anderson, P. (1995). Mutagenesis. *Methods Cell Biol.* 48, 31–58.
- Austin, J., and Kimble, J. (1989). Transcript analysis of *glp-1* and *lin-12*, homologous genes required for cell interactions during development of *C. elegans*. *Cell* 58, 565–571.
- Baier, H., Rotter, S., and Korsching, S. (1994). Connectional topography in the zebrafish olfactory system: random positions but regular spacing of sensory neurons projecting to an individual glomerulus. *Proc. Natl. Acad. Sci. USA* 91, 11646–11650.
- Bargmann, C.I. (1998). Neurobiology of the *Caenorhabditis elegans* genome. *Science* 282, 2028–2033.
- Bargmann, C.I., and Horvitz, H.R. (1991). Chemosensory neurons with overlapping functions direct chemotaxis to multiple chemicals in *C. elegans*. *Neuron* 7, 729–742.
- Bargmann, C.I., Hartwig, E., and Horvitz, H.R. (1993). Odorant-selective genes and neurons mediate olfaction in *C. elegans*. *Cell* 74, 515–527.
- Blair, S.S., Martindale, M.Q., and Shankland, M. (1990). Interactions between adjacent ganglia bring about the bilaterally alternating differentiation of RAS and CAS neurons in the leech nerve cord. *J. Neurosci.* 10, 3183–3193.
- Braun, A.P., and Schulman, H. (1995). The multifunctional calcium/calmodulin-dependent kinase: from form to function. *Annu. Rev. Physiol.* 57, 417–445.
- Buck, L., and Axel, R. (1991). A novel multigene family may encode odorant receptors: a molecular basis for odor recognition. *Cell* 65, 175–187.
- Chess, A., Simon, I., Cedar, H., and Axel, R. (1994). Allelic inactivation regulates olfactory receptor gene expression. *Cell* 78, 823–834.
- Chou, W., Huber, A., Bentrop, J., Schulz, S., Schwab, K., Chadwell, L.V., Paulsen, R., and Britt, S.G. (1999). Patterning of the R7 and R8 photoreceptor cells of *Drosophila*: evidence of induced and default cell-fate specification. *Development* 126, 606–616.
- Clyne, P.J., Warr, C.G., Freeman, M.R., Lessing, D., Kim, J., and Carlson, J.R. (1999). A novel family of divergent seven-transmembrane proteins: candidate odorant receptors in *Drosophila*. *Neuron* 22, 327–338.
- Coburn, C.M., and Bargmann, C.I. (1998). A putative cyclic nucleotide-gated channel is required for sensory development and function in *C. elegans*. *Neuron* 17, 695–706.
- Devries, S.H., and Baylor, D.A. (1997). Mosaic arrangement of ganglion cell receptive fields in rabbit retina. *J. Neurophysiol.* 78, 2048–2060.
- Dwyer, N.D., Troemel, E.R., Sengupta, P., and Bargmann, C.I. (1998). Odorant receptor localization to olfactory cilia is mediated by ODR-4, a novel membrane-associated protein. *Cell* 93, 455–466.
- Govind, C.K. (1992). Claw asymmetry in lobsters: case study in developmental neuroethology. *J. Neurobiol.* 23, 1423–1445.

- Greenwald, I. (1998). LIN-12/Notch signaling: lessons from worms and flies. *Genes Dev.* 12, 1751-1762.
- Grunert, U., Martin, P.R., and Wässle, H. (1994). Immunocytochemical analysis of bipolar cells in the macaque monkey retina. *J. Comp. Neurol.* 348, 607-627.
- Hall, D.H., and Hedgecock, E.M. (1991). Kinesin-related gene *unc-104* is required for axonal transport of synaptic vesicles in *C. elegans*. *Cell* 65, 837-847.
- Hedgecock, E.M., Culotti, J.G., Thomson, J.N., and Perkins, L.A. (1985). Axonal guidance mutants of *Caenorhabditis elegans* identified by filling sensory neurons with fluorescent dyes. *Dev. Biol.* 111, 158-170.
- Huang, L.S., Tzou, P., and Sternberg, P.W. (1994). The *lin-15* locus encodes two negative regulators of *Caenorhabditis elegans* vulval development. *Mol. Biol. Cell* 5, 395-412.
- Jansen, G., Thijssen, K.L., Werner, P., van der Horst, M., Hazendonk, E., and Plastarak, R.H. (1999). The complete family of genes encoding G proteins of *Caenorhabditis elegans*. *Nat. Genet.* 21, 414-419.
- Komatsu, H., Mori, I., Rhee, J.-S., Akaike, N., and Ohshima, Y. (1996). Mutations in a cyclic nucleotide-gated channel lead to abnormal thermosensation and chemosensation in *C. elegans*. *Neuron* 17, 707-718.
- Lee, R.Y., Lobel, L., Hengartner, M., Horvitz, H.R., and Avery, L. (1997). Mutations in the $\alpha 1$ subunit of an L-type voltage-activated Ca^{2+} channel cause myotonia in *Caenorhabditis elegans*. *EMBO J.* 16, 6066-6076.
- MacNeil, M.A., and Masland, R.H. (1998). Extreme diversity among amacrine cells: Implications for function. *Neuron* 20, 971-982.
- Malkin, B., Hirono, J., Sato, T., and Buck, L.B. (1999). Combinatorial receptor codes for odors. *Cell* 96, 713-723.
- Maruyama, I.N., and Brenner, S. (1991). A phorbol ester/diacylglycerol-binding protein encoded by the *unc-13* gene of *Caenorhabditis elegans*. *Proc. Natl. Acad. Sci. USA* 88, 5729-5733.
- Mayford, M., Barzilai, A., Keller, F., Schacher, S., and Kandel, E.R. (1992). Modulation of an NCAM-related adhesion molecule with long-term synaptic plasticity in Aplysia. *Science* 256, 638-644.
- Mello, C.C., Kramer, J.M., Stinchcomb, D., and Ambros, V. (1991). Efficient gene transfer in *C. elegans*: extrachromosomal maintenance and integration of transforming sequences. *EMBO J.* 10, 3959-3970.
- Mombaerts, P., Wang, F., Dulac, C., Chao, S.H., Nemes, A., Mendelsohn, M., Edmondson, J., and Axel, R. (1996). Visualizing an olfactory sensory map. *Cell* 87, 675-686.
- Nonet, M.L., Grundahl, K., Meyer, B.J., and Rand, J.B. (1993). Synaptic function is impaired but not eliminated in *C. elegans* mutants lacking synaptotagmin. *Cell* 73, 1291-1305.
- Otsuka, A.J., Franco, R., Yang, B., Shim, K.H., Tang, L.Z., Zhang, Y.Y., Boontrakulpoontawe, P., Jeyaprasath, A., Hedgecock, E., Wheaton, V.I., et al. (1995). An ankyrin-related gene (*unc-44*) is necessary for proper axonal guidance in *Caenorhabditis elegans*. *J. Cell Biol.* 129, 1081-1092.
- Papatsenko, D., Sheng, G., and Desplan, C. (1997). A new rhodopsin in R8 photoreceptors of *Drosophila*: evidence for coordinate expression in Rh3 in R7 cells. *Development* 124, 1665-1673.
- Reiner, D.J., Newton, E.M., Tian, H., and Thomas, J.H. (1999). Regulation of a behavioral clock, muscle excitation, and a genetically defined target by the *C. elegans* *unc-43* CaM Kinase II. *Nature*, in press.
- Roeyale, K., Crump, J.G., Sagasti, A., and Bargmann, C.I. (1998). The $G\alpha$ protein ODR-3 mediates olfactory and nociceptive function and controls cilium morphogenesis in *C. elegans* olfactory neurons. *Neuron* 20, 55-67.
- Robey, E. (1997). Notch in vertebrates. *Curr. Opin. Genet. Dev.* 7, 551-557.
- Sagasti, A., Hobert, O., Troemel, E.R., Ruvkun, G., and Bargmann, C.I. (1999). Alternative olfactory neuron fates are specified by the LIM homeobox gene *lin-4*. *Genes Dev.* 13, 1794-1806.
- Schafer, W.R., and Kenyon, C.J. (1995). A calcium-channel homologue required for adaptation to dopamine and serotonin in *Caenorhabditis elegans*. *Nature* 375, 73-78.
- Schuster, C.M., Davis, G.W., Fetter, R.D., and Goodman, C.S. (1996). Genetic dissection of structural and functional components of synaptic plasticity. II. Fasciclin II controls presynaptic structural plasticity. *Neuron* 17, 655-667.
- Sengupta, P., Colbert, H.A., and Bargmann, C.I. (1994). The *C. elegans* gene *odr-7* encodes an olfactory-specific member of the nuclear receptor superfamily. *Cell* 79, 971-980.
- Sengupta, P., Chou, J.C., and Bargmann, C.I. (1996). *odr-10* encodes a seven transmembrane domain olfactory receptor required for responses to the odorant diacetyl. *Cell* 84, 899-909.
- Starich, T.A., Herman, R.K., and Shaw, J.E. (1993). Molecular and genetic analysis of *unc-7*, a *Caenorhabditis elegans* gene required for coordinated locomotion. *Genetics* 133, 527-541.
- Troemel, E.R., Chou, J.H., Dwyer, N.D., Colbert, H.A., and Bargmann, C.I. (1995). Divergent seven transmembrane receptors are candidate chemosensory receptors in *C. elegans*. *Cell* 83, 207-218.
- Troemel, E.R., Kimmel, B.E., and Bargmann, C.I. (1997). Reprogramming chemotaxis responses: sensory neurons define olfactory preferences in *C. elegans*. *Cell* 91, 161-169.
- Vosshall, L.B., Amrein, H., Morozov, P.S., Rzhetsky, A., and Axel, R. (1999). A spatial map of olfactory receptor expression in the *Drosophila* antenna. *Cell* 96, 725-736.
- Wässle, H., and Boycott, B.B. (1991). Functional architecture of the mammalian retina. *Physiol. Rev.* 71, 447-480.
- Weinshenker, D.Z., Wei, A., Salkoff, L., and Thomas, J.H. (1999). An *eag K⁺* channel links cell excitation and antidepressant action in *C. elegans*. *J. Neurosci.*, in press.
- White, J.G., Southgate, E., Thomson, J.N., and Brenner, S. (1986). The structure of the nervous system of the nematode *Caenorhabditis elegans*. *Phil. Trans. R. Soc. Lond. B* 314, 1-340.
- Williams, B.D., Schrank, B., Huynh, C., Shownkeen, R., and Waterston, R.H. (1992). A genetic mapping system in *Caenorhabditis elegans* based on polymorphic sequence-tagged sites. *Genetics* 131, 609-624.
- Yochem, J., and Greenwald, I. (1989). *gip-1* and *lin-12*, genes implicated in distinct cell-cell interactions in *C. elegans*, encode similar transmembrane proteins. *Cell* 58, 553-563.
- Yochem, J., Weston, K., and Greenwald, I. (1988). The *Caenorhabditis elegans* *lin-12* gene encodes a transmembrane protein with overall similarity to *Drosophila* Notch. *Nature* 335, 547-550.
- Yu, S., Avery, L., Baude, E., and Garbers, D.L. (1997). Guanylyl cyclase expression in specific sensory neurons: a new family of chemosensory receptors. *Proc. Natl. Acad. Sci. USA* 94, 3384-3387.
- Zallen, J.A., Yi, B.A., and Bargmann, C.I. (1998). The conserved immunoglobulin superfamily member SAX-3/Robo directs multiple aspects of axon guidance in *C. elegans*. *Cell* 92, 217-227.
- Zallen, J.A., Kirch, S., and Bargmann, C.I. (1999). Genes required for axon pathfinding and extension in the *C. elegans* nerve ring. *Development* 126, 3679-3692.
- Zoran, M.J., Furuta, L.R., Kater, S.B., and Haydon, P.G. (1993). Neuron-muscle contact changes presynaptic resting calcium set-point. *Dev. Biol.* 158, 163-171.

Chapter 4

The CaMKII UNC-43 activates the MAPKKK NSY-1 to execute a lateral signaling decision required for asymmetric olfactory neuron fates

(Published in Cell, April 20, 2001, 105: 221-232)

The CaMKII UNC-43 Activates the MAPKKK NSY-1 to Execute a Lateral Signaling Decision Required for Asymmetric Olfactory Neuron Fates

Alvaro Sagasti,* Naoki Hisamoto,† Junko Hyodo,† Miho Tanaka-Hino,† Kunihiro Matsumoto,† and Cornelia I. Bargmann*‡

*Howard Hughes Medical Institute Programs in Developmental Biology, Neuroscience, and Genetics

Department of Anatomy and Department of Biochemistry and Biophysics

The University of California, San Francisco San Francisco, California 94143

†Department of Molecular Biology Graduate School of Science

Nagoya University and CREST, Japan Science and Technology Corporation

Chikusa-ku, Nagoya 464-8602 Japan

Summary

A stochastic cell fate decision mediated by axon contact and calcium signaling causes one of the two bilaterally symmetric AWC neurons, either AWCL or AWCR, to express the candidate olfactory receptor *str-2*. *nsy-1* mutants express *str-2* in both neurons, disrupting AWC asymmetry. *nsy-1* encodes a homolog of the human MAP kinase kinase kinase (MAPKKK) ASK1, an activator of JNK and p38 kinases. Based on genetic epistasis analysis, *nsy-1* appears to act downstream of the CaMKII *unc-43*, and NSY-1 associates with UNC-43, suggesting that UNC-43/CaMKII activates the NSY-1 MAP kinase cassette. Mosaic analysis demonstrates that UNC-43 and NSY-1 act primarily in a cell-autonomous execution step that represses *str-2* expression in one AWC cell, downstream of the initial lateral signaling pathway that coordinates the fates of the two cells.

Introduction

Olfactory neurons fall into many distinct classes that can be distinguished by the expression of different odorant receptor genes. This diversity is observed even in the simple nervous system of the nematode *C. elegans*, which includes at least fourteen functionally different classes of chemosensory neurons (White et al., 1986). In general, the chemosensory neurons of *C. elegans* exhibit bilateral symmetry, with pairs of similar neurons located on the left and right sides of the animal. A further level of diversity is achieved in the AWC olfactory neuron pair through a cell interaction between the two AWC cells (AWCL and AWCR). The candidate olfactory receptor gene *str-2* is expressed asymmetrically and stochastically in only one of the two AWC neurons: half of a population of animals expresses a *str-2::GFP* reporter

gene in AWCR and half expresses it in AWCL (Troemel et al., 1999). Asymmetry between the two AWC neurons enables the animal to detect more odors and discriminate between them in complex environments (Wes and Bargmann, 2001). The AWC cells can be defined as AWC^{ON} and AWC^{OFF} based on their pattern of *str-2::GFP* expression. If the precursor to one AWC neuron is killed early in development, the surviving neuron always becomes AWC^{OFF}, suggesting that the two cells communicate to establish the AWC^{ON} fate. In mutants in which the AWC axons terminate prematurely, both neurons become AWC^{OFF}, suggesting that axon contact between the AWC neurons is required for cell communication.

The cell interaction that determines AWC asymmetry is reminiscent of lateral signaling, but appears to use a unique signaling pathway that is not affected by mutations in the *C. elegans* Notch genes *lin-12* and *glp-1* (Kimble and Simpson, 1997). A screen for Neuronal symmetry (*Nsy*) mutants that express *str-2::GFP* in both AWC cells yielded mutations in three genes involved in calcium signaling (Troemel et al., 1999). *unc-2* and *unc-36* encode *C. elegans* homologs of subunits of an N/P-type voltage-gated calcium channel (Lee et al., 1997; Schafer and Kenyon, 1995) and *unc-43* encodes the single *C. elegans* homolog of the calcium/calmodulin-dependent serine/threonine protein kinase CaMKII (Reiner et al., 1999). These observations suggest that the interaction between the AWC neurons inhibits the activity of the calcium channel-CaMKII signaling pathway, which represses *str-2* expression in one cell. The decision is made early in development and is stabilized by a separate cGMP-dependent maintenance pathway.

The screen for mutants with two AWC^{ON} neurons also yielded three *nsy* genes that map to novel loci. We show here that the AWC asymmetry gene *nsy-1* encodes a protein homologous to a human MAPKKK, the apoptosis signal-regulating kinase ASK1. ASK1 activates the JNK and p38 MAP kinases in mammalian cells and induces cell death in response to TNF α (Ichijo et al., 1997). Our results suggest that the ASK1 JNK/p38 pathway is a central component of the AWC cell fate decision. *nsy-1* is genetically downstream of the CaMKII homolog *unc-43* in the regulation of AWC asymmetry. Mosaic analysis reveals that CaMKII acts in a strictly cell-autonomous manner in AWC^{OFF} to execute the cell fate decision made by the AWC lateral signaling pathway. NSY-1 also acts primarily to execute cell fate in AWC^{OFF} but may play an additional minor, *unc-43*-independent role in coordinating the fates of the two AWC neurons. The related functions of the CaMKII *unc-43* and the MAPKKK *nsy-1* in the execution of AWC cell fate reveal a novel link between calcium signaling and a MAPK signaling cassette, suggesting a strategy by which neurons use calcium signals to achieve an all-or-none developmental response.

Results

NSY-1 is a Homolog of the Human MAPKKK ASK1
Mutations in the *nsy-1*, *nsy-2*, and *nsy-3* genes cause *str-2::GFP* to be expressed in both AWC neurons (2

‡To whom correspondence should be addressed (e-mail: cori@itsa.ucsf.edu).

AWC^{ON}) (Troemel et al., 1999). We mapped the *nsy-1* gene and cloned it by transgene rescue of the mutant *str-2::GFP* expression phenotype. A clone that contained only the complete open reading frame for the gene F59A6.1 rescued the *nsy-1(ky397)* mutant phenotype (see Experimental Procedures), and RNA interference of the F59A6.1 gene caused a mild 2 AWC^{ON} phenotype in wild-type animals (data not shown). Nonsense mutations in F59A6.1 were identified in all three *nsy-1* alleles (Figure 1A and below). We conclude that the *nsy-1* gene corresponds to the open reading frame F59A6.1.

nsy-1 encodes a homolog of the human MAP kinase kinase kinase (MAPKKK) ASK1 (Ichijo et al., 1997). We generated a full-length cDNA for *nsy-1* and found that the two proteins are 44% identical over 884 amino acids and 63% identical in their kinase domains (Figure 1A). It is likely that *nsy-1* and ASK1 are orthologs (Plowman et al., 1999). The mutations in *nsy-1(ky400)* and *nsy-1(ky542)* result in premature stop codons just before the kinase domain, and the mutation in *nsy-1(ky397)* creates a premature stop codon after the kinase domain (Figure 1A). All of these alleles have similar *str-2::GFP* misexpression phenotypes and are likely to represent null alleles of the *nsy-1* gene.

MAPKKKs are a conserved family of serine/threonine kinases that play important developmental and physiological roles in eukaryotic cells (Garrington and Johnson, 1999). These kinases phosphorylate MAP kinase kinases (MAPKK), which in turn phosphorylate and activate MAP kinases (MAPK). ASK1 has been shown to phosphorylate the MAPKK MKK6, and to activate the JNK and p38 MAPKs, but not the ERK MAPK (Ichijo et al., 1997). To confirm that NSY-1 and ASK1 have similar functions, we expressed NSY-1 in mammalian HEK 293 cells. A wild-type form of NSY-1 efficiently phosphorylated MKK6 in vitro, but a kinase-negative form did not (Figure 1B). NSY-1 expression in mammalian cells also stimulated phosphorylation of endogenous p38 kinases (Figure 1B). These results suggest that NSY-1 functions as a MAPKKK with similar specificity to the human protein ASK1.

NSY-1 and UNC-43 Function in the AWC Neurons to Regulate AWC Cell Fate

To determine where NSY-1 is expressed, we made fusions between the *nsy-1* gene and GFP and examined their expression patterns in transgenic animals (Chalfie et al., 1994). A GFP fusion gene containing 10 kb of sequence upstream of the *nsy-1* translational start site was expressed in the intestine, hypodermis, rectal gland cells, and neurons, including both AWC neurons (Figures 2A and 2B). A shorter transcriptional GFP fusion gene with 5 kb of upstream sequence, and a translation fusion of GFP to the entire NSY-1 protein with 3.8 kb of upstream sequence, were expressed in many cells but not in the AWC neurons (data not shown). Full rescue of the *nsy-1* phenotype required more than 3.8 kb of upstream sequence, suggesting that expression of the gene in the AWC neurons was needed for rescue of a *nsy-1* mutant.

To ask whether NSY-1 expression in AWC is sufficient to rescue *nsy-1* mutants, we placed the *nsy-1* cDNA under the control of the *odr-3* promoter. This promoter

drives strong expression in both AWC neurons, weak expression in the AWB neurons, and variable expression in AWA, ADF, and ASH neurons (Roayaie et al., 1998). AWA, AWB, ADF, and ASH do not make synaptic connections with AWC (White et al., 1986). The *odr-3::NSY-1* transgene rescued the 2 AWC^{ON} asymmetry defect of *nsy-1* mutants and occasionally caused a gain-of-function (2 AWC^{OFF}) phenotype, supporting the hypothesis that NSY-1 acts in the AWC neurons to mediate AWC asymmetry (Table 1).

Since the CaMKII homolog *unc-43* has a similar phenotype to *nsy-1*, we asked whether it could also function in AWC neurons. An *unc-43* cDNA (Rongo and Kaplan, 1999) under the control of the *odr-3* promoter rescued the 2 AWC^{ON} *str-2::GFP* phenotype of an *unc-43* mutant and occasionally caused a gain-of-function (2 AWC^{OFF}) phenotype (Table 1), consistent with the possibility that *unc-43* acts in the AWC neurons. A gain-of-function *unc-43* cDNA (Rongo and Kaplan, 1999) under the control of the *odr-3* promoter also caused *str-2::GFP* to turn off in both AWC cells (2 AWC^{OFF}; Table 1).

Because the *odr-3* promoter is reproducibly expressed in both AWC and AWB neurons, it is possible that *nsy-1* and *unc-43* expression in AWB rescues AWC cell fate. To rule out this possibility, we examined mosaic animals that expressed *odr-3::NSY-1* or *odr-3::UNC-43* in the AWB neurons but not the AWC neurons. Mosaic animals arose through the random loss of extrachromosomal arrays containing both *odr-3::NSY-1* (or *odr-3::UNC-43*) and the marker *odr-1::RFP* in a *nsy-1* (or *unc-43*) mutant background (see below and Experimental Procedures). *str-2::GFP* asymmetry was rescued when the arrays were present in AWC neurons, but not when they were present only in AWB neurons (see Experimental Procedures). The *odr-3::UNC-43(GF)* phenotype also correlated with expression in AWC. These results demonstrate that *str-2::GFP* asymmetry is most likely mediated by expression of *nsy-1* and *unc-43* in AWC. Since the *odr-3* promoter drives expression in both AWC cells, asymmetric expression of UNC-43 and NSY-1 is not necessary for asymmetric expression of *str-2*.

nsy-1 May Act Downstream of the CaMKII Homolog *unc-43*

To characterize the roles of the *nsy* genes in AWC asymmetry, we analyzed epistasis relationships between the novel *nsy* genes and genes that affect axon guidance, calcium signaling, and olfactory cGMP signaling. Two AWC^{ON} neurons are present in *nsy* mutants, loss-of-function mutations in the calcium channel subunits *unc-2* and *unc-36*, and null mutants in the CaMKII *unc-43*. Two AWC^{OFF} neurons are present in gain-of-function *unc-43* mutants (*unc-43(gf)*) and in mutants that cause early axon termination, like *unc-76*. *unc-76* and other axon guidance mutants presumably block primary signaling between the two AWC axons. Two AWC^{OFF} neurons are also present in mutants for the *odr-1* transmembrane guanylyl cyclase and other olfactory cGMP signaling molecules that are essential for maintenance of *str-2* expression. Previous epistasis analysis placed the axon guidance gene *unc-76* upstream of the calcium signaling genes, and the guanylyl cyclase *odr-1* downstream of all other genes that affect AWC asymmetry (Troemel et al., 1999).

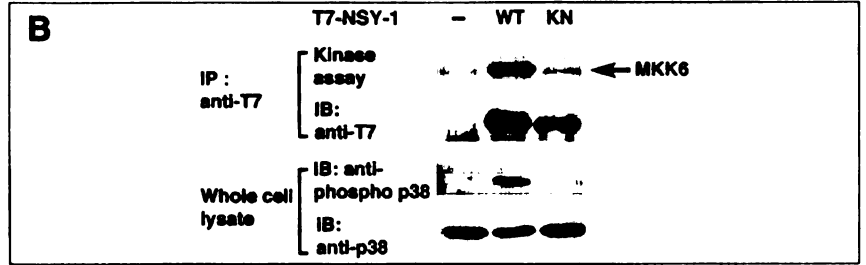
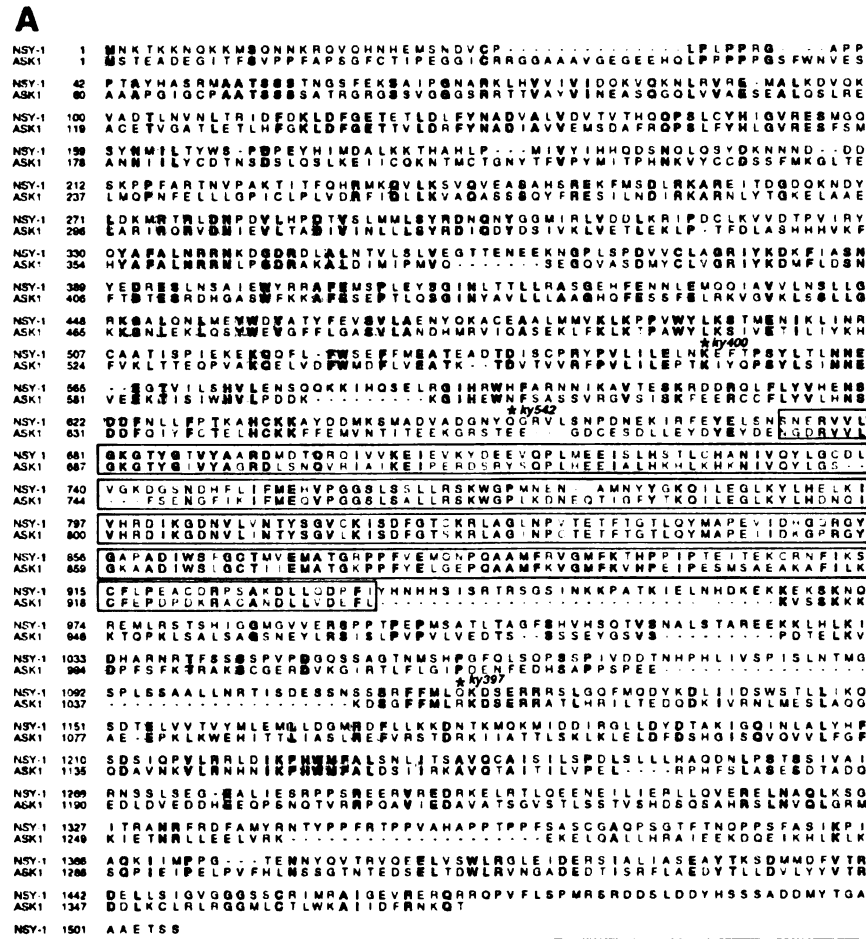


Figure 1. *nsy-1* Encodes a MAPKKK Related to the Human Protein ASK1
(A) ClustalW alignment of the NSY-1 and ASK-1 protein sequences. Shading indicates identical residues. The kinase domain is boxed. Residues that were mutated to stop codons in the three *nsy-1* alleles are indicated by an asterisk and allele number above the mutant residue.
(B) NSY-1 has MAPKKK activity in mammalian cells. Human embryonic 293 cells were transiently transfected with a control vector (-), NSY-1 tagged with a T7 epitope (WT), and a T7-tagged catalytically inactive form of NSY-1, in which Lys-703 in the ATP binding domain was replaced by methionine (KN). The complexes immunoprecipitated (IP) with anti-T7 were tested in *in vitro* kinase reactions with bacterially expressed MKK6 as a substrate (top panel). The immunoprecipitates were also immunoblotted with anti-T7 (second panel). To determine whether NSY-1 is able to activate a mammalian p38 MAPK pathway *in vivo*, whole-cell extracts were immunoblotted with anti-phospho-p38 (third panel), an antibody that specifically recognizes the dually phosphorylated active form of p38, and anti-p38 (bottom panel). NSY-1 efficiently phosphorylated MKK6 *in vitro* and activated p38 in cells, whereas catalytically inactive NSY-1(KN) did not.

We found that *nsy-3* (2 *AWC^{ON}*) was epistatic to the *unc-76* axon guidance mutant (2 *AWC^{OFF}*), whereas a gain-of-function mutant in the CaMKII *unc-43* (2 *AWC^{OFF}*) was epistatic to *nsy-3* (Table 2). These results suggest

that *nsy-3* acts upstream of *unc-43*. Both *nsy-1* and *nsy-2* (2 *AWC^{ON}*) were epistatic to *unc-76* and *unc-43(gf)* (Table 2). These results suggest that *nsy-1* and *nsy-2* act downstream of or in parallel to *unc-43*. The *odr-1*

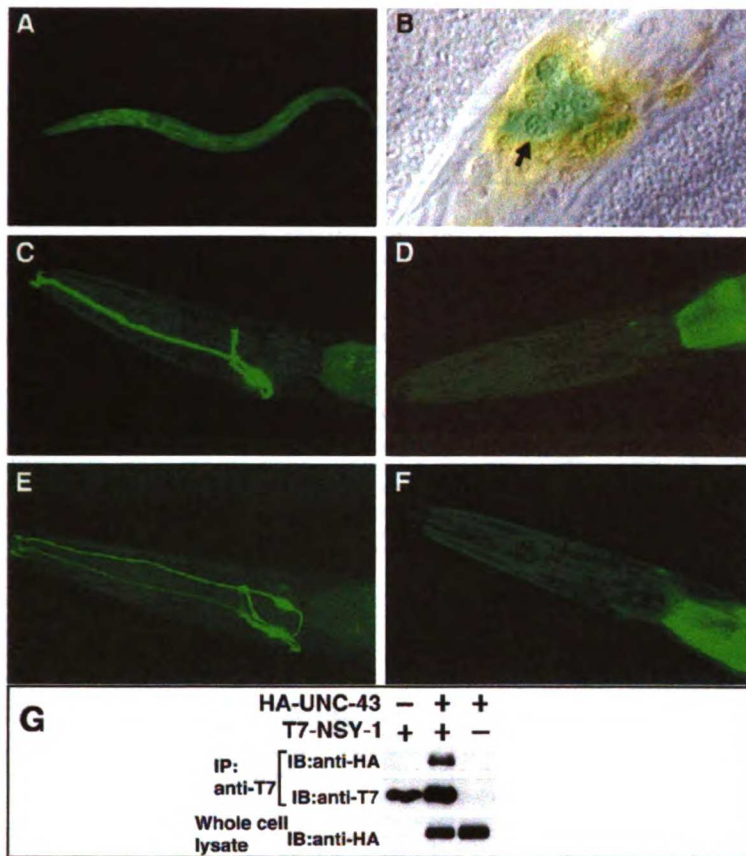


Figure 2. *nsy-1* Is Expressed in the AWC Neurons and May Act Downstream of *unc-43*/CaMKII

(A and B) A *nsy-1::GFP* transgene with ~10 kb of *nsy-1* upstream sequence was expressed in many cells, including AWC. (A) A confocal projection of an L1 larval stage animal with wide expression of *nsy-1::GFP*. (B) Merged *nsy-1::GFP* and Nomarski images of an L1 animal. An arrow indicates AWC.

(C–F) Animals bearing an integrated *str-2::GFP* reporter. Fluorescence posterior to the head is gut autofluorescence or gut expression of the transgene marker *elt-2::GFP*. (C) Wild-type animals expressed *str-2::GFP* in one AWC neuron. (D) Animals expressing *odr-3::NSY-1(GF)* did not express *str-2::GFP* in either AWC neuron. (E) An *unc-43* loss-of-function mutation caused *str-2::GFP* expression in both AWC neurons. (F) An *unc-43* loss-of-function mutant expressing *odr-3::NSY-1(GF)* did not express *str-2::GFP* in either AWC neuron. The dorsally-located, dim-staining cells in (D) and (F) are the ASI neurons, where *str-2::GFP* is sometimes weakly expressed. Dorsal is up and anterior is to the left in all panels.

(G) Association between UNC-43 and NSY-1 in mammalian cells. Human embryonic 293 cells were transfected with a control vector (-); an HA-tagged, calcium-independent, activated form of UNC-43, HA-UNC-43(T284D); and a catalytically inactive, T7-tagged form of NSY-1, T7-NSY-1(K703M). Cell lysates were immunoprecipitated (IP) with anti-T7 antisera. Immunoprecipitates were immunoblotted (IB) with anti-HA (top panel) and anti-T7 (middle panel); UNC-43 was present in the NSY-1 immunoprecipitate (top panel). Whole-cell extracts were also immunoblotted with anti-HA (bottom panel).

guanylyl cyclase mutant (2 AWC^{OFF}) was epistatic to *nsy-1*, *nsy-2*, and *nsy-3*, as predicted by its later role in *str-2* maintenance (Table 2).

As an additional tool for epistasis analysis, a gain-of-function *nsy-1* allele (*nsy-1(gf)*) was made by deleting the N-terminal 640 amino acids encoded by the cDNA. The analogous mutation in the NSY-1 mammalian homolog ASK1 creates a gain-of-function protein (Saitoh et al., 1998). A *nsy-1(gf)* transgene under the control of the *odr-3* promoter conferred a 2 AWC^{OFF} phenotype, the opposite phenotype of *nsy-1(lf)* (Table 1 and Figure 2D). The AWC marker *odr-1::RFP* was expressed normally in *nsy-1(gf)* strains, confirming that the AWC neurons were viable and properly specified. Thus, like *unc-43*, *nsy-1* can act as a switch for AWC cell fates.

To determine whether *nsy-1* acts downstream of or in parallel to *unc-43*, the *nsy-1(gf)* transgene (2 AWC^{OFF}) was crossed into an *unc-43(lf)* mutant (2 AWC^{ON}). The *unc-43(n1186lf)* allele used in these experiments contains an early stop codon in the kinase domain and is a predicted null mutation (Reiner et al., 1999). Just as *nsy-1(lf)* is epistatic to *unc-43(gf)*, the *nsy-1(gf)* phenotype was epistatic to the *unc-43(lf)* phenotype (Figures 2C–2F and Table 2). If *nsy-1* and *unc-43* were required in parallel to repress *str-2::GFP* expression, then loss-of-function mutants would be expected to be epistatic to gain-of-function mutants in both cases. These epistasis

results are therefore consistent with *nsy-1* acting downstream of *unc-43* in a linear genetic pathway to regulate AWC asymmetry.

Given the genetic similarities between *nsy-1* and *unc-43* in the AWC cell fate decision, it is possible that UNC-43 interacts with NSY-1. We tested whether NSY-1 and UNC-43 interact physically by expressing a catalytically inactive form of NSY-1, tagged with a T7 epitope, and a constitutively active form of UNC-43, tagged with HA, in mammalian HEK 293 cells. Immunoprecipitation with anti-T7 antibodies brought down both UNC-43 and NSY-1 (Figure 2G). Similar experiments with a wild-type UNC-43 protein and a kinase-dead UNC-43 protein indicated that all of these forms of UNC-43 interact with NSY-1 (data not shown).

Dissecting the Circuitry of AWC Signaling: *unc-43* Executes the AWC^{OFF} Cell Fate in a Cell-Autonomous Fashion and Does Not Influence the Fate of the AWC^{ON} Cell

Since the two AWC neurons signal to each other, *unc-43* and *nsy-1* could act either in the AWC^{OFF} cell to repress *str-2* expression cell autonomously, or in the AWC^{ON} cell to send a nonautonomous signal to the contralateral AWC^{OFF} cell. Previous experiments suggested that the calcium signaling pathway acts at least partly in AWC^{OFF}. When one AWC precursor cell is killed in a

Table 1. Targeted Gene Expression and Mosaic Analysis

Genetic Background	Transgene	2 AWC ^{OFF} (%)	1 AWC ^{OFF} / 1 AWC ^{ON} (%)	2 AWC ^{ON} (%)	n
Transgene expressed in both AWC cells ¹					
<i>unc-43(n1186)</i>	<i>odr-3::UNC-43 a</i>	16	55	29	778
	<i>odr-3::UNC-43 b</i>	12	68	20	634
Wild-type	<i>odr-3::UNC-43(GF) a</i>	87	13	0	447
	<i>odr-3::UNC-43(GF) b</i>	86	12	1	626
	<i>odr-3::UNC-43(GF) c</i>	85	14	0	240
<i>nsy-1(n397)</i>	<i>odr-3::NSY-1 a</i>	2	93	5	659
	<i>odr-3::NSY-1 b</i>	18	79	4	884
	<i>odr-3::NSY-1 c</i>	17	80	3	646
Wild-type	<i>odr-3::NSY-1(GF) a</i>	90	10	0	626
	<i>odr-3::NSY-1(GF) b</i>	95	4	1	536
	<i>odr-3::NSY-1(GF) c</i>	83	17	0	329
	<i>odr-3::NSY-1(GF) d</i>	91	9	0	862
	<i>odr-3::NSY-1(GF) e</i>	78	22	0	673

Mosaic animals with one wild-type and one mutant AWC neuron¹

Genetic Background	Transgene	1 AWC ^{OFF} / 1 AWC ^{ON} (%) ²			2 AWC ^{ON} (%)	n	χ ² analysis for execution model ²	
		2 AWC ^{OFF} (%)	Wildtype AWC ^{ON} / Mutant AWC ^{OFF}				χ ²	p
			Wildtype AWC ^{OFF} / Mutant AWC ^{ON}					
<i>unc-43(n1186)</i>	<i>odr-3::UNC-43 a</i>	0	3	46	51	71	0.53	0.2-0.5
	<i>odr-3::UNC-43 b</i>	3	7	44	47	146	1.4	0.2-0.5
Wild-type	<i>odr-3::UNC-43(GF) a</i>	34	54	11	1	119	5.72	0.2-0.5
	<i>odr-3::UNC-43(GF) b</i>	46	49	5	0	74	0.13	>0.9
	<i>odr-3::UNC-43(GF) c</i>	47	47	6	0	104	0.79	0.5-0.9
<i>nsy-1(ky397)</i>	<i>odr-3::NSY-1 a</i>	0	3	66	32	79	11.4	<0.001
	<i>odr-3::NSY-1 b</i>	3	10	65	22	124	14.9	<0.001
	<i>odr-3::NSY-1 c</i>	0	5	65	30	82	3.63	0.05-0.20
Wild-type	<i>odr-3::NSY-1(GF) a</i>	43	51	6	0	104	0.30	0.5-0.9
	<i>odr-3::NSY-1(GF) b</i>	78	19	2	2	63	23.6	<0.001
	<i>odr-3::NSY-1(GF) c</i>	44	47	9	0	96	0.42	0.5-0.9
	<i>odr-3::NSY-1(GF) d</i>	54	37	9	0	180	17.10	<0.001
	<i>odr-3::NSY-1(GF) e</i>	38	42	20	0	98	8.7	0.01-0.05

¹Results for single mutants are reported in Table 2. For *unc-43(lf)* analysis, an *odr-3::UNC-43* transgene was introduced into *unc-43(n1186)* mutants. For *unc-43(gf)* analysis, an *odr-3::UNC-43(GF)* transgene was introduced into wild-type animals. Similarly, for *nsy-1(lf)* analysis, an *odr-3::NSY-1* transgene was introduced into *nsy-1(ky397)* mutants and for *nsy-1(gf)* analysis, an *odr-3::NSY-1(GF)* transgene was introduced into wild-type animals. An *odr-1::RFP* transgene was used to identify AWC cells which retained the array. Upper table reports results for animals which retained the array in both AWC cells (2 RFP+ cells). Lower table reports results for mosaic animals which retained the array in only one AWC cell (1 RFP- and 1 RFP+ cell). Lower case letters designate independent lines.

²Statistical analysis was also used to test a lateral interaction model. In all cases, p < 0.001, excluding the model.

³For LF mosaic analysis, the wild-type cell was RFP+, and the mutant cell was RFP-. For GF mosaics, the wild-type cell was RFP- and the GF mutant was RFP+.

wild-type background, the surviving AWC cell takes on the AWC^{OFF} fate. However, killing one AWC precursor in the 2 AWC^{ON} mutant *unc-36* leaves a surviving AWC^{ON} cell, suggesting that *unc-36* can act autonomously in a single AWC cell (Troemel et al., 1999). Similarly, the axon termination mutant *unc-76* has a 2 AWC^{OFF} phenotype, presumably because the AWC axons do not make contact and signal to each other. Double mutants between 2 AWC^{ON} *Nsy* mutants and *unc-76* have a 2 AWC^{ON} phenotype (Table 2; Troemel et al., 1999), suggesting that the *Nsy* genes are required cell autonomously in AWC^{OFF}, even in the absence of direct cell contact. A more definitive mosaic analysis experiment confirmed that *unc-43* and *nsy-1* are required cell autonomously for the AWC^{OFF} fate (Table 1 and below).

To understand the roles of *unc-43* and *nsy-1* in the

signaling circuitry that determines AWC cell fates, it is important to ask whether they have a nonautonomous role in addition to their autonomous one. Since the AWC neurons communicate to coordinate the two AWC cell fates, the AWC cell fate determination pathway can be broken down into two components: a nonautonomous cell interaction pathway that coordinates the fates of the AWC^{ON} and AWC^{OFF} cells and a strictly cell-autonomous pathway that executes the fate determined by the first part of the pathway (Figure 3A). By analogy with the Notch/Delta lateral signaling pathway, the first part of the AWC pathway may include feedback that amplifies small differences in the signaling properties of the two AWC neurons (Kimble and Simpson, 1997). *unc-43* and *nsy-1* could function in a solely cell-autonomous manner to repress *str-2* expression downstream of the cell inter-

Table 2. Epistasis Analysis

Strain	Cells expressing <i>str-2::GFP</i> (%)			n
	2 AWC ^{OFF}	1 AWC ^{ON} /1 AWC ^{OFF}	2 AWC ^{ON}	
Single mutants				
<i>unc-76(e911)</i> ¹	43	57	0	114
<i>odr-1(n1933)</i> ¹	100	0	0	150
<i>unc-43(n1186lf)</i> ¹	3	5	92	101
<i>unc-43(n498gf)</i> ¹	80	20	0	133
<i>nsy-1(ky397)</i> ¹	0	0	100	34
<i>nsy-2(ky388)</i> ¹	0	32	68	62
<i>nsy-3(ky389)</i> ¹	0	4	96	107
<i>odr-3::NSY-1(GF) transgene</i> ²	81	19	0	53
Double mutants				
<i>nsy-1; unc-76</i>	0	12	88	85
<i>nsy-1; unc-43(n498gf)</i>	2	5	93	59
<i>nsy-1; odr-1</i>	98	2	0	58
<i>nsy-2; unc-76</i>	2	24	75	170
<i>nsy-2; unc-43(n498gf)</i>	0	39	61	75
<i>nsy-2; odr-1</i>	100	0	0	75
<i>nsy-3; unc-76</i>	0	12	88	49
<i>nsy-3; unc-43(n498gf)</i>	97	3	0	33
<i>nsy-3; odr-1</i>	100	0	0	40
<i>unc-43(n1186lf); odr-3::NSY-1(GF) transgene</i> ²	76	15	9	102

¹These data are reproduced from Troemel et al., 1999.

²Results of two transgenic lines were combined. Both lines exhibited similar proportions of phenotypic classes.

action machinery, or they could function during feedback and thus act both autonomously and nonautonomously to coordinate the fates of the two AWC neurons.

The cell-autonomous and nonautonomous functions of *unc-43* and *nsy-1* can be defined in mosaic animals containing one wild-type and one mutant AWC neuron. Figures 3B and 3C diagram the distinct predictions for mosaics with either loss-of-function or gain-of-function mutant genes, depending on whether *nsy-1* and *unc-43* act to coordinate the fates of the two AWC cells through cell interaction and feedback, or only to execute the AWC^{OFF} fate. For example, if *unc-43* acted during AWC cell interaction and feedback, *unc-43(lf)* mosaic animals would always have exactly one AWC^{ON} and one AWC^{OFF} cell. The *unc-43* mutant cell would always be AWC^{ON} because the AWC^{OFF} execution pathway could not be activated, and the wild-type cell would always be AWC^{OFF}, the default state, because the *unc-43* mutant cell would not participate in interaction and feedback (Figure 3B). This model predicts both a cell-autonomous and a nonautonomous function for *unc-43*, as is observed for the Notch homolog *lin-12* in the AC/VU decision (Seydoux and Greenwald, 1989; see Discussion). Alternatively, if *unc-43* were only required to execute the AWC^{OFF} fate, the mutant cell would always be AWC^{ON} because of the defect in execution, but the wild-type cell would now adopt the AWC^{ON} or AWC^{OFF} fates with equal frequencies because the initial communication between the two cells occurred normally (Figure 3B). For gain-of-function mosaics, if *unc-43* acted in cell interaction and feedback, the *unc-43(gf)* cell would always be AWC^{OFF} and the wild-type cell would always be AWC^{ON}. However, if *unc-43* acted only to execute the AWC^{OFF} fate, the *unc-43(gf)* cell would again always be AWC^{OFF} but the wild-type cell would be AWC^{OFF} or AWC^{ON} with equal frequency (Figure 3C).

Mosaic analysis was conducted with *unc-43(lf)* ani-

mals bearing a transgenic extra-chromosomal array of *odr-3::UNC-43* and *odr-1::RFP*. The *odr-1* promoter drives expression in the AWB and AWC neurons (Yu et al., 1997). Due to cosegregation of the genes in the extrachromosomal array, AWC neurons that retained the array were wild-type for *unc-43* (*unc-43(+)*) and expressed *odr-1::RFP* (RFP+), whereas AWC neurons that lost the array were *unc-43(-)* and RFP-. Mosaic animals with one RFP+ AWC neuron were identified in two transgenic lines. Internal controls were generated in each transgenic line by scoring animals that retained the array in both AWC cells (to determine the efficacy of the rescuing arrays) and animals that lost the array altogether (to determine the penetrance of the mutant phenotype). Animals that lost the array altogether displayed a high penetrance 2 AWC^{ON} *unc-43* phenotype (see Experimental Procedures). The results for mosaic animals and controls are presented in Table 1 and Figures 4A-4D. Both lines exhibited two major classes of mosaics (Table 1): animals in which *str-2::GFP* was only expressed in the mutant, non-RFP-expressing cell and animals in which both the mutant and wild-type cells expressed *str-2::GFP*. These are the two classes expected if *unc-43* were acting to execute the AWC^{OFF} cell fate, but not to coordinate the two AWC fates via cell interaction and feedback (Figure 3B). Statistical analysis of both lines, using the internal controls to generate predictions, was consistent with the model that *unc-43* acts to execute the AWC^{OFF} cell fate decision (Table 1).

Mosaic analysis was also performed with a wild-type strain bearing a transgenic extrachromosomal array of *odr-3::UNC-43(GF)* and *odr-1::RFP*. AWC neurons that retained the array were *unc-43(gf)* and RFP+, whereas AWC neurons that lost the array were *unc-43(+)* and RFP-. Mosaic animals with one RFP+ AWC neuron were identified in three transgenic lines, and internal controls were generated in each line. The results for

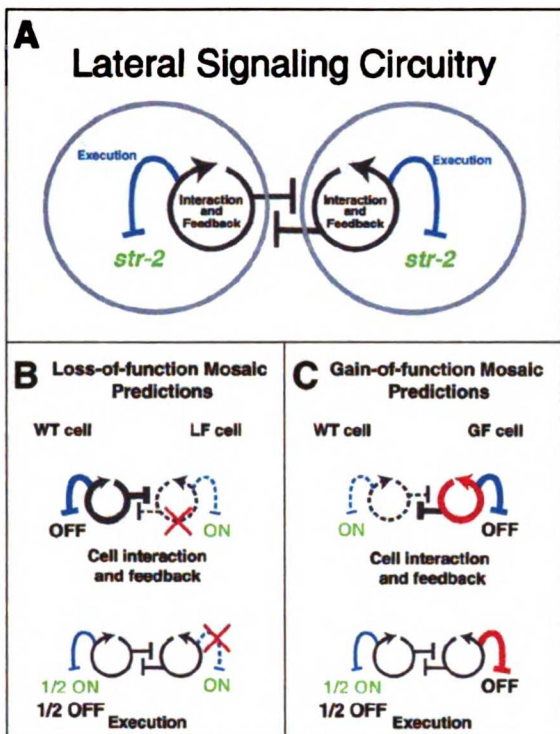


Figure 3. Mosaic Analysis Can Be Used to Analyze the Determination of AWC Fates

(A) Diagram of a hypothetical lateral signaling pathway. The lateral signaling circuitry can be divided into two components. The first component (black) consists of nonautonomous cell interaction with feedback, used by one cell to instruct the other to adopt the opposite fate. The second component (blue) is a pathway that executes the cell fate decision determined by the cell interaction. In the AWC^{OFF} cell, this pathway represses transcription of *str-2*.

(B) Loss-of-function mosaics with one wild-type and one mutant AWC cell can distinguish whether the *nsy-1* and *unc-43* genes function in cell interaction or in executing the AWC^{OFF} fate. A red "X" indicates the defect in a loss-of-function mutant.

(C) Gain-of-function mosaics with one wild-type and one *gf* mutant cell can also distinguish whether *Nsy* genes act in cell communication or execution. Red indicates the focus of a gain-of-function transgene. See text for detailed discussion of models. Dashed lines indicate an inactive pathway, thickened lines indicate an activated pathway, and unbroken, unthickened lines indicate a pathway with the potential to be active or inactive.

controls and mosaic animals are presented in Table 1 and Figures 4I–4L. All three lines yielded two major classes of mosaics. Animals in one class of mosaics expressed *str-2::GFP* in the wild-type cell but not in the gain-of-function, RFP^+ cell, and animals in the second class did not express *str-2::GFP* in either cell. These are the classes expected if *unc-43* were acting to execute the AWC^{OFF} cell fate, but not to coordinate the fates of the two AWC cells via cell interaction (Figure 3C). Statistical analysis for all three lines was consistent with the model that *unc-43* acts only to execute the AWC^{ON} cell fate decision (Table 1). The results of mosaic analysis with both gain-of-function and loss-of function *unc-43* thus support the model that *unc-43* acts cell autonomously to execute the AWC^{OFF} fate and does not contribute to the specification of the AWC^{ON} fate.

nsy-1 Executes the AWC^{OFF} Cell Fate, but May Also Play a Minor Role in Coordinating the Fates of the Two AWC Neurons

Using the approach described above for *unc-43*, we performed mosaic analysis experiments with a *nsy-1* loss-of-function mutant and a *nsy-1* gain-of-function transgene. The results of these experiments are reported in Table 1 and Figure 4.

Three transgenic lines were used in the *nsy-1* loss-of-function mosaic analysis. In all lines, two major classes of mosaics were observed (Table 1, Figures 4E–4H): in one class, only the mutant cell expressed *str-2::GFP*, and in the other class, both cells expressed *str-2::GFP*. These are the same mosaic classes observed in the *unc-43* loss-of-function mosaic analysis and are the two classes expected for a gene involved only in executing the AWC^{OFF} fate (Figure 3B). Statistical analysis of the results, however, revealed that these mosaics did not fit the model that *nsy-1* acts exclusively to execute the AWC^{OFF} fate (Table 1). Two of three lines generated significantly more mosaic animals than expected in the class that expressed *str-2::GFP* in the *nsy-1* mutant AWC cell but not the wild-type AWC cell. This class of mosaics would predominate if *nsy-1* played a role in cell interaction and feedback. The results for *nsy-1(lf)* mosaics therefore support a model in which *nsy-1* acts mostly cell autonomously to execute the AWC^{OFF} cell fate, but may also have a minor influence on cell interaction and feedback in a separate, *unc-43*-independent role.

Mosaic analysis was also performed with five *nsy-1* gain-of-function lines. Again, the two major classes of mosaics expected in the execution model were observed (Table 1, Figures 4M–4P). Two of the lines exhibited approximately equal numbers of the two major classes of mosaics (lines a and c), two of the lines were slightly enriched in mosaics that did not express *str-2::GFP* at all (lines d and e), and one of the lines was strikingly enriched in this class of mosaics (line b). Although all of these results are closer to the execution model than the cell interaction and feedback model, lines a and c statistically fit this model, but lines b, d, and e did not (Table 1). In lines b, d, and e, the *nsy-1(gf)* cell appeared to act as a weak dominant-negative in the cell interaction, not as a gain-of-function. The disruption of the N terminus of *nsy-1*, which is missing in *NSY-1(GF)*, may create a mixed gain-of-function and dominant-negative *nsy-1* allele. The simplest interpretation of the mosaic analyses for *nsy-1(lf)* and *nsy-1(gf)* is that *nsy-1* plays a predominately cell-autonomous role downstream of *unc-43* to execute the AWC^{OFF} cell fate, but also has the potential to play a nonessential, minor role in coordinating the fates of the two AWC cells.

Discussion

The CaMKII UNC-43 Activates the MAPKKK ASK1/NSY-1 to Regulate AWC Cell Fate

nsy-1, a gene involved in determining asymmetric cell fates in the AWC olfactory neurons, encodes the likely ortholog of the human MAPKKK ASK1 (Ichijo et al., 1997). Our genetic results predict that calcium signaling through a voltage-gated calcium channel and the C.

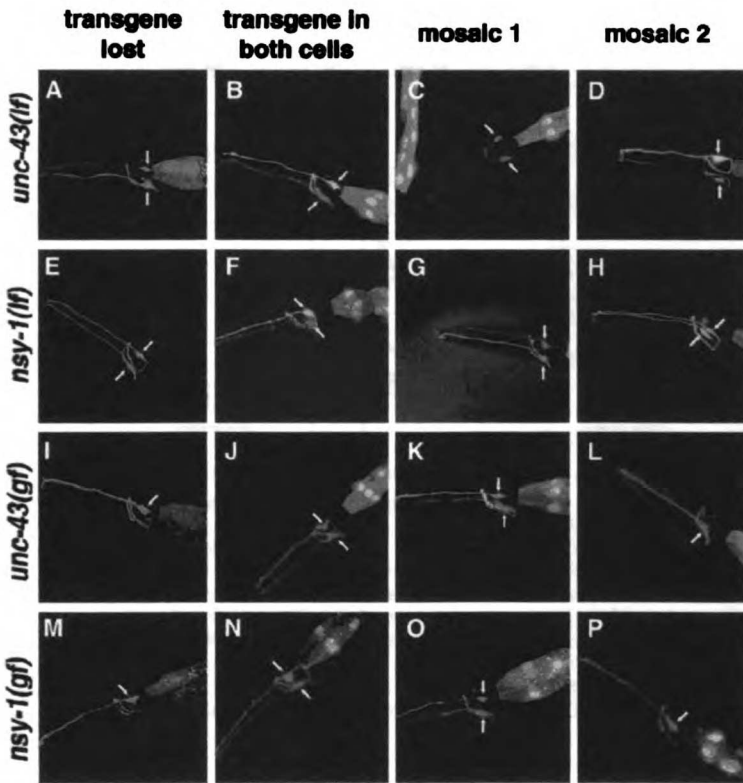


Figure 4. *str-2::GFP* Expression in Control and Mosaic Animals

Confocal projections of animals expressing a stable, integrated *str-2::GFP* transgene and an unstable transgenic array with a test plasmid and *odr-1::RFP*. (A–D) *odr-3::UNC-43* plasmid in an *unc-43(n1186lf)* strain, (E–H) *odr-3::NSY-1* plasmid in a *nsy-1(ky397)* strain, (I–L) *odr-3::UNC-43(GF)* plasmid in a wild-type strain, (M–P) *odr-3::NSY-1(GF)* plasmid in a wild-type strain. *str-2::GFP* fluorescence was false-colored green and *odr-1::RFP* fluorescence was false-colored red. Overlap between red and green appears yellow. AWC cells are indicated by arrows. (A, E, I, and M) Control animals that lost the array from both AWC cells. (A and E) 2 AWC^{ON} phenotype when wild-type rescuing transgenes were lost from *nsy-1(lf)* and *unc-43(lf)* strains. (I and M) Wild-type phenotype (1 AWC^{ON}/1 AWC^{OFF}) when *nsy-1(gf)* and *unc-43(gf)* transgenes were lost from a wild-type strain. (B, F, J, and N) Control animals expressing the array in both AWC cells. (B and F) In *nsy-1(lf)* and *unc-43(lf)* lines, the transgene rescued asymmetric expression of *str-2::GFP* (1 AWC^{ON}/1 AWC^{OFF}). (J and N) In *nsy-1(gf)* and *unc-43(gf)* lines, the transgene caused a 2 AWC^{OFF} phenotype. Mosaic animals: (C and G) In some *nsy-1(lf)* and *unc-43(lf)* AWC mosaics the wild-type RFP⁺ cell was AWC^{OFF}, whereas the mutant RFP[–] cell was AWC^{ON}. (D and H) In some *nsy-1(lf)* and *unc-43(lf)* mosaics, both the wild-type and mutant cells were AWC^{ON}. (K and O) In some *nsy-1(gf)* and *unc-43(gf)*

mosaics, the activated RFP⁺ cell was AWC^{OFF}, and the wild-type RFP[–] cell was AWC^{ON}. (L and P) In some *nsy-1(gf)* and *unc-43(gf)* mosaics both the wild-type and mutant cells were AWC^{OFF}. Dorsal is up and anterior is left in all panels. Fluorescence posterior to the head is gut autofluorescence or gut expression of the transgene marker *elt-2::GFP* (see Experimental Procedures). In (H) and (J), *odr-1::RFP* is also visible in AWB, a smaller cell.

C. elegans CaMKII UNC-43 activates the NSY-1 MAPKKK. *nsy-1* and *unc-43* mutants have identical *str-2::GFP* expression phenotypes, and both can act as switches in the establishment of AWC asymmetry. Mosaic analysis demonstrates that both act in the AWC^{OFF} cell to repress *str-2* expression. Epistasis analysis places *nsy-1* downstream of *unc-43*, and the UNC-43 and NSY-1 proteins associate in heterologous cells, suggesting that their interaction may be direct. Indeed, the NSY-1/ASK1 MAPKKK pathway is activated by CaMKII in both *C. elegans* and mammalian cultured cells, supporting the predictions of the genetic model (M. Tanaka-Hino et al., submitted; K. Takeda et al., submitted).

The link between CaMKII and NSY-1/ASK1 was unanticipated. CaMKII was previously shown to activate ERK, but not p38/JNK MAP kinases (e.g., Watt and Storm, 2001); conversely, several different activators, but not CaMKII, were previously linked to ASK1. In mammalian cells, ASK1 promotes apoptosis in response to tumor necrosis factor- α and activation of the Fas death receptor (Chang et al., 1998; Ichijo et al., 1997). Tumor necrosis factor activation of ASK1 is mediated by the adaptor protein TRAF2, and Fas activation of ASK1 is mediated by the Daxx adaptor (Chang et al., 1998; Nishitoh et al., 1998). ASK1 may also be involved in G protein-coupled receptor signaling through an interaction with β -arrestin (Berestetskaya et al., 1998; McDonald et al., 2000). It

does not always promote cell death; in PC12 cells, ASK1 promotes neuronal differentiation (Takeda et al., 2000).

As predicted by its similarity to ASK1, NSY-1 expression can stimulate the phosphorylation of the MAPKK MEK6 and p38 MAPK in heterologous cells. The *C. elegans* genome contains at least three MAPKKs, ten MAPKKs, and fourteen MAPKs (five ERK class, five JNK class, three p38 class, and one NLK class) (Plowman et al., 1999). Although several candidates have been tested (data not shown), we have not yet identified a *C. elegans* MAPK that affects AWC asymmetry.

The ERK, JNK, and p38 MAP kinases are related to one another by sequence, but different classes are regulated by different inputs and have distinct outputs. Many cell fate decisions are controlled by ERK MAP kinase signaling cassettes, particularly downstream of receptor tyrosine kinase/ras signaling pathways (reviewed in Garrington and Johnson, 1999). Their intrinsic ultrasensitivity and reinforcing feedback loops make MAPK pathways well-suited to all-or-none developmental fate decisions (Ferrell, 1996). The JNK and p38 MAPKs respond to environmental stresses (such as ultraviolet light) and inflammatory cytokines, and regulate apoptosis and nonmitogenic inflammatory responses. JNK also functions in some developmental decisions, including dorsal closure and tissue polarity in *Drosophila* (Noselli, 1998; reviewed in Davis, 2000). The functional divi-

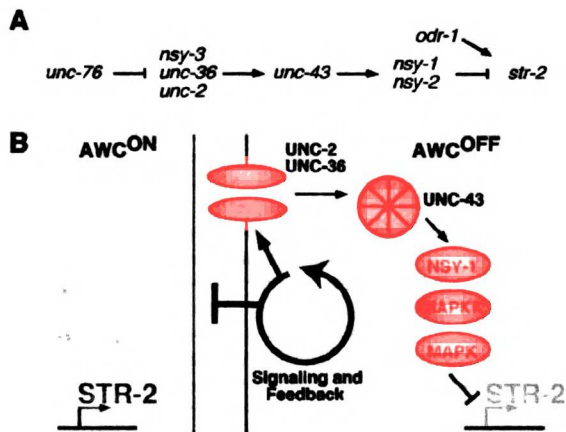


Figure 5. A Model for Execution of the AWC^{OFF} Fate

(A) Epistasis relationships of *nsy* mutants.

(B) In the AWC^{OFF} cell, calcium influx through the UNC-2/UNC-36 calcium channel activates the calcium/calmodulin-dependent kinase UNC-43, which in turn activates the NSY-1 MAPKKK. Activation of the NSY-1 MAPK cascade leads to repression of *str-2* transcription. The CaMKII/NSY-1 pathway is less active in the AWC^{ON} cell, allowing expression of *str-2*. By analogy to Notch, the fates of the two cells are initially specified by a cell interaction that may use feedback to amplify differences between the AWC cells. This pathway acts upstream of the calcium/CaMKII/NSY-1 AWC^{OFF} execution pathway.

sion between MAP kinases is conserved in yeast: the KSS1/FUS3 ERK proteins act in differentiation (mating and filamentous growth), whereas the HOG1 p38 kinase acts in the osmotic stress response. The AWC asymmetry decision represents an unusual case of the p38/JNK pathway acting in a cell fate decision. In addition, AWC asymmetry has the unusual property of using calcium signaling to control cell fate. Because the developing AWC neurons are relatively mature and have sent out axons by the time the decision is made, they may have access to the calcium channels that are more typically involved in neuronal signaling. In one scenario, the AWC cell fate decision may be recruiting a stress response pathway to a developmental decision.

The broad expression pattern of *nsy-1* suggests that it has other functions in addition to its role in controlling *str-2* asymmetry, and might regulate other cell fates. In addition, since calcium entry contributes to stress following prolonged excitation of neurons, the same pathway may contribute to physiological detection of stress in other circumstances. For example, since ASK1 can act as an activator of cell death (Ichijo et al., 1997; Berestetskaya et al., 1998; Chang et al., 1998), we speculate that CaMKII and ASK1 may play a role in excitotoxic cell death in response to calcium influx. Calcium signals can also affect cell migration, axon guidance, and neuronal plasticity. Even among kinases, there are numerous targets for calcium signals: CaMKII activates the ERK MAP kinase in several cell types, including mammalian olfactory neurons (Watt and Storm, 2001), and the *ras*/ERK pathway responds to sensory activity in *C. elegans* olfactory neurons (Hirotsu et al., 2000). JNK can be activated by a CaMKIV pathway in PC12 cells (Enslin et al., 1996). The UNC-43/CaMKII-NSY-1/ASK1 pathway

could act in a variety of calcium-dependent processes, either alone or in combination with other ERK and JNK pathways.

UNC-43/CaMKII and NSY-1/ASK1 Execute the AWC^{OFF} Fate

UNC-43/CaMKII and NSY-1/ASK1 have central roles in a cell interaction that determines cell fates in the olfactory system of *C. elegans* (Troemel et al., 1999). Although most neurons in *C. elegans* exist as bilaterally symmetric, morphologically similar pairs, the two AWC olfactory neurons interact with each other to allow AWCL and AWCR to adopt distinct fates. The stochastic and coordinated interaction that determines AWC asymmetry is reminiscent of lateral signaling, a process that allows two initially equivalent cells to coordinate their fates so that each adopts a distinct identity. The only well-characterized molecular pathway that accomplishes lateral signaling is mediated by Notch family receptors (Kimble and Simpson, 1997). In lateral signaling interactions mediated by Notch, ablating one of the interacting cells causes the remaining cell to adopt a default fate (e.g., Kimble, 1981). Similarly, ablating one of the two AWC cells causes the remaining cell to adopt the AWC^{OFF} fate (Troemel et al., 1999). However, several features of the AWC lateral interaction are not typical for Notch signaling: the signaling between the two AWC neurons is mediated by calcium and a MAPK pathway, and occurs in relatively mature neurons whose axons have made contact with each other. In addition, unlike Notch lateral signaling, UNC-43/NSY-1 signaling primarily affects execution of the AWC^{OFF} fate and not feedback between the AWC neurons.

unc-43 and *nsy-1* act in the AWC neuron pair to control the asymmetric expression of *str-2::GFP*. Expressing either *nsy-1* or *unc-43* in both AWC cells restored asymmetric cell fates in *nsy-1* and *unc-43* mutants, demonstrating that it is not the asymmetric expression of these genes but rather asymmetric activity that controls AWC cell fates. A signal from the AWC^{OFF} cell is required for the AWC^{ON} fate, but *unc-43* and *nsy-1* are required for the AWC^{OFF} fate; their activities may be repressed by the initial signal.

Genetic mosaic analysis was used to ask whether *unc-43* and *nsy-1* are required in a strictly cell autonomous manner to execute the AWC^{OFF} cell fate, or whether they also play roles in coordinating the two cell fates. The mosaic strategy and cell interaction model were based on the AC/VU lateral signaling decision that occurs between two cells in the *C. elegans* hermaphrodite gonad, Z1.ppp and Z4.aaa (Kimble, 1981). Z1.ppp and Z4.aaa make a stochastic, coordinated decision that allows one cell to adopt an anchor cell (AC) fate and the other cell to adopt a ventral uterine precursor cell (VU) fate. This interaction requires the Notch family receptor *lin-12* (Greenwald et al., 1983). Seydoux and Greenwald (1989) used genetic mosaic analysis to show that *lin-12* activity is required in the VU cell to allow it to receive an inducing signal from the AC cell. If *lin-12* was mutant in one of the two AC/VU cells, the mutant cell always adopted the AC fate and the wild-type cell always adopted the VU fate. Because *lin-12* is involved in the feedback loop between AC and VU, loss of *lin-12*



activity in one cell had a nonautonomous effect that forced the other cell to become VU. By analogy, we reasoned that if *unc-43* and *nsy-1* are involved in a feedback loop in the AWC cell fate decision, the loss of *unc-43* and *nsy-1* activity in one AWC neuron would result in mosaic animals with one AWC^{OFF} (wild-type) and one AWC^{ON} (mutant) cell every time. A different result is expected if these genes act to execute the AWC^{OFF} cell fate. The execution model predicts that half of the mosaic animals would have two AWC^{ON} cells. The mutant cell will always adopt the AWC^{ON} fate, whereas the wild-type cell will take on the AWC^{ON} and AWC^{OFF} fates with equal frequency.

Genetic mosaic analyses with *unc-43* gain-of-function and loss-of-function mutants fit the prediction for a strictly cell-autonomous gene that executes the AWC^{OFF} cell fate in one cell. Loss-of-function and gain-of-function mosaics with *nsy-1* were also mostly consistent with the execution model: the presence of two classes of *nsy-1(ff)* and *nsy-1(gf)* mosaics supports the idea that *nsy-1* functions mainly to execute the AWC^{OFF} cell fate autonomously. However, the class of mosaics with one AWC^{ON} (mutant) and one AWC^{OFF} (wild-type) neuron was more prevalent in *nsy-1(ff)* mosaics, suggesting that *nsy-1* has a minor cell nonautonomous effect on AWC fate.

Our results suggest a model for the execution of the AWC^{OFF} cell fate (Figure 5). An initial lateral signaling interaction between the two AWC cells defines one cell as AWC^{ON} and the other as AWC^{OFF}. In the cell defined as AWC^{OFF}, calcium influx through a voltage-gated calcium channel (UNC-2 and UNC-36) activates the calcium-calmodulin dependent kinase UNC-43, which in turn activates the MAPKKK NSY-1. Activation of the MAPKKK pathway represses *str-2* transcription in the AWC^{OFF} cell. In contrast with signaling molecules of Notch pathways, the CaMKII/NSY-1 signaling cassette is not an essential component of lateral signaling and feedback. The genes that participate in the initial AWC cell interaction are not known. One candidate for a molecule involved in this lateral signaling pathway is *nsy-3*, which is genetically upstream of or parallel to the CaMKII *unc-43*. *nsy-2* is a candidate to act at a downstream step in execution, since like *nsy-1* it is epistatic to *unc-43*. Our results, coupled with the observation that NSY-1 and UNC-43 have well-conserved mammalian homologs, raise the possibility that the calcium-to-MAPK signaling cassette used in AWC cell fate determination may be used for cell fate diversification in other animals.

Experimental Procedures

Strains

Wild-type strains were *C. elegans* variety Bristol, strain N2. Unless otherwise noted, strains contained the integrated *str-2::GFP* transgene *kyIs140 (I)* (Troemel et al., 1999). Strains were maintained by standard methods (Brenner, 1974).

Mapping and Cloning *nsy-1*

nsy-1(ky397) was mapped on LGII between *stP196* and *stP36*, two Tc1 transposable element polymorphisms in the DP13 strain (Williams, 1995). The deficiencies *ccDf2* and *maDf4* failed to complement *nsy-1*, whereas the deficiencies *ccDf11* and *maDf30* complemented *nsy-1*. Cosmid clones representing the *nsy-1* genomic region were injected into *nsy-1(ky397)* at a concentration of ~10

μg/ml each. The cosmid C51A9 (overlapping F59A6) rescued asymmetric expression of *str-2::GFP* in three of four transgenic lines (all rescued lines were ≥ 91% 1 AWC^{ON}/1 AWC^{OFF}). A 13.1 kb *SacI* deletion fragment of C51A9 containing only the full open reading frame for the F59A6.1 gene rescued *str-2::GFP* asymmetry in *nsy-1(ky397)* in four of four lines (all lines ≥ 80% 1 AWC^{ON}/1 AWC^{OFF}). A subclone with the F59A6.1 gene and 3.8 kb of upstream sequence partially rescued *str-2::GFP* asymmetry in only one of eight transgenic lines (the one rescued line was 50% 1 AWC^{ON}/1 AWC^{OFF}, 50% 2 AWC^{ON}). The *nsy-1* (F59A6.1) genomic coding region in *ky397*, *ky400*, and *ky542* was amplified by PCR in several pieces and PCR products were directly sequenced.

Plasmid Construction

nsy-1::GFP

A region including ~10 kb of sequence upstream of the *nsy-1* gene was amplified by PCR and subcloned into the pPD95.77 vector.

nsy-1 and *nsy-1(gf)* cDNA Construction

A full-length *nsy-1* cDNA was assembled from the EST yk321g3 (a gift of Y. Kohara) and a partial cDNA amplified by PCR from a *C. elegans* cDNA library (Kawasaki et al., 1999). To make a *nsy-1(gf)* cDNA, the region corresponding to the first 640 amino acids of the cDNA was deleted by PCR.

odr-3::NSY-1 and *odr-3::NSY-1(GF)*

The full-length *nsy-1* cDNA and the *nsy-1(gf)* were subcloned into a vector with an EcoRV fragment of the *odr-3* promoter (Roayale et al., 1998).

odr-3::UNC-43 and *odr-3::UNC-43(GF)*

An *unc-43* cDNA (KP354) and an *unc-43(gf)* cDNA (T284D; KP421) were provided generously by Josh Kaplan (Rongo and Kaplan, 1990). Both were subcloned into the *odr-3* promoter vector (see above).

odr-1::RFP

GFP was replaced by RFP (dsRed, Clontech) in an *odr-1::GFP* plasmid (L'Etoile and Bargmann, 2000).

Further details of plasmid construction are available upon request.

Germ-Line Transformation

Transgenic strains were made as previously described (Mello and Fire, 1995). *odr-1::RFP*, *elt-2::GFP*, and cosmids were injected at 10–15 μg/ml; all other plasmids were injected at 50 μg/ml. For rescue experiments, the dominant pRF4 *rol-6(su1006)* coinjection marker was injected with test plasmids into a *nsy-1(ky397)* strain containing a *str-2::GFP* transgene (*kyIs140*). *nsy-1::GFP* expression was examined by injection of test plasmids and the *lin-15* plasmid pJM23 into *lin-15(n765ts)* strains. For mosaic animals, an *elt-2::GFP* injection marker (a gift of J. McGhee), which causes intense fluorescence in the gut, was injected with test plasmids. Transgenes were maintained by picking Rol animals, nonMuv animals, or animals expressing *elt-2::GFP*.

Biochemistry

Immunoprecipitation from mammalian cells, in vitro kinase assays, and immunoblotting were carried out as described (Kawasaki et al., 1999). Mammalian expression vectors were transfected into HEK 293 cells using the calcium phosphate precipitation method. Proteins from the cell lysates were immunoprecipitated with anti-T7 antibodies (Novagen). For kinase assays, aliquots of immunoprecipitates were incubated with bacterially expressed His-MKK6 in kinase buffer at 25°C for 2 min. Samples were analyzed by SDS-PAGE and autoradiography. The immunoprecipitates and aliquots of total lysates were analyzed by immunoblotting and visualized by Enhanced Chemiluminescence (ECL) Western Blotting System (Amersham).

Genetic Mosaic Analysis

Mosaic analysis was performed according to the general method described by Herman (1984). Animals of the appropriate background (see Table 1) were injected with a mix of transgenes including *elt-2::GFP*, *odr-1::RFP* and either *odr-3::UNC-43*, *odr-3::NSY-1*, *odr-3::UNC-43(GF)*, or *odr-3::NSY-1(GF)*. Transgenic lines were passaged for ten generations to allow the transgenes to stabilize before screening for mosaics. The presence of the array could be scored

in the AWC and AWB neurons, which express the *odr-1::RFP* transgene.

Since the *odr-3* promoter is expressed in both AWB and AWC, we asked whether AWB has a role in regulating AWC cell fate. Control animals were generated that lost the array in both AWC neurons but maintained expression in AWB neurons. The results of these experiments excluded a function for *unc-43* or *nsy-1* in AWB. Results for transgenes in which neither AWC neuron, but one or both AWB neurons expressed RFP: For *odr-3::UNC-43* rescue of *unc-43(n1186)*, 0/8 animals with one AWB+ and 0/6 animals with two AWB+ neurons were rescued; for *odr-3::NSY-1* rescue of *nsy-1(n397)*, 1/30 animals with one AWB+ and 0/1 animals with two AWB+ neurons were rescued; for *odr-3::UNC-43(GF)* introduced into wild-type, 0/11 animals with one AWB+ and 0/7 animals with two AWB+ neurons exhibited the gain-of-function phenotype; for *odr-3::NSY-1(GF)* introduced into wild-type, 0/30 animals with one AWB+ and 0/17 animals with two AWB+ neurons exhibited the gain-of-function phenotype.

To dissect the circuitry of signaling between the two AWC cells, mosaic animals that lost the array in one AWC cell (1 RFP+ and 1 RFP- AWC cell) were scored for each line. Internal controls were generated by scoring animals that lost the array in both AWC neurons (RFP-) and animals that retained the array in both AWC neurons (RFP+). For *unc-43(lf)* and *nsy-1(lf)* analysis, animals that lost the wild-type transgene from both AWC cells (2 RFP-) expressed *str-2::GFP* in both cells (all lines $\geq 97\%$ 2 AWC^{off}, $n \geq 311$). For *unc-43(gf)* and *nsy-1(gf)* analysis, animals that lost the gain-of-function transgene from both AWC cells (2 RFP-), expressed *str-2::GFP* in one AWC cell (all lines $\geq 98\%$ 1 AWC^{on}/1 AWC^{off}, $n \geq 50$).

Statistical Analysis

Data from all lines were analyzed with χ^2 tests to determine whether *unc-43* or *nsy-1* fit models that they act in cell interaction and feedback or solely in the execution of the AWC^{off} fate (see Table 1 for results of these analyses). Models for statistical analyses were generated from results for internal controls expressing the transgene in both AWC cells (2 RFP+). For example, when the *odr-3::UNC-43* transgene was expressed in both AWC cells in the *unc-43(lf)* mosaic line "a", 16% of the animals had a 2 AWC^{off} (gain-of-function) phenotype, 55% of the animals had a 1 AWC^{on}/1 AWC^{off} (rescued) phenotype, and 29% of the animals had a 2 AWC^{on} (mutant) phenotype. The model that *unc-43* acts in execution was generated as follows: In all cases, the mutant RFP- cell was predicted to be AWC^{on}; this prediction was correct in >90% of animals. The anomalous cases in which the RFP- cell was AWC^{off} (<10% of animals) were not included in statistical analysis. Sixteen percent of mosaics were expected to have a gain-of-function transgene in the RFP+ cell and were thus expected to have a transgenic cell that was AWC^{off} and a nontransgenic (mutant) cell that was AWC^{on}. Fifty-five percent of mosaics were expected to have a "rescued" RFP+ cell that had an equal chance of being AWC^{on} or AWC^{off}, so, in our model, half of this percentage (27.5%) was expected to have a 1 AWC^{on} (mutant)/1 AWC^{off} (rescued cell) phenotype and the other 27.5% was expected to have a 2 AWC^{on} phenotype. In 29% of controls, the transgene did not rescue the *unc-43* mutant phenotype, so the corresponding 29% of mosaics were expected to have a 2 AWC^{on} phenotype. Thus, our model predicted that 43.5% (16 + 27.5) of mosaics would have an AWC^{off} (RFP+) cell and an AWC^{on} (RFP-) cell, and 56.5% (27.5 + 29) would have 2 AWC^{on} cells. For the cell interaction model, all 55% of the "rescued" RFP+ cells were expected to be AWC^{off} in the presence of a mutant AWC^{on} cell, predicting 71% (16 + 55) 1 AWC^{on}/1 AWC^{off} animals and 29% 2 AWC^{on} animals. These percentages were multiplied by the number of mosaics generated in the experiment (in this case 71), and the resulting numbers were compared by χ^2 analysis with the actual numbers of mosaics observed. Analogous logic was applied to generate models for both loss-of-function and gain-of-function mosaic experiments with *unc-43* and *nsy-1*.

One possible explanation for the skewed proportions of mosaics in *nsy-1(lf)* mosaics is that the *odr-3* promoter is expressed at a low level in AWC precursors, and that even if expression is lost in AWC itself (as determined by lack of RFP expression), perdurance of the NSY-1 protein was able to rescue *str-2::GFP* asymmetry. This model could explain the existence of a small number of anomalous animals in a third class of mutants (wild-type (RFP+) AWC^{on}/mutant (RFP-) AWC^{off}). We tested this possibility statistically by removing this

anomalous class from our analysis, as well as an equal number of animals from the overrepresented class (wild-type (RFP+) AWC^{off}/mutant (RFP-) AWC^{on}). Following this analysis, *nsy-1(lf)* lines (a) and (b) were still statistically different from the pure execution model. Therefore perdurance could account for some, but not all, of the nonautonomous effects of *nsy-1*.

Acknowledgments

We are grateful to Mike Springer for insightful comments on statistical interpretation, Oliver Hobert, Amanda Kahn, Miri VanHoven, and Paul Wes for helpful discussions and comments on the manuscript, and Jason Much and Hai Nguyen for excellent technical support. We thank Lisa Williams for examining cell migrations in *nsy-1* and *unc-43* mutants, Maria Gallegos for help with microscopy, Kang Shen for RFP PCR product, Alan Coulson and the Sanger Center for cosmids, Yuji Kohara for EST clones, Andy Fire for *C. elegans* vectors, Josh Kaplan for the *unc-43* cDNAs, and Jim McGhee for *elt-2::GFP*. This work was supported by the National Institutes of Health (C. I. B.) and special grants from CREST, Advanced Research on Cancer from the Ministry of Education, Culture and Science of Japan, the Uehara Memorial Foundation, and the Daiko Foundation (to K. M.). A. S. is a Howard Hughes Medical Institute predoctoral fellow and C. I. B. is an investigator of the Howard Hughes Medical Institute.

Received December, 2000; revised March 22, 2001.

References

- Beresetskaya, Y.V., Faure, M.P., Ichijo, H., and Voyno-Yasenetskaya, T.A. (1998). Regulation of apoptosis by alpha-subunits of G12 and G13 proteins via apoptosis signal-regulating kinase-1. *J. Biol. Chem.* 273, 27816-27823.
- Brenner, S. (1974). The genetics of *Caenorhabditis elegans*. *Genetics* 77, 71-94.
- Chalfie, M., Tu, Y., Euskirchen, G., Ward, W.W., and Prasher, D.C. (1994). Green fluorescent protein as a marker for gene expression. *Science* 263, 802-805.
- Chang, H.Y., Nishitoh, H., Yang, X., Ichijo, H., and Baltimore, D. (1998). Activation of apoptosis signal-regulating kinase 1 (ASK1) by the adapter protein Daxx. *Science* 281, 1860-1863.
- Davis, R.J. (2000). Signal transduction by the JNK group of MAP kinases. *Cell* 103, 239-252.
- Enslin, H., Tokumitsu, H., Stork, P.J., Davis, R.J., and Soderling, T.R. (1996). Regulation of mitogen-activated protein kinases by a calcium/calmodulin-dependent protein kinase cascade. *Proc. Natl. Acad. Sci. USA* 93, 10803-10808.
- Ferrell, J.E., Jr. (1996). Tripping the switch fantastic: how a protein kinase cascade can convert graded inputs into switch-like outputs. *Trends Biochem. Sci.* 21, 460-466.
- Garrington, T.P., and Johnson, G.L. (1999). Organization and regulation of mitogen-activated protein kinase signaling pathways. *Curr. Opin. Cell Biol.* 11, 211-218.
- Greenwald, I.S., Sternberg, P.W., and Horvitz, H.R. (1983). The *lin-12* locus specifies cell fates in *Caenorhabditis elegans*. *Cell* 34, 435-444.
- Herman, R.K. (1984). Analysis of genetic mosaics of the nematode *Caenorhabditis elegans*. *Genetics* 108, 165-180.
- Hirotsu, T., Saeki, S., Yamamoto, M., and Iino, Y. (2000). The Ras-MAPK pathway is important for olfaction in *Caenorhabditis elegans*. *Nature* 404, 289-293.
- Ichijo, H., Nishida, E., Irie, K., ten Dijke, P., Saitoh, M., Moriguchi, T., Takagi, M., Matsumoto, K., Miyazono, K., and Gotoh, Y. (1997). Induction of apoptosis by ASK1, a mammalian MAPKKK that activates SAPK/JNK and p38 signaling pathways. *Science* 275, 90-94.
- Kawasaki, M., Hisamoto, N., Iino, Y., Yamamoto, M., Ninomiya-Tsuji, J., and Matsumoto, K. (1999). A *Caenorhabditis elegans* JNK signal transduction pathway regulates coordinated movement via type-D GABAergic motor neurons. *EMBO J.* 18, 3604-3615.

- Kimble, J. (1981). Alterations in cell lineage following laser ablation of cells in the somatic gonad of *Caenorhabditis elegans*. *Dev. Biol.* 87, 286-300.
- Kimble, J., and Simpson, P. (1997). The LIN-12/Notch signaling pathway and its regulation. *Annu. Rev. Cell Dev. Biol.* 13, 333-361.
- L'Etoile, N.D., and Bargmann, C.I. (2000). Olfaction and odor discrimination are mediated by the *C. elegans* guanylyl cyclase ODR-1. *Neuron* 25, 575-586.
- Lee, R.Y., Lobel, L., Hengartner, M., Horvitz, H.R., and Avery, L. (1997). Mutations in the alpha1 subunit of an L-type voltage-activated Ca²⁺ channel cause myotonia in *Caenorhabditis elegans*. *EMBO J.* 16, 6066-6076.
- McDonald, P.H., Chow, C.W., Miller, W.E., Laporte, S.A., Field, M.E., Lin, F.T., Davis, R.J., and Lefkowitz, R.J. (2000). beta-Arrestin 2: A receptor-regulated MAPK scaffold for the activation of JNK3. *Science* 290, 1574-1577.
- Mello, C., and Fire, A. (1995). DNA transformation. *Methods Cell Biol.* 48, 451-482.
- Nishitoh, H., Saitoh, M., Mochida, Y., Takeda, K., Nakano, H., Rothe, M., Miyazono, K., and Ichijo, H. (1998). ASK1 is essential for JNK/SAPK activation by TRAF2. *Mol. Cell* 2, 389-395.
- Noselli, S. (1998). JNK signaling and morphogenesis in *Drosophila*. *Trends Genet.* 14, 33-38.
- Plowman, G.D., Sudarsanam, S., Blingham, J., Whyte, D., and Hunter, T. (1999). The protein kinases of *Caenorhabditis elegans*: a model for signal transduction in multicellular organisms. *Proc. Natl. Acad. Sci. USA* 96, 13603-13610.
- Reiner, D.J., Newton, E.M., Tian, H., and Thomas, J.H. (1999). Diverse behavioural defects caused by mutations in *Caenorhabditis elegans* *unc-43* CaM kinase II. *Nature* 402, 199-203.
- Roayale, K., Crump, J.G., Sagasti, A., and Bargmann, C.I. (1998). The G alpha protein ODR-3 mediates olfactory and nociceptive function and controls cilium morphogenesis in *C. elegans* olfactory neurons. *Neuron* 20, 55-67.
- Rongo, C., and Kaplan, J.M. (1999). CaMKII regulates the density of central glutamatergic synapses *in vivo*. *Nature* 402, 195-199.
- Saitoh, M., Nishitoh, H., Fujii, M., Takeda, K., Tobiume, K., Sawada, Y., Kawabata, M., Miyazono, K., and Ichijo, H. (1998). Mammalian thioredoxin is a direct inhibitor of apoptosis signal-regulating kinase (ASK) 1. *EMBO J.* 17, 2596-2606.
- Schafer, W.R., and Kenyon, C.J. (1995). A calcium-channel homologue required for adaptation to dopamine and serotonin in *Caenorhabditis elegans*. *Nature* 375, 73-78.
- Seydoux, G., and Greenwald, I. (1989). Cell autonomy of *lin-12* function in a cell fate decision in *C. elegans*. *Cell* 57, 1237-1245.
- Takeda, K., Hatai, T., Hamazaki, T.S., Nishitoh, H., Saitoh, M., and Ichijo, H. (2000). Apoptosis signal-regulating kinase 1 (ASK1) induces neuronal differentiation and survival of PC12 cells. *J. Biol. Chem.* 275, 9805-9813.
- Troemel, E.R., Sagasti, A., and Bargmann, C.I. (1999). Lateral signaling mediated by axon contact and calcium entry regulates asymmetric odorant receptor expression in *C. elegans*. *Cell* 99, 387-398.
- Watt, W.C., and Storm, D.R. (2001). Odorants stimulate the Erk/MAP kinase pathway and activate CRE-mediated transcription in olfactory sensory neurons. *J. Biol. Chem.* 276, 2047-2052.
- Wee, P.D., and Bargmann, C.I. (2001). *C. elegans* odour discrimination requires asymmetric diversity in olfactory neurons. *Nature* 410, 698-701.
- White, J.G., Southgate, E., Thomson, J.N., and Brenner, S. (1986). The structure of the nervous system of the nematode *Caenorhabditis elegans*. *Phil. Trans. R. Soc. Lond. B* 314, 1-340.
- Williams, B.D. (1995). Genetic mapping with polymorphic sequence-tagged sites. *Methods Cell Biol.* 48, 81-96.
- Yu, S., Avery, L., Baude, E., and Garbers, D.L. (1997). Guanylyl cyclase expression in specific sensory neurons: a new family of chemosensory receptors. *Proc. Natl. Acad. Sci. USA* 94, 3384-3387.

Chapter 5

Conclusions and Future Directions

Specification of olfactory neuron subtypes in *C. elegans*

A LIM code for olfactory neurons?

Motor neuron axon pathways in the vertebrate spinal cord are specified by the particular combination of LIM homeobox genes they express (Tsuchida et al., 1994; Sharma et al., 1998). LIM homeobox genes can be both necessary and sufficient to specify a particular motor neuron subtype in mammals and flies (Sharma et al., 1998; Thor et al., 1999). Although only axon trajectories were assayed in these studies of motor neuron specification, it is presumed that the "LIM code" controls all aspects of cell fate. Analysis of *lim-4* in *C. elegans* olfactory neurons (chapter 2) demonstrated that this class of transcription factors can be both necessary and sufficient to specify multiple aspects of cell fate. *lim-4* specifies the expression of signal transduction genes (receptors and a G-protein α subunit), axon morphology, dendrite morphology, and most likely the synaptic connections of the AWB olfactory neurons.

Although LIM homeobox gene function in *C. elegans* does not in occur in a coherent, combinatorial pattern like the vertebrate LIM genes in the spinal cord, there are hints that clusters of LIM genes may play a role in differentiating similar neuron subtypes. For example, one sensory neuron and two interneurons involved in the thermotaxis circuit are specified by distinct LIM genes. *ttx-3* is required for specification

of the interneuron AIY, *lin-11* is required to specify the interneuron AIZ, and *ceh-14* is required for the specification of the sensory neuron AFD (Cassata et al., 2000; Hobert et al., 1997; Hobert et al., 1998). Thus, all three neurons in this simple circuit are specified by LIM homeobox genes. This thermotaxis "code" differs from the vertebrate spinal cord code, however, in that absence of a LIM homeobox gene does not cause these cells to transdifferentiate into another neuron subtype.

Another possible set of neurons with a simple "LIM code" in *C. elegans* are the three olfactory neurons pairs, AWA, AWB, and AWC. *lim-4* is required for the AWB cell fate (chapter 2). Loss of *lim-4* in AWB causes it to adopt an AWC cell fate. All aspects of the AWB cell fate that were assayed (with the notable exception of the AWC left/right asymmetry) were transformed towards an AWC fate in *lim-4* mutants. Recent work from the lab of Piali Sengupta has implicated the LIM homeobox gene *lin-11* in specifying AWA cell fate (Sarafi-Reinach, Melkman, Hobert and Sengupta, in press). Loss of *lin-11* causes the AWA cells to adopt an AWC-like fate. A similar defect is observed following the loss of the nuclear hormone receptor *odr-7* in AWA (chapter 2). *lin-11* acts upstream of *odr-7* in the transcription factor hierarchy that controls AWA cell fate. Therefore, like the vertebrate spinal cord, a simple LIM code controls the fates of the three olfactory neuron cell types in *C. elegans*: expression of *lin-11* specifies the AWA cell fate, expression of *lim-4* specifies AWB, and lack of LIM homeobox gene expression specifies AWC.

AWC as a primordial cell fate

Removing *lim-4* from AWB causes it to adopt an AWC-like fate. Similarly, removing *odr-7* or *lin-11* causes AWA to take on AWC-like characteristics. These results suggest a model whereby AWC serves as a ground state olfactory fate (chapter 2, figure 7), despite the fact that the three neuron subtypes are lineally unrelated. Transcription factors like *lim-4* and *lin-11* act to modify this olfactory cell "blueprint" to create a more diverse array of cell types.

Work from Piali Sengupta's lab has extended these results and suggests that the AWC cell fate may be a default not only for olfactory cells, but perhaps for other sensory cell types as well. In the absence of the forkhead transcription factor *unc-130* the ASG chemosensory neurons adopt the fate of their lineal sister AWA (Sarafi-Reinach and Sengupta, 2000). In an *unc-130; odr-7* double mutant both the presumptive AWA and ASG neurons adopt the AWC default fate. Similarly, in a *ttx-1* mutant the AFD thermosensory neurons adopt an AWC-like fate (Satterlee and Sengupta, in press). Thus, four sensory neuron cell types, AWA, AWB, ASG, and AFD, in addition to AWC itself, are capable of adopting the AWC default fate in different mutant backgrounds. These results together suggest an intriguing evolutionary scenario, in which a more simple *C. elegans* ancestor, with much less chemosensory diversity, possessed only AWC-like sensory cells. As the animal evolved, factors like *lim-4* and *lin-11* were recruited to

diversify this fate, increasing the animal's cellular complexity and its behavioral sophistication.

It is important to note that in all of these cases, AWC cell fate was assayed by the expression of the receptor *str-2* (chapter 3). As discussed in this thesis, *str-2* is a marker for only one of the two AWC cells. In these various mutant backgrounds, both homologs of the transformed cells express *str-2*, indicating that they have not acquired the ability to perform lateral signaling like the native AWC cells. A separate factor, not controlled by *lim-4*, *odr-7*, or *lin-11*, must therefore specify the ability to perform this signaling interaction in the AWC cells. This factor could be a local cue, since cell body positions are not drastically changed in these mutant backgrounds, or a separate factor deposited by the lineage. Because there are so far no markers available for the AWC^{OFF} cell, it is unclear whether the AWC fate that these cells are acquiring is the AWC^{ON} fate, or a mixture of the AWC^{OFF} and AWC^{ON} fates. Given the functional differences between the two AWC cells (Wes and Bargmann, 2001), these possibilities could be distinguished with behavioral assays.

Finding the olfactory fate determinant

The possibility that the AWC fate is a default sensory neuron fate suggests that a factor that specifies this generic cell fate may exist. Since none of the cells with AWC fate potential are lineally related to one another, this factor could be deposited several

times in the lineage, or could be activated by a cue that makes contact with the appropriate cells. In the extreme case that all amphid sensory neurons are derivatives of the AWC default fates, all of the cells in the amphid may be endowed with this factor.

Finding this generic "olfactory cell determinant" will require identifying genes required for the specification of the AWC cells themselves. Screening for the loss of *str-2::GFP* by itself could be problematic, since such mutants could identify genes involved in the later lateral signaling decision. A more specific screen is being conducted by Piali Sengupta's lab, looking for loss of an *odr-1* marker that is expressed in both AWC cells. Another strategy would be to screen for loss of *str-2* expression in an *odr-7; lim-4* background. These animals would express the marker in as many as five cells, making it potentially easy to spot animals that have completely lost the ability to specify the AWC cell fate.

Lateral signaling in the AWC olfactory neuron pair

A model for olfactory fate execution in AWC

The results of a screen designed to isolate genes involved in the AWC lateral signaling decision are described in chapters 3 and 4. Animals expressing the *str-2::GFP* reporter were mutagenized, and mutants expressing this reporter in both AWC cells were isolated. Although the initial goal of this screen was to isolate genes involved in the non-autonomous signaling interaction, analogous to the Delta and Notch genes in other lateral

signaling decisions, a mosaic analysis experiment (chapter 4) demonstrated that most of the genes isolated in the screen function in a cell-autonomous execution pathway for the AWC^{OFF} cell fate. This pathway makes use of a novel combination of signal transduction molecules.

Mapping and complementation tests allowed the relatively rapid identification of the defective gene in several of these mutants (chapter 3), including a calcium channel (*unc-2* and *unc-36*), and a calcium-dependent kinase (*unc-43*). Positional cloning identified one novel gene involved in this pathway, *nsy-1*, a MAP kinase kinase kinase (chapter 4). In collaboration with Kunihiro Matsumoto's lab, a candidate gene approach allowed us to identify the *sek-1* MAP kinase kinase as an additional component of this pathway (Tanaka-Hino et al., submitted). Engineered gain-of-function forms of the *nsy-1* and *unc-43* genes had the opposite, two AWC^{OFF} phenotype, making extensive epistasis analysis possible. Assuming that these genes fall into a linear genetic pathway, a simple pathway emerged from this analysis and allowed the generation of a model for the AWC^{OFF} execution pathway (chapter 4, figure 5). The calcium channel subunit genes are the most upstream component of the pathway, suggesting that calcium influx through this channel triggers downstream events. Next in the pathway is the CaMKII *unc-43*, which is activated by a calcium/calmodulin complex, followed by the MAP kinase kinase kinase *nsy-1*. We suggest that *nsy-1* may be directly activated by *unc-43* phosphorylation. This proposed link between a CaMKII and a MAPKKK is a novel signal transduction

interaction, but the hypothesis is supported by both genetic and biochemical experiments (chapter 4). Activated *nsy-1* phosphorylates and activates the MAP kinase kinase *sek-1* (Tanaka-Hino et al., submitted).

The link between genes involved in neuronal excitability (calcium channels, CaMKII), and genes more traditionally involved in developmental decisions (a MAPK pathway), may be more broadly used to transduce signals in the nervous system. Work from Hidenori Ichijo's lab has demonstrated a similar relationship between the mammalian counterparts of *unc-43* and *nsy-1* (submitted).

Epistasis analysis suggests that *nsy-2* is a downstream component of the execution pathway. *nsy-2* has been mapped to a small region of about 25 cosmids on linkage group III. No candidate MAP kinases have been identified in this region, suggesting that *nsy-2* may encode a transcription factor that represses *str-2* expression. Temperature shift experiments performed by Chiou-Fen Chuang have pinpointed *nsy-2* gene action to late embryogenesis, just before asymmetric *str-2* expression in AWC becomes apparent (personal communication). These results suggest that *nsy-2* most likely acts in the *unc-43/nsy-1* execution pathway, rather than a later maintenance pathway. Positional cloning efforts by Chiou-Fen are likely to reveal *nsy-2*'s molecular identity in the near future.

Identifying the gene responsible for the *nsy-2* phenotype should reveal whether it is indeed a transcription factor or another intermediate step in the pathway. Finding the transcription factor that directly impinges on the *str-2* promoter would make it possible to

address several important questions. These questions include whether the *unc-43/nsy-1* execution pathway directly represses the *str-2* promoter, or instead sets off a transcriptional cascade, whether other genes are candidates for regulation by this pathway, and how exactly the *unc-43/nsy-1* pathway regulates gene expression. For example, does the pathway control import of a transcription factor to the nucleus or its access to DNA? *In vivo* DNA binding assays in worms should make it possible to visualize directly any differences in transcription factor regulation between the two AWC cells (e.g. Carmi et al., 1998).

If *nsy-2* does not encode the transcription factor that represses *str-2* expression, alternative approaches can be employed to identify it. Preliminary promoter dissection experiments have yet to reveal a compact DNA element that controls *str-2* asymmetry (Emily Troemel, Steve McCarroll, and Alvaro Sagasti, unpublished results). More careful promoter dissection experiments could reveal such an element, allowing the identification of factors that bind to it.

Finding the upstream lateral signaling molecules

The major remaining question about *str-2* regulation is the identity of the molecules mediating the lateral cell communication. Examination of several mutations in the *C. elegans* Notch genes *lin-12* and *glp-1* did not reveal any role for these genes in regulating *str-2* transcription (chapter 3, and Miri VanHoven and Alvaro Sagasti,

unpublished results). This raises the intriguing possibility that a completely novel set of genes mediates AWC lateral signaling. One mutant from the original neuronal asymmetry screen, *nsy-3*, is a good candidate for being involved in this process (chapters 3 and 4). Epistasis analysis places *nsy-3* upstream of the *unc-43/nsy-1* pathway. A double mutant between *nsy-3* and the axon guidance mutant *unc-76* displays the two AWC^{ON} *nsy-3* phenotype, indicating that it acts cell autonomously. However, this does not exclude the possibility that it also has a cell non-autonomous function that coordinates the two cell fates, like the Notch receptor (Seydoux and Greenwald, 1989). *nsy-3* could therefore play a role either in receiving the lateral signal, or in transducing information from the lateral signaling pathway to the *unc-43/nsy-1* execution pathway.

nsy-3 is a semi-dominant mutant, but it remains unclear whether the two *nsy-3* alleles are gain-of-function or haplo-insufficient. Determining the nature of *nsy-3* dominance could alter interpretation of its epistasis relationships. *nsy-3* has been localized to the right arm of linkage group V. Cloning efforts by Miri VanHoven promise to shed light on the molecular nature of the *nsy-3* lesion.

The *str-2::GFP* expression phenotype of axon guidance mutants, and the results of laser ablation experiments performed by Emily Troemel (chapter 3), suggest that the default state for *str-2::GFP* expression is two AWC^{OFF}. In other words, if an AWC neuron can not locate its signaling partner, it will adopt an AWC^{OFF} cell fate. It is therefore likely that mutations in molecules involved directly in communication between

the two AWC neurons will exhibit a two AWC^{OFF} phenotype, rather than the two AWC^{ON} phenotype displayed by the mutants isolated in the screen described in chapter 3.

A pilot screen for two AWC^{OFF} mutants was performed by Stephanie Albin, and resulted in the isolation of one mutant, *nsy-4* (personal communication). Epistasis analysis placed *nsy-4* downstream of *nsy-3* and upstream of the calcium channel subunit *unc-36* (Alvaro Sagasti and Miri VanHoven, unpublished results). Behavioral experiments suggest that the two AWC cells in *nsy-4* have adopted the AWC^{OFF} phenotype, rather than having been mispecified (Miri VanHoven and Paul Wes, personal communication). These results make *nsy-4* an excellent candidate to be involved either in the lateral interaction between the two cells, or in transducing information from the lateral signaling pathway to the *unc-43/nsy-1* execution pathway. Miri VanHoven has mapped the *nsy-4* gene to a small region on linkage group IV and is continuing efforts to identify the gene responsible for the mutant phenotype. A more extensive screen for two AWC^{OFF} mutants has been performed by Sarah Bauer and Miri VanHoven and may reveal new genes that act in the AWC lateral signaling pathway.

A role for secretion in AWC lateral signaling?

Electron micrograph reconstructions of two worms reveal an asymmetric arrangement of synapses in the two AWC cells (White, 1986). Experiments performed by Emily Troemel, however, suggest that classical synaptic transmission is unlikely to be

involved in the AWC asymmetry decision (chapter 3). Mutations in *unc-104*, *unc-13*, and *snt-1*, all proteins required for synaptic transmission, do not affect AWC asymmetry. Nonetheless, it is possible that synaptic transmission does play a role, but that the synaptic mutations examined retain enough residual activity to support normal AWC signaling. Alternatively, a separate secretion pathway distinct from the pathway required for classical clear vesicle synaptic transmission, could be involved in AWC signaling. A more thorough survey of proteins involved in synaptic development and transmission, dense core vesicle transmission, neurotransmitter synthesis, and neuropeptide processing would address this question more definitively.

To test more thoroughly whether synaptic activity could be involved in AWC asymmetry, I placed the tetanus toxin light chain under the control of the *odr-3* promoter, which drives expression in both AWC neurons. This transgene causes a two AWC^{ON} phenotype in up to 50% of animals. A compromised form of tetanus toxin causes at most 10% of animals to display the two AWC^{ON} phenotype.

The tetanus toxin light chain is a protease that cleaves synaptobrevin, a SNARE protein required for synaptic vesicle fusion. Expressing this protein in *Drosophila* neurons inactivates them without affecting their morphology (Sweeney et al., 1995). Tetanus toxin in flies seems to be specific for synaptobrevin and not the paralogous protein, cellubrevin, which is more broadly required for secretion. There is no evidence yet whether tetanus toxin is specific for synaptobrevin in *C. elegans*, but this could be

tested by introducing a non-cleavable form of synaptobrevin into worms and looking for rescue of the *str-2* misexpression phenotype. Another experiment that could address whether tetanus toxin affects synaptic transmission is to determine whether mutations in synaptic release proteins such as *unc-13*, or the dense core vesicle release protein *unc-31*, can enhance the phenotype caused by expressing tetanus toxin in AWC.

Although these results are preliminary, they suggest that secretion may play a role in controlling *str-2* expression. The fact that tetanus toxin-expressing animals exhibit the two AWC^{ON} phenotype, rather than the two AWC^{OFF} phenotype caused by lack of axon contact, suggests that two non-autonomous steps may act to control *str-2* asymmetry. In this scenario, axon contact would cause both AWC cells to express *str-2*, and a secretion mediated step would cause one of the two cells to turn it off, perhaps by activating the *unc-43/nsy-1* pathway. Secretion could be acting in several ways: it could play a role in the feedback part of the lateral interaction, it could activate the *unc-43/nsy-1* pathway non-autonomously, or it could have an autonomous function to place a signaling molecule on the cell surface. A combination of epistasis analysis and mosaic analysis with the tetanus toxin-expressing animals should help distinguish between these models.

Many of the molecular details of the lateral signaling pathway that causes asymmetric cell fates in AWC remain a mystery. A plethora of uncloned mutants, including *nsy-2*, *nsy-3*, *nsy-4*, the recently isolated two AWC^{OFF} mutants, and perhaps

secretion mutants, provide a promising resource for fleshing out the details of this pathway. The powerful epistasis, mosaic, and behavioral techniques that have been developed will make it possible to understand the role that individual genes play in this pathway. Understanding the molecular control of AWC asymmetry may provide a paradigm for understanding other cell fate decisions and signaling interactions in the nervous system.

References

- Carmi, I., Kopczynski, J. B., and Meyer, B. J. (1998). The nuclear hormone receptor SEX-1 is an X-chromosome signal that determines nematode sex. *Nature* 396, 168-173.
- Cassata, G., Kagoshima, H., Andachi, Y., Kohara, Y., Durrenberger, M. B., Hall, D. H., and Burglin, T. R. (2000). The LIM homeobox gene *ceh-14* confers thermosensory function to the AFD neurons in *Caenorhabditis elegans*. *Neuron* 25, 587-597.
- Hobert, O., D'Alberti, T., Liu, Y., and Ruvkun, G. (1998). Control of neural development and function in a thermoregulatory network by the LIM homeobox gene *lin-11*. *J Neurosci* 18, 2084-2096.
- Hobert, O., Mori, I., Yamashita, Y., Honda, H., Ohshima, Y., Liu, Y., and Ruvkun, G. (1997). Regulation of interneuron function in the *C. elegans* thermoregulatory pathway by the *ttx-3* LIM homeobox gene. *Neuron* 19, 345-357.
- Sarafi-Reinach, T. R., and Sengupta, P. (2000). The forkhead domain gene *unc-130* generates chemosensory neuron diversity in *C. elegans*. *Genes Dev* 14, 2472-2485.
- Seydoux, G., and Greenwald, I. (1989). Cell autonomy of *lin-12* function in a cell fate decision in *C. elegans*. *Cell* 57, 1237-1245.
- Sharma, K., Sheng, H. Z., Lettieri, K., Li, H., Karavanov, A., Potter, S., Westphal, H., and Pfaff, S. L. (1998). LIM homeodomain factors Lhx3 and Lhx4 assign subtype identities for motor neurons. *Cell* 95, 817-828.

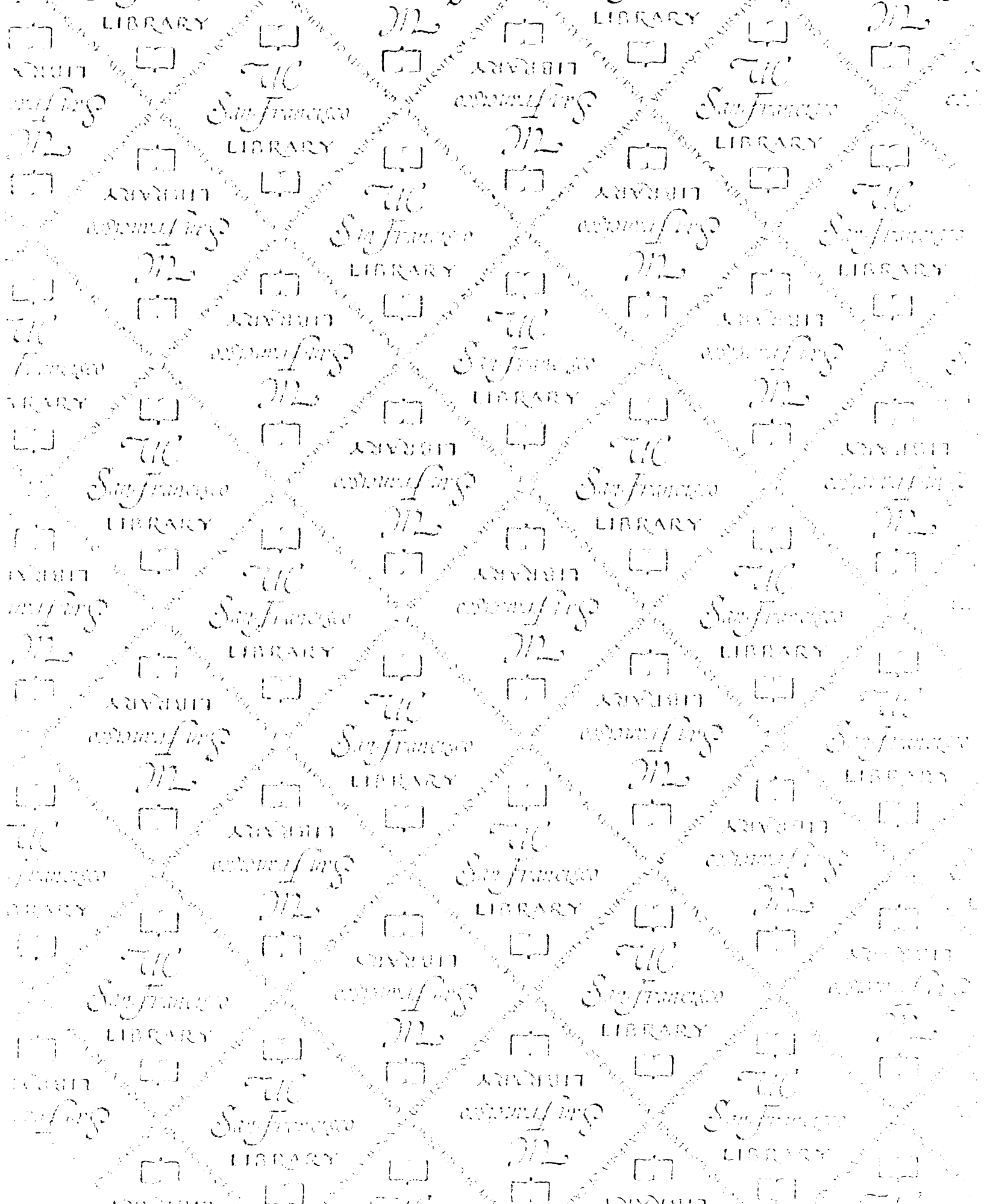
Sweeney, S. T., Broadie, K., Keane, J., Niemann, H., and O'Kane, C. J. (1995). Targeted expression of tetanus toxin light chain in *Drosophila* specifically eliminates synaptic transmission and causes behavioral defects. *Neuron* 14, 341-351.

Thor, S., Andersson, S. G., Tomlinson, A., and Thomas, J. B. (1999). A LIM-homeodomain combinatorial code for motor-neuron pathway selection. *Nature* 397, 76-80.

Tsuchida, T., Ensini, M., Morton, S. B., Baldassare, M., Edlund, T., Jessell, T. M., and Pfaff, S. L. (1994). Topographic organization of embryonic motor neurons defined by expression of LIM homeobox genes. *Cell* 79, 957-970.

Wes, P. D., and Bargmann, C. I. (2001). *C. elegans* odour discrimination requires asymmetric diversity in olfactory neurons. *Nature* 410, 698-701.

White, J. G., Southgate, E., Thomson, J. N., Brenner, S. (1986). The structure of the nervous system of the nematode *Caenorhaditis elegans*. *Phil Trans R Soc Lond B* 314, 1-340.



For Not to be taken
from the room.
reference

